EPA/600/R-14/191 | August 2014 | www.epa.gov/research

United States Environmental Protection Agency

Atmospheric LiDar Coupled with Point Measurement Air Quality Samplers to Measure Fine Particle Matter (PM) Emissions from Agricultural Operations. Part 2 of the California 2007 – 2008 Tillage Campaigns: Spring 2008 Data Analysis

RESEARCH AND DEVELOPMENT

Atmospheric LiDar Coupled with Point Measurement Air Quality Samplers to Measure Fine Particle Matter (PM) Emissions from Agricultural Operations. Part 2 of the California 2007 – 2008 Tillage Campaigns: Spring 2008 Data Analysis

David J. Williams
Office of Research and Development
National Exposure Research Laboratory
Environmental Sciences Division
Landscape Characterization Branch
Research Triangle Park, North Carolina

Jerry Hatfield
National Soil Tilth Laboratory
Agricultural Research Service
United States Department of Agriculture
Ames, Iowa

U.S. Environmental Protection Agency
Office of Research and Development
Washington, DC 20460

Atmospheric LiDAR coupled with point measurement air quality samplers to measure fine particulate matter (PM) emissions from agricultural operations. Part 2 of the California 2007-2008 Tillage Campaigns: Spring 2008 Data Analysis

Authors:

Jerry Hatfield
National Soil Tilth Laboratory
Agricultural Research Service
United States Department of Agriculture
Ames, Iowa

David Williams*
Environmental Sciences Division
National Exposure Research Laboratory
U.S. Environmental Protection Agency
Research Triangle Park, NC

James Sweet
Planning Division
Central Region Office
San Joaquin Valley Air Pollution Control District
Fresno, CA

Sona Chilingaryan
Air Division
Region 9
U.S. Environmental Protection Agency
San Francisco, CA

*Corresponding author. (919) 541-2573; williams.davidj@epa.gov

Disclaimer Notice: The United States Environmental Protection Agency through its Office of Research and Development partially funded and collaborated in the research described here under Interagency Agreement: DW 12922568 to Space Dynamics Laboratory. It has been subjected to Agency review and approved for publication. Mention of trade names or commercial products does not constitute endorsement or recommendation for use.

Report Prepared By:

Dr. Gail Bingham
SDL Chief Scientist & Civil Space and Environment Division Leader
Space Dynamics Laboratory
1695 North Research Park Way
North Logan, UT 84341

Jennifer Bowman
Senior Manager, Internal Communications
ATK Aerospace Systems
P.O. Box 98
5000 S. 8400 W.
Magna, UT 84044

Christian Marchant
Energy Dynamics Laboratory
1695 North Research Park Way
North Logan, UT 84341

Dr. Randal Martin
Research Associate Professor
Department of Civil and Environmental Engineering
Utah State University
41 10 Old Main Hill
Logan, UT 84322

Kori Moore
Environmental Engineer
Energy Dynamics Laboratory
1695 North Research Park Way
North Logan, UT 84341

Dr. Philip Silva
Environmental Chemist
Animal Waste Management Research Unit
USDA Agricultural Research Service
230 Bennett Lane
Bowling Green, KY 42 104

Dr. Michael Wojcik
Branch Chief for Environmental Measurement
Energy Dynamics Laboratory
1695 North Research Park Way
North Logan, UT 84341

Space Dynamics Laboratory
Utah State University Research Foundation

California Spring 2008 Tillage Campaign: Data Analysis

A project performed for the San Joaquin Valleywide Air Pollution Study Agency, Contract 07-1 AG

Submitted To:

James Sweet
Planning Division
Central Region Office
San Joaquin Valley Air Pollution Control District
Fresno, CA

David Williams
Environmental Sciences Division
National Exposure Research Laboratory
U.S. Environmental Protection Agency
RTP, NC

Sona Chilingaryan
Air Division
Region 9
U.S. Environmental Protection Agency
San Francisco, CA

Dr. Jerry Hatfield
National Laboratory for Agriculture and the Environment
Agricultural Research Service
United States Department of Agriculture
Ames, IA

Submitted By:

Space Dynamics Laboratory/ Utah State University Research Foundation
1695 North Research Park Way
North Logan, Utah 84341

DOCUMENT NUMBER: SDL/08-556
REVISION: -
DATE: JUNE 21, 2013

TABLE OF CONTENTS

TABLE OF FIGURES

LIST OF TABLES

TABLE OF ABBREVIATIONS/VARIABLES

Abbr./Var.	Definition
β_E	backscatter values measured by lidar in vector form (1/m-steradians)
β_V	particle normalized backscatter from OPC data in vector form (1/m-steradians)
η	control efficiency
µg	micrograms ($1x10^{-6}$ gram)
µL	microliter ($1x10^{-6}$ liter)
µm	micrometers ($1x10^{-6}$ meter)
ρ_v	density of water vapor
σ	standard deviation
σ_w	standard deviation of the vertical wind (m/s)
σ_y	horizontal plume spread parameter (meter)
σ_z	vertical plume spread parameter (meter)
2D	two-dimensional
3D	three-dimensional
A	acres of land tilled
ACS	American Chemical Society
Activity	amount of time the engine is active during the year (hr/yr)
AERMOD	American Meteorological Society/Environmental Protection Agency Regulatory Model
agl	above ground level
AMS	aerosol mass spectrometer
AQT	air quality trailer
ARS	Agricultural Research Service
Avg	average
AvgHp	maximum rated average horsepower (bhp)
bhp	brake horsepower
C_{10}	10 minute average pollutant concentration (µg/m^3)
C_D	downwind PM_K concentration (µg/m^3)
$C_{measured}$	measured PM concentration (µg/m^3)
$C_{modeled}$	modeled concentration (µg/m^3)
$C_{\bar{U}}$	scan area average upwind PM_K concentration (µg/m^3)
c	Carbon dioxide concentration
c_E	constant, 4.8 lb/acre-pass
CFR	Code of Federal Regulations
Ca^{+2}	Calcium ion
CARB	State of California Air Resources Board
CCF	counting correction factor (unitless)
CCV	continuing calibration verification
CF	conversion factor from (g/yr) to (tons/day)
CHrs	cumulative engine operation hours (hr)
CI	confidence interval
CIMIS	California Irrigation Management Information System
Cl^-	Chloride ion
CMP	conservation management practice
CO_2	Carbon dioxide
CT	conservation tillage
d	particle diameter (µm)

Abbr./Var.	Definition
d_{aero}	aerodynamic diameter (μm)
$d_{i,\ upper}$	upper edge of bin *i* (μm)
$d_{i,\ lower}$	lower edge of bin *i* (μm)
d_k	particle of diameter *k* (μm)
d_{PA}	projected area diameter (μm)
DDI	double-distilled, de-ionized water
DF	engine deterioration factor (unitless)
dr	engine deterioration rate (g/bhp-hr^2)
E	east
E	flux of water vapor from the soil surface
E_{CT}	emission rate for the conventional tillage method
$E_{estimated}$	derived emission rate (μg/s-m^2)
E_{PM}	PM emission (lbs)
E_{seed}	seed emission rate (μg/s-m^2)
E_{STT}	emission rate for the strip-till tillage method
EC	elemental Carbon particulate matter
EC	eddy covariance
EC/OC	elemental Carbon/organic Carbon particulate sampler
EF	emission factor (g/bhp-hr)
$EF_{adj(PM)}$	adjusted PM emission factor (g/hp-hr)
EF_{ss}	steady-state measured emission factor (g/hp-hr)
Emissions	amount of pollutant released (tons/day)
EPA	United States Environmental Protection Agency
F	particulate flux in lidar scans (μg/s)
F^-	Fluoride ion
FRM	federal reference method
GMD	geometric mean diameter (μm)
GPS	global positioning system
H	sensible heat
H	effective stack height (meter)
H_2SO_4	Hydrogen sulfate
HCl	Hydrogen chloride
hp	horsepower
$hr_{tractor}$	tractor operation hour
IC	ion chromatography
IRGA	infrared gas analyzers
ISCST3	Industrial Source Complex, Short Term Ver. 3
k	dimensionless particle size multiplier
K^+	Potassium ion
LE	latent heat
Load	load factor
Lpm	liters per minute
M	molar
m	meter
MCF	mass conversion factor (g/cm^3)
MDL	minimum detection level
Mg^{+2}	Magnesium ion

Abbr./Var.	Definition
N	north
N_{ij}	average number concentration per bin *i* for OPC *j* (number/cm^3)
$\check{N}_i$	mean of the averages across all OPCs for bin *i* (number/cm^3)
n	number of samples
n(r)	relative amplitude of the aerosol component of total atmospheric backscatter at range *r* (unitless)
Na^+	Sodium ion
NAAQS	National Ambient Air Quality Standard
NaOH	Sodium hydroxide
NC	not calculated
NEVES	Nonroad Engine and Vehicle Emission Study
ng	nanogram (1x10^{-9} gram)
NH_4^+	Ammonium ion
NO_2^-	Nitrite ion
NO_3^-	Nitrate ion
NO_x	Oxides of nitrogen
NONROAD	U.S. EPA Nonroad Emissions Model
NRCS	Natural Resources Conservation Service
OC	Organic Carbon
OFFROAD	CARB Offroad Emissions Model
OPC	optical particle counter
p	power law wind speed coefficient (unitless)
p_{ij}	raw OPC particle counts in bin *i* (number)
PM	particulate matter
$PM_{1.0}$	particulate matter with an aerodynamic diameter less than or equal to 1.0 micrometers
$PM_{2.5}$	particulate matter with an aerodynamic diameter less than or equal to 2.5 micrometers
PM_{10}	particulate matter with an aerodynamic diameter less than or equal to 10 micrometers
PM_k	particulate matter with an aerodynamic diameter less than or equal to *k* micrometers
$PM_K(r)$	particulate matter with an aerodynamic diameter less than or equal to K micrometers, calculated from lidar data, at range *r*
ppm	parts per million
PSL	polystyrene latex sphere
Q	emission rate (µg/s)
q	water vapor concentration
q_j	average measured sample flow for OPC *j* (cm^3/min)
RARE	Regional Applied Research Effort
RD	respirable dust
S	south
s	silt content of surface soil (%)
SDL	Space Dynamics Laboratory
SO_4^{-2}	Sulfate ion
S_{PMadj}	diesel sulfur content adjustment factor (g/hp-hr)
ST	standard tillage
t_j	sample time for OPC j (min)
tp	number of passes or tillings per year
TAF	transient adjustment factor (unitless)
TD	total dust
TSP	total suspended particulate

Abbr./Var.	Definition
u	wind speed in the streamwise direction (m/s)
u^*	friction velocity (m/s)
u_1	Measured reference wind speed (m/s)
u_2	Calculated wind speed based on the reference wind speed (m/s)
u_{GM}	mean wind speed at the release height H (m/s)
$\overline{u\,w}$	momentum term of the streamwise and vertical wind directions (m^2/s^2)
UC	University of California
USDA	United States Department of Agriculture
UWRL	Utah Water Research Laboratory
$\mathbf{V_E}$	particle normalized volume concentration vector ($\mu m^3/cm^3$)
V_k	OPC cumulative volume concentration up to a diameter of k ($\mu m^3/cm^3$)
$V_K(r)$	cumulative volume concentration from lidar data at range r ($\mu m^3/cm^3$)
V	wind speed in the lateral direction (m/s)
$\overline{v_{\parallel}}(r, h)$	average wind speed component at range r and height h that is parallel to the long axis of the lidar staple box
$\overline{v\,w}$	momentum term of the lateral and vertical wind directions (m^2/s^2)
W	west
W	watt
$\mathbf{W}$	diagonal weighting matrix used in lidar data analysis (unitless)
w	wind speed in the vertical direction (m/s)
WSS	web soil survey
y	horizontal distance of the modeled receptor from the centerline of the plume (meter)
z	height of modeled receptor above ground level (meter)
z_1	height at which the reference wind speed was measured (m)
z_2	height of the calculated wind speed (m)
ZH	zero-hour engine emission rate (g/bhp-hr)

The statements and conclusions in this report are those of SDL and not necessarily those of the California Air Resources Board, the San Joaquin Valleywide Air Pollution Study Agency, or its Policy Committee, their employees or their members. The mention of commercial products, their source, or their use in connection with material reported herein is not to be construed as actual or implied endorsement of such products.

EXECUTIVE SUMMARY

Airborne particles, especially particulate matter 10 micrometers (μm) or smaller in aerodynamic diameter (PM_{10}) and fine particulate matter 2.5 μm or smaller in aerodynamic diameter ($PM_{2.5}$), are microscopic solids or liquid droplets in the air that can cause serious health problems (e.g., coughing, difficulty breathing, decreased lung function, asthma, heart attacks, and premature death), especially in people with heart and lung disease. Concern with health effects resulting from PM_{10} exposure is drawing increased regulatory scrutiny and research toward local agricultural tillage operations. To investigate the control effectiveness of one of the current Conservation Management Practices (CMPs) written for agricultural land preparation on the generation of particulate matter (PM) levels, the San Joaquin Valleywide Air Pollution Study Agency funded a project to study:

1) The magnitude, flux, and transport of PM emissions produced by agricultural practices for row crops where tillage CMPs are implemented vs. the magnitude, flux, and transport of PM emissions produced by agricultural practices where CMPs are not implemented.
2) The control efficiencies of equipment used to implement the "conservation tillage" CMP. If resources allow assessing additional CMPs, what are the control efficiencies of the "equipment change/technological improvements" CMP?
3) If these CMPs for a specific crop can be quantitatively compared, controlling for soil type, soil moisture, and meteorological conditions.

This study used advanced measurement technologies, which link lidar systems with conventional point-measurement air quality samplers, to map PM emissions at high spatial and temporal resolution in order to accurately compare CMPs with conventional tillage systems. The purpose of this field study was to determine if and how much particulate emissions differ between the conventional method of agricultural fall tillage and a conservation tillage CMP. It is a companion study to an earlier study performed in October 2007 near Los Banos, CA investigating the control efficiency of combined operations CMP versus conventional tillage in the fall tillage sequence. Findings from that study are detailed in a previous report [7].

The test location and CMP to be evaluated were chosen in discussion with stakeholders, regulatory agencies, and researchers. The current study was performed in the San Joaquin Valley of California in May and June of 2008 during the spring tillage sequence between a winter wheat crop and corn. The conventional 13-pass spring tillage sequence for a field going from winter wheat into corn was: two passes for in-field irrigation border breakdown, chisel, two disc passes, lister, two cultivator passes, roll, plant, fertilizer injection, and two more cultivator passes. The spring conservation tillage CMP sequence consisted of only three tractor passes: strip-till, plant/fertilize, and herbicide spray; specifically, the CMP implement investigated was the strip-till implement.

An extensive network of measurement systems were used during this study, including a scanning lidar, a full meteorology suite, four sonic anemometers (for turbulence information), and filter and optical aerosol point samplers. Two additional aerosol chemical analysis systems were employed from a sampling trailer located on the downwind side of the field under test.

Tillage particulate emission rates were determined using two methods: 1) inverse modeling coupled with observed facility-derived concentrations from filter- and optical-based instruments,

and 2) a mass balance approach applied to upwind and downwind PM concentrations measured by the lidar. The tillage emissions were modeled using two different air dispersion models: the Industrial Source Complex Short-Term Model, version 3 (ISCST3) and the American Meteorological Society/Environmental Protection Agency Regulatory Model (AERMOD). Emission data calculated for each measurement method for the conventional and conservation tillage operations are presented herein. The study showed that the conservation practice required < 1/4 of the number of tractor passes when compared to conventional tillage; similar reductions in fuel use and tractor exhaust associated PM_{10} emissions were expected to have occurred.

Lidar-derived and inverse modeling emission rates for $PM_{2.5}$, PM_{10}, and total suspended particulate (TSP) by operation, as well as the average tillage rate in hours per hectare are summarized herein. Based on lidar data, the conservation tillage method reduced $PM_{2.5}$ emission by 91%, PM_{10} by 94%, and TSP by 91%, which were all statistically significant differences. Reduced emissions as calculated using inverse modeling and optical particle counter data are very close to lidar-derived reductions at 85%, 87%, and 90% for $PM_{2.5}$, PM_{10}, and TSP, respectively. The time per hectare required to perform the conservation tillage was about 14% of the conventional method. The control efficiency of the Conservation Management Practice for particulate emissions was 0.905, 0.937, and 0.909 for $PM_{2.5}$, PM_{10}, and TSP, respectively, based on lidar data and 0.853, 0.872, and 0.903 for $PM_{2.5}$, PM_{10}, and TSP, respectively, based on inverse modeling with optical particle counter data.

Some of the derived PM_{10} emission rates from this experiment agree with those reported in the literature, as well as the emission factors used by the State of California Air Resources Board (CARB) to calculate area source PM_{10} contributions from agricultural tilling [14]; others do not agree and are significantly higher, such as the emission rates for the chisel, disc 1, disc 2, and lister passes. Emissions factor values estimated through inverse modeling for these operations are below the 95% level predicted by statistical distributions fitted to published data; emissions estimates from lidar for the same operations are above the 95% level. While values from published studies are generally not in close agreement, they are within the range of the variability expected from measurements made under different meteorological and soil conditions, as demonstrated by the wide range of values in the literature [12][16]. In general, the emission rates calculated from this study are higher than others reported but are within the variability of other reported emission rates.

1. BACKGROUND

Airborne particles, especially particulate matter 10 micrometers (μm) or smaller in aerodynamic diameter (PM_{10}) and fine particulate matter 2.5 μm or smaller in aerodynamic diameter ($PM_{2.5}$), are microscopic solids or liquid droplets in the air that can cause serious health problems (e.g., coughing or difficulty breathing, decreased lung function, aggravated asthma, development of chronic bronchitis, irregular heartbeat, heart attacks, and premature death), especially in people with heart or lung disease [3]. Particles larger than 1.0 μm tend to be prevented from entering the lungs by the nose and throat [4]. The U.S. Environmental Protection Agency (U.S. EPA) has established limits for $PM_{2.5}$ and PM_{10} levels in order to protect public health as part of the National Ambient Air Quality Standards (NAAQS) [5][6]. The U.S. EPA requires state air quality management agencies to monitor ambient $PM_{2.5}$ and PM_{10} concentrations in order to identify possibly hazardous conditions for the population; to report areas that exceed the NAAQS beyond the allowed number of times; and to establish procedures to reduce particulate concentrations to meet the standards.

To address the problems associated with exposure to high particulate matter (PM) levels, the U.S. EPA has been working with the San Joaquin Valley Air Pollution Control District to support PM research. In 2007 the Environmental Sciences Division, National Exposure Research Laboratory was awarded a Regional Applied Research Effort (RARE) grant to determine the control effectiveness of a Conservation Management Practice (CMP) for agricultural tillage, targeted toward reducing PM_{10} emissions, using advanced measurement technologies such as atmospheric light detection and ranging (lidar) systems. The field study was carried out in October 2007 in the San Joaquin Valley [7]. This report describes the 2008 tillage comparison project that was supported by the San Joaquin Valleywide Air Pollution Study Agency to follow-up the 2007 RARE project. The lidar system, when coupled with point-measurement air quality samplers, can map PM emissions at high spatial and temporal resolutions, allowing for accurate comparisons of various CMPs for a variety of agricultural practices [8]. The purpose of this project was to deploy an elastic lidar system, together with a network of air samplers, to measure PM emissions from agricultural operations in order to answer the following research questions:

1. What are the magnitude, flux, and transport of PM emissions produced by agricultural practices for row crops where tillage CMPs are implemented vs. the magnitude, flux, and transport of PM emissions produced by agricultural practices where CMPs are not implemented?

2. What are the control efficiencies of implementing the “conservation tillage” CMP?

3. Can this CMP for a specific crop be quantitatively compared, controlling for soil type, soil moisture, and meteorological conditions?

In November 2008, EPA redesignated the San Joaquin Valley to attainment for the PM_{10} NAAQS, but sources in the Valley must continue to implement measures that helped the District attain the PM_{10} standard, including CMPs. The Valley continues to violate the $PM_{2.5}$ NAAQS. The CMP chosen for comparison against the conventional tillage method was conservation tillage, which is defined as a method in which the soil is being tilled or cultivated to a lesser extent compared to a conventional system [9]. There are several different conservation tillage systems that vary in the amount of the soil tilled; the system chosen for examination in this study

was the strip-till system. Data collected May 17 – June 25, 2008 at a site in the San Joaquin Valley of California are included in this report.

1.1 LITERATURE REVIEW

A handful of published articles pertain to PM emissions from agricultural tillage, with the majority of the studies performed in the State of California. There are also several papers that collectively examine impacts of a variety of conservation tillage practices with respect to soil characteristics, fuel consumption, cost of production, and air emissions.

The companion study to this experiment was conducted in October 2007 near Los Banos, CA [7]. It examined differences between conventional fall tillage practices and a Combined Operations CMP. This involved using an implement designed to do the work of multiple implements in one pass called the Optimizer[1] on two fields that were adjacent and similar to one another. The conventional method consisted of four different passes over the field in the following order: 1) disc pass, 2) chisel pass, 3) another disc pass, and 4) land plane pass. The CMP was applied in two steps in the following order: 1) chisel pass, and 2) the Optimizer pass. This study found that the CMP used 51% less fuel per unit area and took 62% less time per unit area. Using a lidar mass balance approach, it was determined that the CMP produced 71%, 40%, and 76% as much $PM_{2.5}$, PM_{10}, and total suspended particulate (TSP) as the conventional method. Table 1 presents the lidar-based $PM_{2.5}$, PM_{10}, and TSP emissions rates for each tillage step. Comparisons using inverse modeling coupled with PM measurements were not complete due to insufficient differences between upwind and downwind $PM_{2.5}$ concentrations during some measurement periods; however, operation-specific emission rates calculated using inverse modeling were similar to those reported by the calibrated lidar measurements.

Table 1. Emission rates ± 95% confidence intervals found by SDL [7] using lidar measurements for a conventional fall tillage sequence and a Combined Operations CMP sequence.

Operation	$PM_{2.5}$ (mg/m^2)	PM_{10} (mg/m^2)	TSP (mg/m^2)
Combined: Chisel	45.3 ± 13.1	69.0 ± 19.9	265.9 ± 76.6
Combined: Optimizer	32.5 ± 5.1	42.7 ± 6.6	169.9 ± 26.2
Sum for Combined Operation Method	**77.8 ± 14.0**	**111.6 ± 20.9**	**435.8 ± 80.9**
Conventional: Disc 1	20.4 ± 2.6	99.7 ± 12.5	159.8 ± 20.0
Conventional: Chisel	35.8 ± 5.9	79.5 ± 13.1	235.1 ± 38.8
Conventional: Disc 2	39.5 ± 11.2	80.7 ± 20.5	149.3 ± 40.3
Conventional: Land plane	13.8 ± 3.9	21.9 ± 6.2	33.4 ± 9.4
Sum for Conventional Method	**109.5 ± 13.5**	**281.9 ± 28.0**	**577.6 ± 60.1**

The use of an elastic lidar system by the University of California at Davis (UC Davis) to examine dust plumes resulting from tillage activities was presented by Holmen et al.[8]. Qualitatively, the constructed system was able to track the plume emitted from the moving source and provide a 2D vertical, downwind map of the plume. It was observed that the plume

[1] Mention of a specific tradename or manufacturer does not imply endorsement or preferential treatment by the USDA-ARS or Space Dynamics Laboratory or Utah State University

heights were often above the point samplers located at 10 m along the downwind plane. The authors suggested that the best fugitive dust sampling procedures would include a combination of elastic lidar and strategically placed point samplers.

Two papers by Holmen et al., both published in 2001, further discuss tillage PM_{10} emission rate investigations by UC Davis using filter-based mass concentration samplers and qualitative measurements from the previously mentioned elastic lidar system [10][11]. The 24 samples labeled as valid were collected from Fall 1996 to Winter 1998 in the San Joaquin Valley during a wide range of environmental (temperature 7-35 °C, relative humidity 20-90%, and from prior to the season's first precipitation to periods between winter storms) and soil moisture conditions (1.5-20%). Tillage operations examined were discing, listing, root cutting, and ripping. Calculated PM_{10} emission rates ranged from 0 to 800 mg/m^2 (0 to 6.9 lb/acre), the mean ± one standard deviation was 152 ± 240 mg/m^2 (1.4 ± 2.1 lb/acre), and the median was 43 mg/m^2 (0.4 lb/acre). One point made by Holmen et al. [11] is that several environmental conditions (e.g., temperature profile, relative humidity, soil moisture) can significantly affect PM emissions and should be monitored and accounted for in emission rate measurement and reporting. As a result, the reliability of direct comparisons of emission rates measured under different environmental conditions must be carefully examined.

The studies published by researchers at UC Davis and herein previously discussed were part of a much larger investigation of agricultural PM_{10} emission rates in the San Joaquin Valley as funded by the U.S. Department of Agriculture Special Research Grant Program. Findings of this broad study are published in Flocchini et al. (2001) [12]. Table 2 presents emission factors published in this study for different types of agricultural tillage along with the crop and time of year. As seen in results measured by Holmen et al., the emission rates reported by Flocchini et al. for agricultural tillage were influenced more by environmental conditions, such as the near-ground temperature profile, relative humidity, and soil moisture, than by the type of crop or equipment used for tilling [11][12].

The California Air Resources Board (CARB) developed area source emission inventory calculation methodologies for agricultural tillage and harvesting operations based on the report by Flocchini et al. [12][13][14]. A summary of the resulting emission factors appears in Table 3. The given unit for the emission factor can be explained as the mass of PM_{10} particles released per acre for each operation, or pass. Specific tillage operations were assigned to one of these five categories and the displayed emission factor was used for all operations in each category.

The U.S. EPA (2001) uses the empirically derived equation shown below to estimate the quantity of particulate matter emitted from all agricultural tilling processes [15].

$$E \quad c_E \times k \times s^{0.6} \times p \times a \tag{1}$$

where E PM emission in lbs, c_E constant 4.8 lb/acre-pass, k dimensionless particle size multiplier (TSP = 1.0, PM_{10} 0.21, $PM_{2.5}$ 0.042), s silt content of surface soil (%), p = number of passes or tillage operations in a year, and a acres of land tilled. The above equation was developed to estimate TSP emissions (k 1.0) and has since been scaled to estimate PM_{10} and $PM_{2.5}$ emissions by using the respective k value. Average values of s are tabulated in Table 4.8-6 in U.S. EPA (2001) as a function of soil type on the soil texture classification triangle [15]. Based on the k values, PM released by tillage operations is dominated by large particles (> 10 μm).

Table 2. Emission factors and uncertainties for land preparation as reported by Flocchini et al. (2001) [12].

Date	Emission Factor (mg/m^2)	Uncertainty		Date	Emission Factor (mg/m^2)	Uncertainty
Stubble Disc						
10/27/1995	257.7	NC		11/6/1998	50.0	146%
11/3/1995	49.3	9%		11/6/1998	28.4	145%
11/3/1995	27.4	470%		11/6/1998	35.0	NC
11/3/1995	231.0	4%		11/6/1998	28.0	10%
11/3/1995	136.7	7%		11/6/1998	117.0	18%
11/3/1995	140.8	6%		11/6/1998	32.4	9%
11/3/1995	286.1	5%		11/6/1998	58.9	8%
11/15/1995	537.9	9%		11/6/1998	93.5	9%
11/15/1995	542.2	125%		11/6/1998	74.2	8%
6/24/1997	430.0	17%				
Finish disc						
11/26/1996	124.3	3%		12/4/1996	9.2	NC
11/26/1996	142.4	4%		12/4/1996	0.6	NC
11/26/1996	97.5	5%		12/4/1996	3.5	NC
12/2/1996	91.0	9%		12/5/1996	-0.5	NC
Ripping/chisel						
6/24/1997	765.0	5%		6/25/1997	331.0	5%
6/26/1997	112.0	5%		6/25/1997	577.0	6%
6/26/1997	776.0	3%				
Root cutting						
11/16/1996	30.0	12%		11/16/1996	36.0	8%

Table 3. Emission factors used by the California Air Resources Board in estimating agricultural tilling PM_{10} emissions [13].

Agricultural Tilling Operation	Emission Factor	
	(lb PM_{10}/acre-pass)	(mg PM_{10}/m^2-pass)
Root cutting	0.3	33.6
Discing, Tilling, Chiseling	1.2	134.5
Ripping, Subsoiling	4.6	515.6
Land Planing Floating	12.5	1401.0
Weeding	0.8	89.7

A comparison between standard tilling practices and conservation tilling (strip-till) in dairy forage production on two farms in the San Joaquin Valley is given by Madden et al. (2008) [16]. Both strip-till and standard till operations were monitored for PM_{10} emissions over two tillage cycles at both farms. Results show that conservation tillage practices reduce PM_{10} emissions from one farm by 86% and 52% for 2004 and 2005, respectively. At the second farm, conservation tillage emissions were reduced by 85% and 93% for 2004 and 2005, respectively. Derived emission rates are presented in Table 4. Madden et al. attribute these reductions, in part, to a reduced total number of passes (from 3-6 passes in standard tillage to 1 pass in conservation tillage) and the ability for conservation tillage operations to be done under a higher soil moisture content than standard operations.

Table 4. Conventional and conservation tillage emission rates reported by Madden et al. (2008) for tillage in a dairy forage crop rotation [16]. ST= standard tillage method, CT = conservation tillage method.

Season/Year	Sweet Haven Dairy		Barcellos Farms	
	Operation	Avg Emission Factor (mg/m^2)	Operation	Avg Emission Factor (mg/m^2)
Spring 2004	ST: 1st discing	198	ST: 1st discing	259
	ST: 2nd discing (w/ roller)	1035	ST: 2nd discing	917
	ST: 3rd discing (w/roller)	114	ST: Listing	615
	ST: Planting	103	ST: Bed discing	25
	CT: Strip-tilling	181	ST: Bed mulching	89
	CT: Planting	26	ST: Ring roller	566
			ST: Planting	96
			ST: Ring roller	104
			CT: Planting	394
Spring 2005	ST: 1st discing	139	ST: 1st discing	51
	ST: 2nd discing (w/ roller)	375	ST: 2nd discing	123
	ST: 3rd discing (w/roller)	404	ST: Circle harrow	337
	ST: Planting	263	ST: Listing	466
	CT: Strip-tilling	180	ST: Bed discing	109
	CT: Planting	385	ST: Bed mulching	384
			ST: Planting	481
			CT: Planting	130

Conventional tillage emissions factors were reported by Wang et al. (2010) and Kasumba et al. (2011) from different field experiments conducted in cotton fields on the same farm in New Mexico [17][18]. Kasumba et al. 2011 reported emission rates from six different discing operation tests, resulting in averages of 154.6 ± 6.9 mg/m^2, 78.3 ± 2.9 mg/m^2, 238.7 ± 8.8 mg/m^2, 89.2 ± 3.7 mg/m^2, 8.4 ± 2.5 mg/m^2, and 68.4 ± 2.3 mg/m^2 where the uncertainty represents the standard deviation (σ) about the average. Wang et al. reported operation average emissions ± 1σ of 12.1 ± 9.7 mg/m^2 for a rolling operation, 210.7 ± 115.3 mg/m^2 for listing, 176.7 ± 77.0 mg/m^2 for planting, 10.4 ± 6.5 mg/m^2 for harvesting, and 44.8 ± 29.3 mg/m^2 and 202.8 ± 79.8 mg/m^2 for discing operations during different years. Wang et al. also developed an empirical relationship relating emissions to soil moisture, silt fraction, crop type, and operation.

Dust concentrations produced by agricultural implements used at a UC Davis research farm were reported by Clausnitzer and Singer (1996) [19]. Personal exposure samplers measuring respirable dust (RD) concentrations--particles that may reach the alveolar region of the lungs when breathed in (with a 50% cut-point diameter of 4 μm)--were mounted on implements in 22 different operations over a seven month period in 1994; replicate samples were collected during 18 operations. Average RD concentrations measured on the implement ranged from 0.33 mg/m^3 for discing corn stubble to 10.3 mg/m^3 for both land planing and ripping operations. While RD concentration was heavily influenced by operation, other factors determined to be significant in dust production were relative humidity, air temperature, soil moisture, wind speed, and tractor speed.

Further investigation of the data set presented by Clausnitzer and Singer (1996) [19] and of another data set collected on a different UC Davis research farm was reported by Clausnitzer and Singer (2000) [20]. Both sets of data focus on RD concentrations as measured on the agricultural implement. The analysis examined environmental influences on the measured concentration. Again, soil moisture and air temperature were found to be significant factors in RD production. The RD production with respect to soil moisture was well fit by a power function, with the curve predicting RD concentrations becoming significantly steeper below 5%. Air temperature was hypothesized to be significant in that it was a surrogate measurement of atmospheric instability: as temperature increases near the surface, the atmosphere becomes less stable and may carry greater quantities of dust upwards.

Baker et al. (2005) examined differences between dust concentrations resulting from standard and conservation tillage practices in the San Joaquin Valley over a two year cotton/tomato crop rotation, each under two different cover crop scenarios: 1) no cover crop and 2) a cover crop forage mixture [21]. Total dust (TD), particles < 100 μm in aerodynamic diameter, and RD samplers were stationed on the implements to collect samples in the plume. For both TD and RD, the presence or lack of a cover crop in the standard till treatment did not seem to affect concentrations. Summed concentrations for conservation tillage without a cover crop were about one-third of standard tillage; for conservation tillage with a cover crop, they were about two-thirds for both dust fractions measured. Reductions in summed concentrations with conservation tillage were attributed to fewer operations, including the elimination of the dustiest (discing and power incorporation). When comparing operations common to all four treatments, tomato planting and harvesting in conservation till produced higher concentrations than standard till (thought to be due to increased organic matter on the surface) and concentrations during cotton harvesting, which does not disturb the soil, were equivalent for all treatments. This study was part of a larger effort to quantify the effects of conservation tillage in California on crop production, soil quality, and time and resources dedicated to production as outlined by Mitchell et al. (2008) and Veenstra et al. (2006) [22][23].

Upadhyaya et al. (2001) compared the Incorpramaster, a one-pass tillage instrument against a conventional combination of discing twice and land planing twice based on fuel consumption, timeliness, and effect on soil [24]. Studies on four experimental fields at UC Davis showed no statistical difference between resulting soil conditions (bulk density changes, soil moisture changes, and aggregate size), but the Incorpramaster used between 19% and 81% less fuel with a mean of 50%. The time savings ranged from 67% to 83% with a mean of 72%. In most cases, two passes with the Incorpramaster were required to achieve the same soil conditions as the four passes in the conventional till.

Three conservation tillage methods were compared in Mitchell et al. (2006) against the standard tillage method in cotton production in terms of yield, yield quality, tractor passes, fuel, and production [25]. A single field near Fresno, CA was divided in area among seven tillage treatments: 1) standard, 2) no till/chop, 3) no till, 4) ridge till/chop, 5) ridge till, 6) strip-till/chop, and 7) strip-till. Prior to both cotton growing seasons examined, a small grain wheat was planted in the field to enhance soil properties; this crop was sprayed with herbicide, and in treatments 2, 4, and 6, it was chopped with a mower prior to tillage activities. In the other treatments (1, 3, 5, and 7), the dead wheat was either incorporated by the tilling or left standing. Yield and yield quality were statistically the same for both years for all treatments, though the standard treatment was numerically higher in both yield and yield quality the 2nd year. Conservation tillage

treatments reduced tractor passes by 41% to 53% over the standard method and estimated fuel reduction was 48% to 62% for the conservation practices. The estimated overall production costs of the conservation tillage systems were 14% to 18% lower than the conventional system. Mitchell et al. estimated, by extrapolation from other work, that whole-tillage process particulate matter emissions would also be decreased.

Particulate matter is released during agricultural tillage activities from both the operational activity of the tillage implement, as well as the tractor in use. Emissions from the tractor mainly originate from the tires kicking up dust from the soil and the combustion engine. Attempts to quantify the PM emitted in agricultural tractor exhaust have been made by the U.S. EPA and the CARB in software designed to estimate off-road engine emissions on a county or regional scale. The U.S. EPA developed the NONROAD software program, with the latest version distributed in 2005 [26]. Emission factors from compression ignition (diesel) engines used in the NONROAD model are calculated by adjusting a zero-hour (ZH), steady-state measured emission factor (EF_{ss}) for engine deterioration with operation time (DF) and a transient adjustment factor (TAF) that accounts for variations from steady-state engine loading and speed, as shown in the following equation [27].

$$EF_{adj(PM)} \quad EF_{ss} \times TAF \times DF - S_{PMadj} \tag{2}$$

where $EF_{adj(PM)}$ is the adjusted PM emission factor and S_{PMadj} is the emission factor adjustment accounting for the use of a diesel fuel with a sulfur content different than the default concentrations; fuel sulfur level is known to affect PM emissions. The units for $EF_{adj(PM)}$, EF_{ss}, and S_{PMadj} are g/hp-hr, where hp stands for horsepower, and TAF and DF are both unitless. All four variables on the right side of Eq. 2 vary with model year and engine size, expressed in horsepower (hp), according to measured values and/or the emission standards each model year and engine size was designed to meet. The selection of values for steady-state emission factors and all the adjustment variables given in U.S. EPA (2004) [27] was performed using a variety of tests and resources, including the Nonroad Engine and Vehicle Emission Study (NEVES) Report [28], or by setting the values such that the adjusted PM emissions were equal to model year-specific emission standards.

The CARB has also developed a model to forecast and backcast daily exhaust emissions from off-road engines, including agricultural tractors, herein called OFFROAD. Similarly to the U.S. EPA's NONROAD model, emission factors (EF) for each engine size and model year are calculated based on a ZH emission rate with a deterioration factor (dr) applied to account for engine wear with use, as in Eq. 3. The derived emission factor is then multiplied by the load factor (Load), the maximum rated average horsepower (AvgHp), and the amount of time the engine is active through the year (Activity) in hr/yr.

$$EF \quad ZH + dr * CHrs \tag{3}$$

$$\text{Emissions} \quad EF * AvgHp * Load * Activity * CF \tag{4}$$

where CHrs is the cumulative engine operation hours, Emissions is the amount of pollutant released in tons/day, and CF is the conversion factor from units of grams per year to tons per day and has a value of 3.02×10^{-9}. The values for the EF and DR are derived from measured values or they are calculated based on requirements to meet the proposed emissions limits for future years [29].

Kean et al. (2000) estimated off-road diesel engine, locomotive, and marine vehicle emissions of NO_x and PM_{10} for 1996 based on fuel sales [30]. Diesel engine exhaust emission factors were developed based on information provided in the development of the U.S. EPA NONROAD off-road vehicle emissions model with supplemental information in order to calculate emissions based on fuel consumption. A fleet-wide average PM_{10} emission factor was determined for farm diesel equipment to be 3.8 g/kg of fuel used, at an average mass per volume of 0.85 kg/L of diesel fuel. Fuel sales surveys from 1996 were used to calculate regional and national emissions. In the off-road category, which includes farm equipment, the U.S. EPA NONROAD model calculated on average 2.3 times higher emissions, which was attributed to higher engine activity assumed in the EPA model than represented in the reported fuel sales data.

An uncertainty analysis was conducted to determine the statistics of the preceding PM_{10} emissions factors reported from measurements. This analysis was performed following the emissions factor dataset analysis technique used by RTI International in "Emission Factor Uncertainty Assessment, Review Draft" [31]. Data points were categorized according to the following tillage operations, with the number of values given in parenthesis: chisel (2), disc (67), land planing (1), listing (8), ripping (5), root cutting (3), standard tillage planting (11), strip-till planting (9), strip-tilling (6), and weeding (15). In cases where a report/paper only provided an average emissions factor, the average value was used only once. RTI International found that two parametric models, the lognormal and Weibull distributions, best fit the analyzed datasets. These same two parametric models were fitted to the tillage operation datasets with eight or more data points. The estimated parameters for these models and the corresponding goodness-of-fit to the available data points, expressed as the root mean square error (RMSE), are given in Table 5 with the better fit model values in bold. Note that a smaller RMSE represents a better fit to the data. The Weibull distribution proved to be a better fit for four out of the five examined datasets. The fits to the disc and weeding datasets were better than that for the remaining three, both visually and based on the RMSE values. Figure 1 presents the histogram for the disc operation dataset and cumulative density functions developed from the data and the Weibull distribution fit to the data. The mean and median values of the fitted Weibull distribution are shown on the cumulative density function line, along with the emissions factor value given by ARB for a disc operation. The ARB emissions factor of 134.5 mg/m^2 is very close to the Weibull distribution median of 136.3 mg/m^2. The emissions factor values corresponding to the 5%, 25%, median, 75%, and 95% levels along the cumulative distribution curve, as well as the average emissions factor, were calculated for the five operations and are presented in Table 6. The 95% level emissions factors for the three operations with poorer fits (i.e., higher RMSE) seem very high; this is likely an artifact of fitting the distributions to a limited number of data points. In this analysis, the better fits were obtained for datasets with $n \geq 15$.

Table 5. Estimated distribution parameters and goodness-of-fit, as root mean square error (RMSE), for the lognormal and Weibull distributions fit to tillage operation datasets with ≥ 8 data points. Values in bold represent model with a better fit.

Operation	*n*	Lognormal			Weibull		
		Mean	σ	RMSE	Scale	Shape	RMSE
Disc	67	4.61	2.18	0.10	**214.1**	**0.82**	**0.04**
Weeding	15	**3.90**	**1.22**	**0.06**	89.3	0.91	0.07
Standard-till Planting	11	3.92	4.45	0.19	**197.0**	**0.58**	**0.13**
Strip-till Planting	9	3.21	4.99	0.17	**143.3**	**0.43**	**0.15**
Listing	8	4.21	5.44	0.23	**366.0**	**0.50**	**0.22**

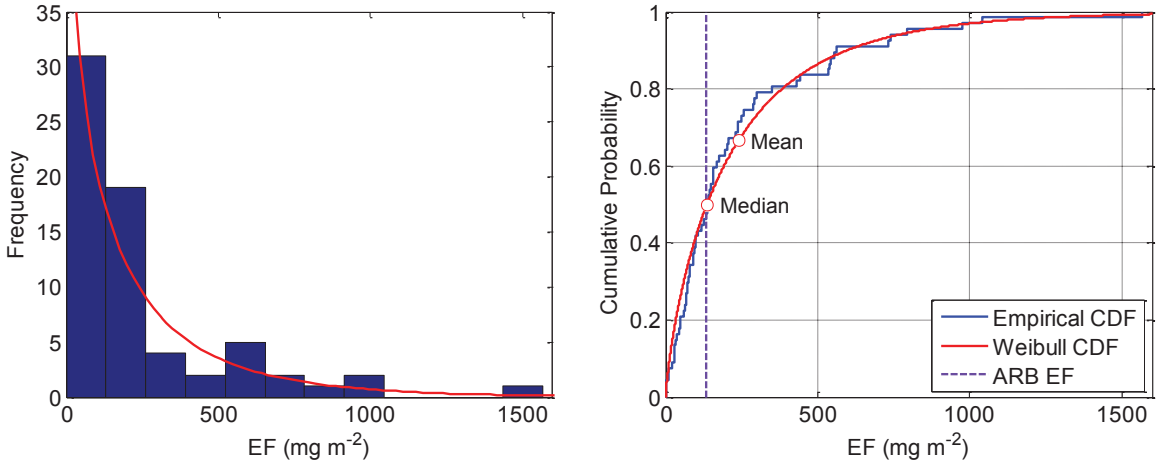

Figure 1. Histogram of disc operation emissions factors and both the empirical and the Weibull cumulative distribution functions (CDFs).

Table 6. Emissions factor values corresponding to statistical measures of interest for the distributions fitted to the various tillage operation datasets.

Operation	Emissions Factor (mg/m^2)					
	5%	25%	Median	Mean	75%	95%
Disc	5.5	46.1	136.3	240.6	320.1	827.1
Weeding	6.5	21.6	49.2	104.1	112.4	368.5
Standard-till Planting	1.2	23.4	105.2	306.8	344.4	1,286.6
Strip-till Planting	0.2	7.9	61.0	396.0	306.5	1,843.4
Listing	1.0	30.7	176.6	724.8	701.0	3,246.4

2. EXPERIMENT DESIGN

2.1 SITE DESCRIPTION

After discussion among stakeholders, regulatory agencies, and researchers, it was collectively determined that the appropriate type of tillage for this experiment would be the tillage sequence following the harvest of a winter wheat crop in preparation for planting of corn. An appropriate site was identified in the San Joaquin Valley of California (see Figure 2) consisting of two adjacent fields. Both fields were cultivated in winter wheat in late 2007 and were to be planted in corn for the 2008 summer growing season. The focus of this study was comparing emissions resulting from the tillage operations in each field. Therefore, no data were collected to make comparisons of other potentially varying characteristics, such as crop yield, soil organic matter, etc., between the two management practices. Tillage management practices are often crop specific and are not appropriate for use in all crop production activities. The effectiveness of CMPs used in other crop systems at reducing PM emissions should be investigated.

An aerial photograph and soil classification map of the experimental site is shown in Figure 3. These data were obtained from the Web Soil Survey (WSS), a website maintained by the USDA Natural Resources Conservation Service (NRCS) [32]. The photo was slightly modified from its original format to reflect current land use, to delineate and label study fields, and to make soil type boundaries and labels more visible. The study fields are outlined and labeled in yellow. The soil type boundaries and labels are in white. The two fields that were used for this experiment are labeled as Field 4 and Field 5. The fields are referred to by these names throughout this experiment and reflect the designation given to them by the landowner. Both Field 4 and Field 5 are rectangular in shape, contain an area of approximately 25 acres and are completely dominated by soil type 130 (Kimberlina fine sandy loam, saline-alkali).

The area immediately surrounding the experiment fields is dominated by agricultural practices. Field 4 has adjacent cultivated cropland on three sides and the fourth side is bounded by an active dairy. Field 5 has adjacent cultivated cropland on two and a half sides and the other side and a half are adjacent to active dairies. Both fields are surrounded on all sides by roads. These roads, with the exception of one, are dirt roads used for field access by farm machinery. The paved road is a heavily travelled, two-lane asphalt road that was downwind of the fields during all measurements. Additionally, railroad tracks are located to the north of this site and two to three trains pass by per day with varying numbers of cars. The crops observed in the area at the time of the experiment were grain, corn, almond orchards and grape vineyards.

The terrain surrounding the fields was relatively flat in all directions. Figure 4 is a photo taken on the southern edge of Field 5 looking across Field 5 and Field 4. The main form of topographical terrain relief was provided by the drainage and irrigation ditches and canals.

2.2 OPERATION DESCRIPTION

The purpose of this field study was to measure and compare the quantity of particulate emissions between the conventional method (of spring tillage between a winter wheat crop and a summer crop of feed corn) and a Conservation Tillage CMP. As described in the Conservation Management Practices Program Report (2006), the conservation tillage CMP "involves using a system in which the soil is being tilled or cultivated to a lesser extent compared to a conventional system" and it is "intended to reduce primary soil disturbance operation such as plowing, discing, ripping, and chiseling".

Figure 2. Shaded relief map of the State of California, USA, with the location of the selected sample site shown by the white star. Image from geology.com [33].

The Conservation Tillage CMP under study is a strip-till method which combines multiple operations to reduce the number of passes required and disturbs the soil only in 8”-wide strips centered every 30” instead of disturbing the entire surface like the plowing, discing, and listing operations of a conventional method. This strip-till method therefore reduces the tilled surface by up to 75% while leaving a lot of the wheat stubble as ground cover in addition to reducing the number of passes. The implement used in this study was the Orthman 1-tRIPr, shown in Figure 5. The level of precision and repeatability required by the strip-till method makes the use of accurate GPS systems a necessity. The cooperating farm has been using the Orthman 1-tRIPr for seedbed preparation on all of its fields for several years with the exception of Field 4 which has continued to be prepared by conventional tillage methods.

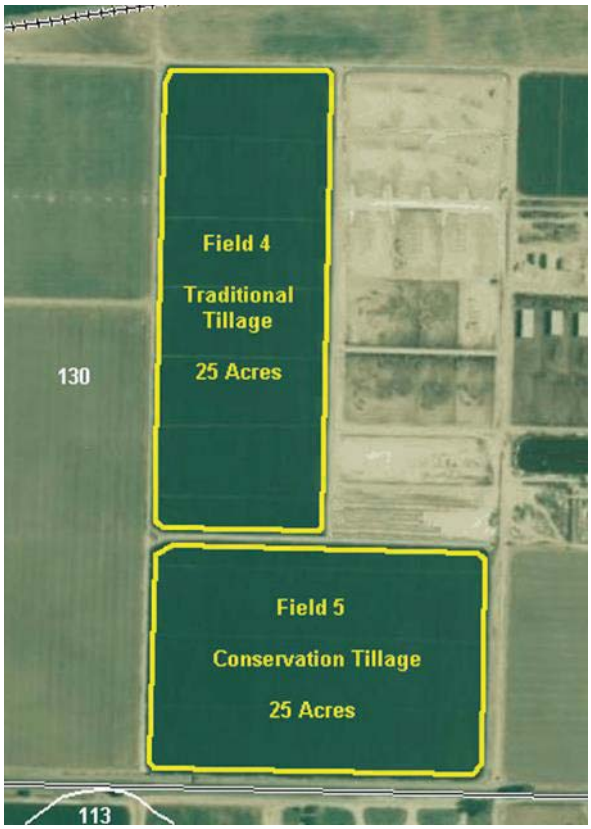

Figure 3. Satellite image of the study location with soil types shown in white. The study fields are outlined within the two rectangles. Soil type 130 represents Kimberlina fine sandy loam, saline-alkali [34].

The conservation tillage CMP applied in this study consisted of three operations totaling three passes across the field, with all three being measured in separate sample periods. In comparison, the conventional tillage method as applied here had nine different operations totaling 13 passes, excluding the building and removal of a ditch and in-field borders, with 12 of them being measured in nine sample periods.

The conventional tillage method was employed in Field 4, and the conservation tillage CMP was used in Field 5. The operations that were performed in each method are shown in order in Table 7, with their corresponding dates. In both the CMP and conventional tillage sequences, ditches and field-edge borders were built and then broken down between 5/20/2008 and 6/5/2008 to allow for flood irrigation of the field prior to planting. Drainage ditches on the east side of both fields returned excess water to the wastewater lagoon of the adjacent dairy. As the ditch and field-edge border construction and removal were not measured in Field 5, the corresponding step for the conventional tillage method was not considered in the total emissions per method. Also, the in-field borders in Field 5 were not broken down and smoothed out, but instead were used for the summer corn crop. The term in-field borders as used here applies to low ridges of soil that separate the field into smaller areas for flood irrigation. Prior to any spring tillage activities, both Fields 4 and 5 had in-field borders running in roughly an east/west direction, with the irrigation water sources located on the west side of the fields. In Field 5 the borders were not broken down, but in Field 4 they were removed and the irrigation water moved from west to east between the ridges in which the corn was planted.

Figure 4. Photo taken standing near the southern edge of Field 5 looking north across Field 5 towards Field 4. Note the relative flatness of the terrain.

The cultivator passes in the conventional tillage sequence function as mechanical weed control, whereas a chemical weed control (herbicide) is used in the CMP sequence. Additionally, the cultivator pass 4 was carried out the day after the cultivator pass 3, but unmovable schedules prevented its measurement. It is assumed, in calculating the total PM emissions, that the emission rates of both passes 3 and 4 were equal. In general, two cultivator passes are done right after the other in opposite directions down the rows to ensure adequate weed control.

The tractors and implements used during all the tillage operations are listed in Table 8 by date and operation. In cases where multiple tractors and implements were used, they are listed in the order of use. A single, handheld GPS unit was used to actively log the tractors' positions over time for each run. During the first part of the lister operation, unharvested plant material along the border lines caused clogging of the lister blades, decreasing its effectiveness. A second tractor with the disc set was brought in to go over the border lines again to further reduce the size of residual plant material. Note that the cultivator passes 1 and 2 and the roller pass were not finished when the planter arrived to begin planting Field 4. Therefore, the first sample period on 6/5/2008 was stopped and the second sample period was started shortly thereafter with the cultivator and roller still operating in the north end of the field – the implement locations in the north end of the field and meteorological conditions likely prevented significant impacts from the cultivator and roller operations on downwind samples.

Field personnel observed operations continually and recorded notes on tractor operation times, potential contamination issues due to traffic on surrounding dirt roads and wind-blown dust, general meteorological observations, etc.

Figure 5. Orthman 1-tRIPr in operation during this field experiment.

Table 7. Tillage operations and dates performed for the comparison study.

Sequence	Operation	Date
Conservation Tillage (Field 5)		
1	Strip-Till	5/17/2008
2	Plant and Fertilize	6/7/2008
3	Herbicide Application	6/11/2008
Conventional Tillage (Field 4)		
1	Break down in-field irrigation borders	5/17/2008
2	Chisel	5/18/2008
3	Disc 1	5/19/2008
4	Disc 2	5/19/2008
5	Lister	5/20/2008
6	Build up ditch and field-edge borders	5/20/2008
7	Break down ditch and field-edge borders, Cultivator passes 1 and 2, and Roller	6/5/2008
8	Plant	6/5/2008
9	Fertilize	6/18/2008
10	Cultivator pass 3	6/25/2008

Table 8. Agricultural equipment used to perform the tillage operations.

Operation	Field # *	Date	Tractor	Implement (1 per tractor)
Strip-till	5	5/17/08	Case MX255	Orthman 1-tRIPr, 6 row, 30 in. spacing
Break down in-field borders	4	5/17/08	Case Puma 195	Custom border buster (2 sets of 3 discs that move soil from center to edges)
Chisel	4	5/18/08	Case MX255	Custom chisel, 13 ft. wide, 22 in. depth, w/ edged roller
Disc 1	4	5/19/08	Case Puma 195	International Offset Disc, 19 ft. wide, pulling a single axle (2 smooth road tires), pulling a 19 ft. wide spiked roller
Disc 2	4	5/19/08	Case Puma 195	International Offset Disc, 19 ft. wide, pulling a single axle (2 smooth road tires), pulling a 19 ft. wide spiked roller
Lister	4	5/20/08	1) Case MX255	Custom lister, 6 row, 38 in. spacing
			2) Case Puma 195	International Offset Disc, 19 ft. wide
Building borders and ditches	4	5/20/08	1) Kubota M8030DT	Custom 1-way ditch digger (2 sets of 3 discs that move soil toward center)
			2) Case 870	Custom border ridger (2 sets of 3 discs that move soil from center to edges)
Break borders and ditches, cultivate, and roll	4	6/5/08	1) Kubota M8030DT	Custom 1-way disc (1 set of 3 discs that move soil from one side to the other)
			2) Case 870	Custom border buster (2 sets of 3 discs that move soil from center to edges)
			3) Case Puma 195	Lilliston Rolling Cultivator, 6 rows wide, 38 in. spacing
			4) Case 2290	Flat roller, 6 rows wide
Planting	4	6/5/08	1) Case Puma 195	Lilliston Rolling Cultivator, 6 rows wide, 38 in. spacing
			2) Case 2290	Flat roller, 6 rows wide
			3) John Deere 4055	John Deere MaxEmerge 2 Row Planter, single row, 6 rows wide, 38 in. spacing
Planting	5	6/7/08	Case MX255	Monosem Twin-Row Planter Model 6x2, 6 rows, 30 in. spacing
Herbicide Application	5	6/11/08	Kubota B-Series	Hardi ATV Sprayer, 40 ft. boom
Fertilizer Application	4	6/18/08	Case 2290	Custom side-dress fertilizer, 6 rows wide, 38 in. spacing, pulling a fertilizer tank (1 axle, 2 small smooth tractor tires)
Cultivator	4	6/25/08	Case 1370	Lilliston Rolling Cultivator, 6 rows wide, 38 in. spacing

* Note: Field 4 = conventional tillage practice, Field 5 = conservation tillage CMP

2.3 TILLAGE OPERATION DATA

Based on field notes and GPS data points, the total tractor run time in tractor hours ($hr_{tractor}$), or the sum of individual tractor operation times, and the total area tilled per day were calculated. This tractor run time only includes times when the tractor was moving and performing the specified operation in the field. The tractor hours we report therefore do not include time the tractor spent motionless in the field with or without an idling engine. Operation delays observed were refueling, implement adjustments, changing equipment, and corrections to the on-board GPS system. The tillage rate (hectares/$hr_{tractor}$) and the operation rate of the tractors ($hr_{tractor}$/hectares) were calculated from the tractor run time and total area tilled. While both fields were 25 acres (10.1 hectares) in area, measurement equipment had to be placed inside of the field edge in Field 5 used for conservation tillage, reducing the monitored area to about 22.4 acres (9.05 hectares). The tractor operation rates were summed to provide the total amount of time per hectare spent preparing the ground for the next crop. All of these data are presented in Table 9. In this study, the tillage rate of the conservation tillage operation was 0.86 $hr_{tractor}$/hectare and the conventional tillage rate was about five times that amount at 4.90 $hr_{tractor}$/hectare.

Table 9. Operation data for both the conventional and conservation tillage studies as recorded by field personnel.

Operation	Date	Total Tractor Time ($hr_{tractor}$)	Total Area worked (hectares)	Tillage Rate (hectares/$hr_{tractor}$)	Tractor Rate ($hr_{tractor}$/hectare)
Conservation Tillage (study area = 9.05 hectares)					
Strip till	5/17	3.05	9.05	2.97	0.337
Plant	6/7	3.82	9.05	2.37	0.422
Herbicide application	6/11	0.93	9.05	9.73	0.103
				Sum	**0.862**
Conventional Tillage (study area = 10.05 hectares)					
Break down borders	5/17	0.92	2.02	2.20	0.455
Chisel	5/18	6.18	8.51	1.38	0.726
Disc 1	5/19	4.83	10.05	2.08	0.481
Disc 2	5/19	4.73	10.05	2.12	0.471
Lister	5/20	5.07	12.48	2.46	0.406
Build ditches	5/20	0.83	0.77	0.93	1.078
Break down ditches, Cultivator passes 1 and 2, & Roller	6/5	7.43	23.86	3.21	0.311
Plant	6/5	3.82	13.21	3.46	0.289
Fertilizer application	6/18	1.08	3.81	3.53	0.283
Cultivator pass 3	6/25	4.02	10.05	2.50	0.400
				Sum	**4.90**

Due to the breaks in tractor run time and variation in the presence of other tractors, the ratio of the sample period length and total tractor operation time was slightly different for each run, as shown in Table 10 below. The difference between total tractor operation time and sample period time is important because the source strength also varies based on how many tractors, if any, are operating at a given time. All calculations of emission rates herein have accounted for these differences in source strength with time, with final emission rates based on time reported as the emission rate of a single tractor.

Table 10. Sample period, total tractor operation time, and the sample period-to-tractor operation time ratio for all sample periods.

Sample	Sample Time (hr)	Total Tractor Time (hr)	Sample time/Tractor time
5/17 Run 1	3.92	3.05	1.29
5/17 Run 2	0.92	0.92	1.00
5/18	6.58	6.18	1.06
5/19 Run 1	4.92	4.83	1.02
5/19 Run 2	5.25	4.73	1.11
5/20 Run 1	3.83	5.07	0.76
5/20 Run 2	1.07	0.83	1.29
6/5 Run 1	7.25	7.43	0.98
6/5 Run 2	2.00	3.82	0.52
6/7	5.33	3.82	1.40
6/11	1.58	0.93	1.70
6/18	2.17	1.08	2.00
6/25	4.25	4.02	1.06

3. MEASUREMENTS AND METHODS

3.1 MEASUREMENT OVERVIEW

A wide variety of air quality and meteorological sampling equipment was employed during this field study. These instruments are described in the following sections along with their functions, data analysis procedures, and calibration verification procedures which were performed before, during, and after the campaign to ensure the accuracy of data collected.

As wind direction and wind speed are important factors in obtaining accurate and representative data from the tillage operations, it was necessary to determine the dominant wind direction for this period of year in the area. Meteorological data from the California Irrigation Management Information System (CIMIS) database were downloaded for May and June of 2005 through 2007 for the Stratford station (#15) [35]. Based on these data, the dominant wind direction for the months of May and June in the area was determined to be from the north to the northwest, as shown in Figure 6.

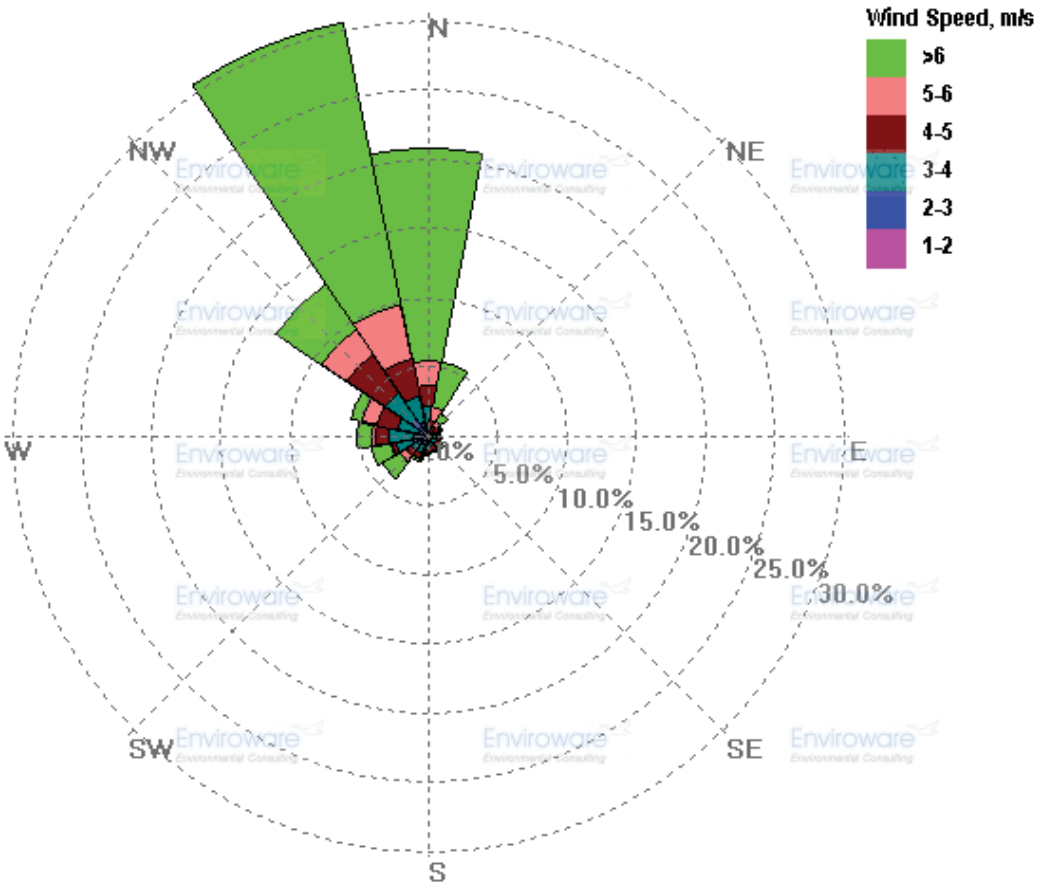

Figure 6. Wind rose for May and June of 2005 - 2007 as recorded by the CIMIS Station # 15 (Stratford). No calm periods were recorded.

Due to the layout of the fields and adjacent dairy, the preferred wind direction for sampling was from the north to northwest. Assuming a northwest wind, instrument deployment was such that samplers meant to measure background aerosol parameters were to the west and northwest of the fields of interest. Samplers meant to measure background plus plume parameters were to the south and east. Similar sample layouts were arranged around each field using the same instruments. Some equipment, such as the lidar and air quality trailers, remained in the same place for samples in both fields while more portable samplers were moved between fields.

The first layout, shown in Figure 7, presents the sample layout for monitoring conventional tillage practices in Field 4. Table 11 summarizes the types of instruments that were located at each site and the dates certain instruments were used if they were not used during the entire study. The greatest deviations in the daily layout occurred during the runs on June 18th and 25th, which are due to the following situations: 1) a separate study of particulate and gaseous emissions from the adjacent dairy was carried out from June 13th to the 20th during the break in tillage operations that required the relocation of most samplers, including both the Aglite lidar and Air Quality trailers; and 2) a failure in the Aglite lidar system on June 19th prevented the lidar from being used in subsequent sample periods. The lidar system was located at position L2 throughout the dairy investigation and for the June 18th sample of the fertilizer application in Field 4.

The sample array arranged to monitor the conservation tillage activities in Field 5 is shown in Figure 8. Table 12 summarizes the type of instruments that were located at each site. In contrast to the sampling changes to measure operations in Field 4, there were not significant deviations from the original sample layout used around this field as all sampling occurred prior to moving equipment for the dairy emissions study.

3.1.1 Meteorological Measurements

A Vantage Pro2 Plus weather station from Davis Instruments, Inc. (Hayward, CA) was used to monitor wind speed, wind direction, temperature, humidity, precipitation, barometric pressure, and solar radiation. It was located on top of the Air Quality sampling trailer, at an approximate height of 5 m above ground level. It was wired to a datalogger and a display panel inside the trailer, which was connected to a computer for data storage.

Two 15.2 m towers were instrumented with 3-cup anemometers (model 12102) at five heights (2.5, 3.9, 6.2, 9.7 and 15.3 m) to measure the vertical wind speed profile. Relative humidity/temperature sensors (Vaisala HMP45C) from Campbell Scientific, Inc. (Logan, UT) were also stationed at five heights (1.5, 2.5, 3.9, 6.2, and 9.7 m) to provide profiles of temperature and relative humidity. A Met One Instruments, Inc. (model 024A, Grants Pass, OR) Wind Vane was stationed at a height of 15.3 m on each tower. Data from each tower were stored as one minute averages on the Campbell Scientific CR23X dataloggers and were downloaded daily.

The eddy covariance (*EC)* instrumentation was comprised of four Campbell Scientific Inc. (Logan, UT) 3D sonic anemometers (CSAT) and four LiCOR 7500 infrared gas analyzers (IRGA). The sensor separation for all four *EC* systems was 10 cm. All data were stored on to a Campbell Scientific data logger (CR5000). Together the CSAT and LiCOR measured water vapor (q) and carbon dioxide (c) concentrations, and velocity components of the wind flow in three spatial dimensions: x, y, and z. These measurements were made at a scan rate of 20 Hz, 20 measurements per second for u, v, w, q and c. Each EC instrumentation group was visited daily

between 06:00-07:00 hours for maintenance. Maintenance performed included exchanging compact flash cards for data storage on the CR5000, sensor interrogation at the data logger screen to evaluate measurement status, cleaning dust from the surface of the IRGA lens with de-ionized water, and removing spider webs from the transducer arms.

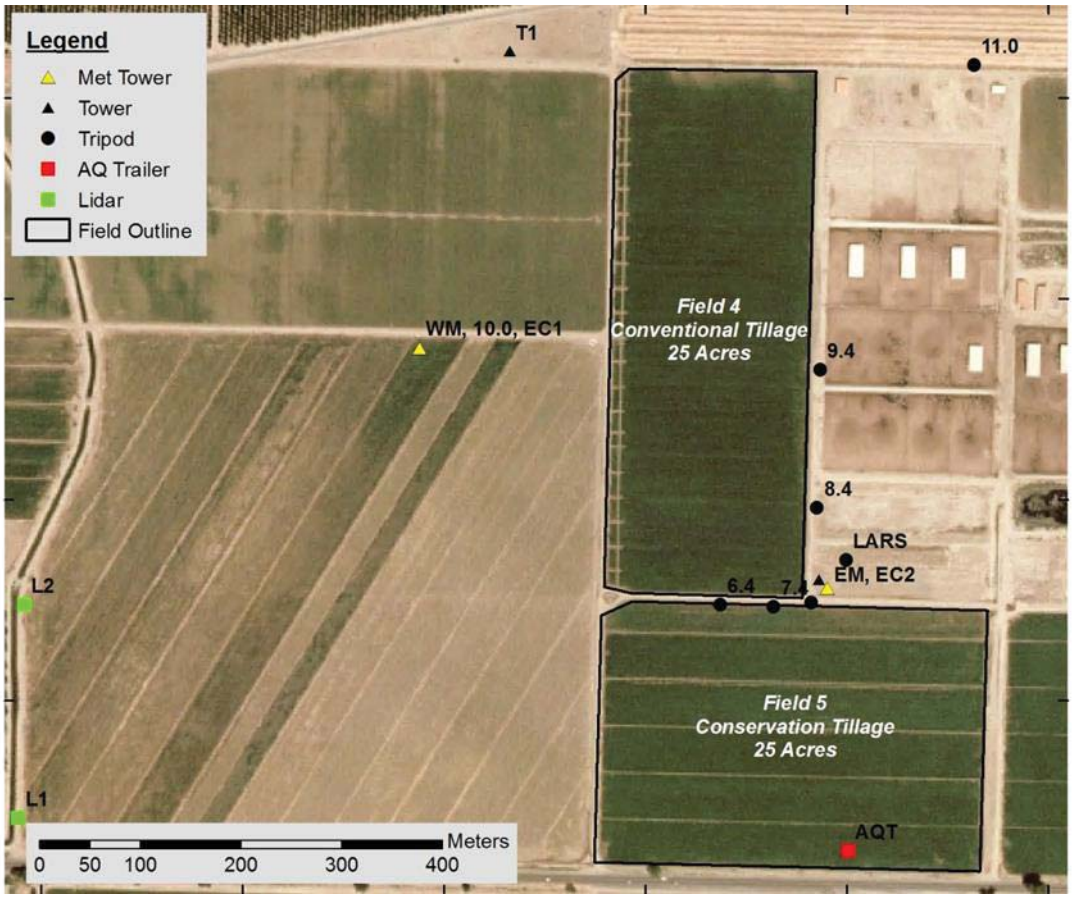

Figure 7. Sample layout used for Field 4.

Table 11. Summary of instruments located at each position for the conventional tillage study of Field 4. All heights given as above ground level (agl).

Instrument Location	Description
T1	1 - 10 m tower 1 - OPC: 1 @ 9 m 3 - MiniVols: 3 @ 9 m (TSP, PM_{10} and $PM_{2.5}$)
T2	1 - 10 m tower 1 - OPC: 1 @ 9 m 3 - MiniVols: 3 @ 9 m (TSP, PM_{10} and $PM_{2.5}$)
WM	1 - 15 m tower 5 - cup anemometers: 1 each @ 2.5, 3.9, 6.2, 9.7 and 15.3 m 1 - wind vane: 1 @ 15.3 m 5 - temp/RH sensors: 1 each @ 1.5, 2.5, 3.9, 6.2, and 9.7 m 2 - Campbell Scientific dataloggers 1 - sonic anemometers: 1 @ 11.3 m 1 - energy balance systems: 1 @ 2 m

Instrument Location	Description
EM	1 - 15 m tower 5 - cup anemometers: 1 each @ 2.5, 3.9, 6.2, 9.7 and 15.3 m 1 - wind vane: 1 @ 15.3 m 5 - temp/RH sensors: 1 each @ 1.5, 2.5, 3.9, 6.2, and 9.7 m 2 - Campbell Scientific dataloggers 1 - sonic anemometers: 1 @ 11.3 m 1 - energy balance systems: 1 @ 2 m 2 - OPCs: 1 @ 9 m, 1 @ 14.5 m
L1	1 - Lidar data collection system (5/14 - 6/11) 1 - Davis met station for lidar operator's reference
L2	1 - Lidar data collection system (6/18) 1 - Davis met station for lidar operator's reference
EC1	1 - Campbell Scientific CSAT @ 1.6 m 1 - LiCOR IRGA @ 1.6 m
EC2	1 - Campbell Scientific CSAT @ 2.9 m 1 - LiCOR IRGA @ 2.9 m
EC3	1 - Campbell Scientific CSAT @ 1.6 m 1 - LiCOR IRGA @ 1.6 m
2.4	1 - 2 m tripod 1 - OPC: 1 @ 2 m 3 - MiniVols: 3 @ 2 m (TSP, PM_{10} and $PM_{2.5}$)
6.4	1 - 2 m tripod 2 - MiniVols: 2 @ 2 m (PM_{10} and $PM_{2.5}$)
7.4	1 - 2 m tripod 1 - OPC: 1 @ 2 m 2 - MiniVols: 2 @ 2 m (PM_{10} and $PM_{2.5}$)
8.4	1 - 2 m tripod 2 - MiniVols: 2 @ 2 m (PM_{10} and $PM_{2.5}$)
9.4	1 - 2 m tripod 2 - MiniVols: 2 @ 2 m (PM_{10} and $PM_{2.5}$)
10.0	1 - 2 m tripod (5/18 - 6/11) 1 - OPC: 1 @ 2 m 3 - MiniVols: 3 @ 2 m (TSP, PM_{10} and $PM_{2.5}$)
11.0	1 - 2 m tripod (6/18, 6/25) 1 - OPC: 1 @ 2 m 3 - MiniVols: 3 @ 2 m (TSP, PM_{10} and $PM_{2.5}$)
12.0	1 - 2 m tripod (6/25) 1 - OPC: 1 @ 2 m 3 - MiniVols: 3 @ 2 m (TSP, PM_{10} and $PM_{2.5}$)
LARS	1 - OPC: 1 @ 2.8 m
AQT	1 - OPC: 1 @ 5 m 3 - MiniVols: 3 @ 5 m (TSP, PM_{10} and $PM_{2.5}$) 1 - Davis met station: 1 @ 5 m 1 - OC/EC Analyzer: 1 inlet @ 4.5 m 1 - AMS: 1 inlet @ 4 m 1 - radio and laptop for OPC Data collection ***Note:*** *The Air Quality Trailer was in the position indicated on the map for the tillage practices that occurred from 5/17/2008 through 6/11/2008. For the two remaining runs on 6/18/2008 and 6/25/2008 the Air Quality Trailer was in a different location and the analysis equipment were either not used or located in a different downwind position.*

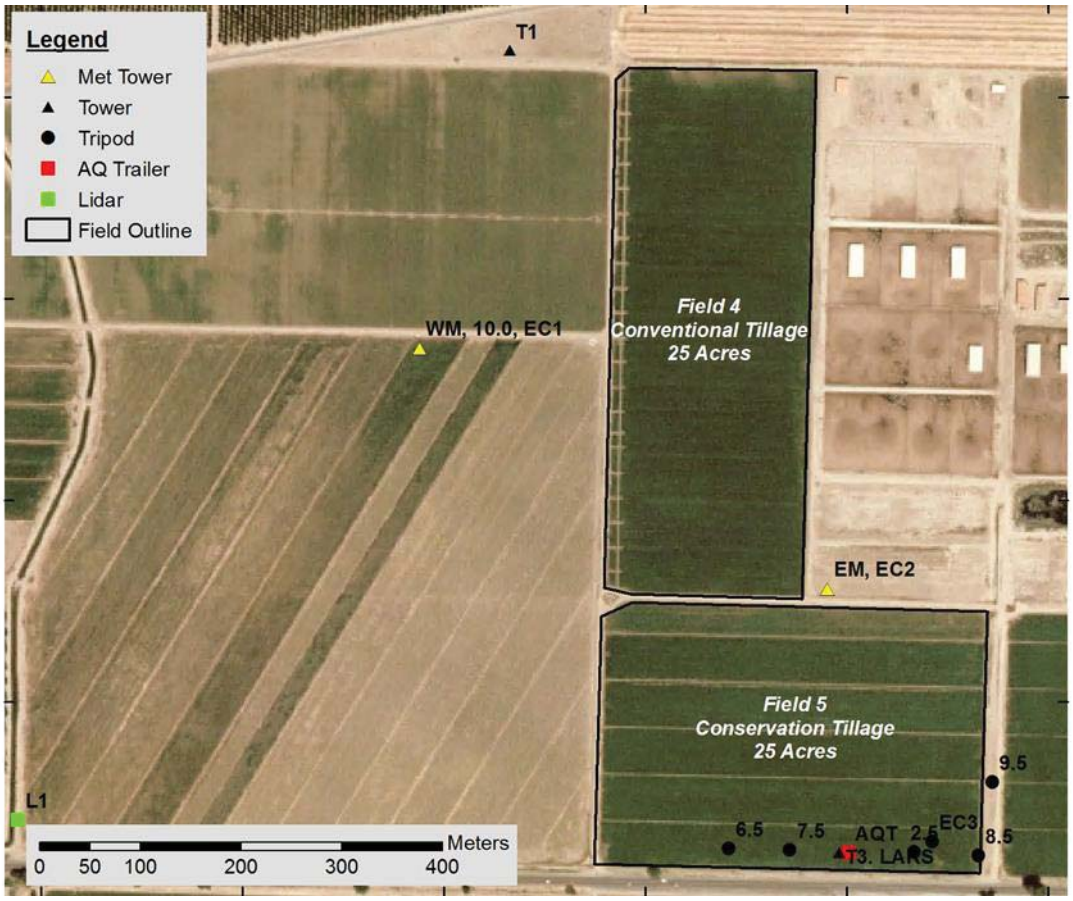

Figure 8. Sample layout used for Field 5.

Table 12. Summary of instruments located at each position for the Conservation tillage study of Field 5. All heights given as above ground level (agl).

Instrument Location	Description
T1	1 - 10 m tower 1 - OPC: 1 @ 9 m 3 - MiniVols: 3 @ 9 m (TSP, PM_{10} and $PM_{2.5}$)
T2	1 – 10 m tower 1 – OPC: 1 @ 9 m
T3	1 - 10 m tower 1 - OPC: 1 @ 9 m 3 - MiniVols: 3 @ 9 m (TSP, PM_{10} and $PM_{2.5}$)
WM	1 - 15 m tower 5 - cup anemometers: 1 each @ 2.5, 3.9, 6.2, 9.7 and 15.3 m 1 - wind vanes: 1 @ 15.3 m 5 - temp/RH sensors: 1 each @ 1.5, 2.5, 3.9, 6.2, and 9.7 m 2 - Campbell Scientific dataloggers 1 - sonic anemometers: 1 @ 11.3 m 1 - energy balance systems: 1 @ 2 m

EM	1 - 15 m tower 5 - cup anemometers: 1 each @ 2.5, 3.9, 6.2, 9.7 and 15.3 m 1 - wind vanes: 1 @ 15.3 m 5 - temp/RH sensors: 1 each @ 1.5, 2.5, 3.9, 6.2, and 9.7 m 2 - Campbell Scientific dataloggers 1 - sonic anemometers: 1 @ 11.3 m 1 - energy balance systems: 1 @ 2 m 2 - OPCs: 1 @ 9 m, 1 @ 14.5 m
L1	1 - Lidar data collection system 1 - Davis met station for lidar operator's reference
EC1	1 - Campbell Scientific CSAT @ 1.6 m 1 - LiCOR IRGA @ 1.6 m
EC2	1 - Campbell Scientific CSAT @ 2.9 m 1 - LiCOR IRGA @ 2.9 m
EC3	1 - Campbell Scientific CSAT @ 1.6 m 1 - LiCOR IRGA @ 1.6 m
2.5	1 - 2 m tripod 1 - OPC: 1 @ 2 m 3 - MiniVols: 3 @ 2 m (TSP, PM_{10} and $PM_{2.5}$)
6.5	1 - 2 m tripod 2 - MiniVols: 2 @ 2 m (PM_{10} and $PM_{2.5}$)
7.5	1 - 2 m tripod 1 - OPC: 1 @ 2 m 2 - MiniVols: 2 @ 2 m (PM_{10} and $PM_{2.5}$)
8.5	1 - 2 m tripod 2 - MiniVols: 2 @ 2 m (PM_{10} and $PM_{2.5}$)
9.5	1 - 2 m tripod 2 - MiniVols: 2 @ 2 m (PM_{10} and $PM_{2.5}$)
10.0	1 - 2 m tripod (6/7 – 6/11) 1 - OPC: 1 @ 2 m 3 - MiniVols: 3 @ 2 m (TSP, PM_{10} and $PM_{2.5}$)
LARS	1 - OPC: 1 @ 2.8 m
AQT	2 - OPC: 2 @ 5 m 3 - MiniVols: 3 @ 5 m (TSP, PM_{10} and $PM_{2.5}$) 1 - Davis met station: 1 @ 5 m 1 - OC/EC Analyzer: 1 inlet @ 4.5 m 1 - AMS: 1 inlet @ 4 m 1 - radio and laptop for OPC Data collection

3.1.2 Wind Profile Calculations

Wind profiles near the ground surface were calculated based on one-minute averaged wind speed data from the logarithmically spaced cup anemometers on the 15 m meteorological tower at the WM location, which was the meteorological tower located upwind/crosswind of both tillage sites. A power law wind speed profile fit to the tower data was extrapolated up to 250 m to estimate the wind speed at higher elevations. The power law for calculating wind speed (u_2) at height z_2 based on a measured wind speed (u_1) at height z_1 is shown in Eq. 5 from Cooper and Alley (2002) [36].

$$\frac{u_2}{u_1} = \left(\frac{z_2}{z_1}\right)^p \tag{5}$$

where wind speeds are in m/s, height is in meters, and p is a unitless coefficient that varies based on atmospheric stability and surface roughness. The approximate value of p is 0.5 for very stable conditions and 0.15 for very unstable conditions.

An error in the code used to calculate the one-minute average wind directions from the wind vane at the top of the meteorological towers (15.3 m) was discovered in post-processing of the data taken during the 2007 fall tillage CMP study [7]. For both the 2007 fall tillage and the 2008 spring tillage datasets, one-minute averaged horizontal wind directions calculated from the sonic anemometer data were used in subsequent analyses. The wind direction measured by the sonic anemometer was applied to the entire wind speed profile. For most sample periods, wind profiles above 150 m were not required for the lidar emission rate calculations. Averaged horizontal wind speed data from the sonic anemometer (11.3 m agl) on N Met were compared with the nearest cup anemometer (9.7 m agl) wind speed measurements as a quality check. Both data sets showed the same patterns and recorded wind speeds were close (< 0.25 m/s difference), with the observed difference likely due to a combination of vertically separated sample heights and instrument error.

3.1.3 Soil Characterization

Soil characterization involved collecting soil samples for analysis of bulk density, soil moisture, and sand/silt/clay content. Bulk density samples were collected in each field prior to tillage operations. A manual device consisting of a 7.6 cm-diameter and 7.6 cm-deep cylinder was hand driven into the soil until the top of the cylinder was level with the soil surface. Samples were removed and placed into pre-weighed cans. Post-weights were performed in the field for determination of wet weight. All weights were determined using a Mettler balance (Columbus, OH), Model PM2000.

Samples for soil moisture were taken for each day of operation at random locations in the field and collected in pre-weighed cans 7 cm in diameter and 4 cm deep. Samples were collected immediately prior to the tillage period or shortly after commencement in areas that had not been tilled. The can was pushed into the soil approximately 3cm then removed. The can was closed and weighed in the field for determination of wet weight.

All soil samples were dried at the Agricultural Research Service (ARS) National Laboratory for Agriculture and the Environment (NLAE) in Ames, IA at a temperature of 105 °C until a constant weight was achieved (~60 hours). Samples were then weighed to determine dry weight. Calculations for soil moisture and bulk density were performed according to the following equations as found in Doran and Jones 1996 [37].

$$\text{field water content (\%)} = \frac{\text{weight of moist soil} - \text{weight of oven dried soil}}{\text{weight of oven dried soil}} \times 100 \quad (6)$$

$$\text{\% moisture} = \frac{\text{weight of moist soil} - \text{weight of oven dried soil}}{\text{weight of moist soil}} \times 100 \quad (7)$$

$$\text{bulk density} = \frac{\text{weight of moist soil} \times (1 - \text{field water content})}{\text{volume of soil collected}} \quad (8)$$

where "volume of soil collected" = π x radius^2 x length of cylinder = π x 3.81^2 x 7.62 = 347.3 cm^3 and "field water content" is the value given by Eq. 6 expressed as a fraction.

A composite was made of all the samples collected. It was analyzed for the percent of sand, silt, and clay according to the Hygrometer Procedure, as given in Soil Sampling and Methods of Analysis (1993) [38]. The percent of stable aggregates was also determined from the composite sample according to the Dry-Sieve Method, as given in the Soil Sampling and Methods of Analysis (1993) [39].

3.1.4 Air Quality Point Samplers

The suite of air quality point samplers deployed around the tillage plots to quantify both the ambient and ambient plus operations emissions values were summarized in Table 11 and Table 12. Details of each of these sensors and their data processing methods are presented below.

3.1.4.1 MiniVol Portable Air Sampler

Twenty-four MiniVol Portable Air Samplers (Airmetrics, Eugene, OR) were distributed to gravimetrically measure the time-averaged mass concentrations of aerosols at multiple locations surrounding the fields of interest. The MiniVol is a battery operated, ambient air sampler that gives results that closely approximate air quality data collected by a Federal Reference Method (FRM) PM sampler [40][41]. The MiniVol is neither designated as an FRM nor a Federal Equivalency Method (FEM) by the EPA, and results should be considered as approximate measures of PM. The sampler draws air through a particle size separator, or impactor head, and then through a filter medium [42]. The photo in Figure 9 shows MiniVols mounted on a rechargeable battery pack with attached impactor sample heads deployed during the reported study.

Particulate concentrations in the PM_{10} and $PM_{2.5}$ size fractions were measured using impactor heads for size separation based on aerodynamic diameter, while Total Suspended Particulate (TSP) was measured with the impactor head removed. Each PM sampler was assigned to sample a specific size fraction at a specific location throughout the study, with location changes made as deemed necessary. Clusters of three PM samplers were assigned to four locations, two upwind and two downwind, in order to provide size fractionated, mass-based particle loading distributions.

Figure 9. Two Airmetrics MiniVol Portable Air Samplers and a Met One Instruments Optical Particle Counter (OPC) deployed for field sampling during Spring 2008 tillage study.

Filters used in the PM samplers were pre-conditioned according to the protocols outlined in 40 CFR 50 Appendix J before obtaining pre- and post-sample filter weights. Final average weights were found using a Mettler Toledo Microbalance, Type MT5 located at the Utah Water Research Laboratory (UWRL) in Logan, UT to determine three stable weights within ± 5 µg, measured on different days. Filters were transported to and from the site and stored on-site in dessicators to maintain filter conditioning. Flow calibrations on each MiniVol were performed using a slant manometer prior to the study and the actual sample flow was adjusted daily on each instrument in order to maintain the required 5.0 L/min for accurate particle size separation.

During this study it was found that the $PM_{2.5}$ and PM_{10} impactor heads were being overloaded with particulates due to high wind conditions and extremely high ambient particle loading. Therefore, for June sample periods, we installed a PM_{10} impactor in series with a $PM_{2.5}$ impactor to serve as an additional filter. These efforts are described more fully in Appendix B.

3.1.4.2 Optical Particle Counter

Ten Optical Particle Counters (OPCs), Model 9722 from Met One Instruments, Inc. (Grants Pass, OR), were collocated with MiniVols in order to describe the particle count and size distribution at locations measuring background aerosols and those locations measuring background plus plume aerosols. Figure 9 shows a Met One OPC collocated with MiniVols for sampling in Field 5. The 9722 particle counter uses scattered light to size and count airborne particles. Particle counts are reported in eight, user-defined channels over a user-defined sample time. For this study, the OPCs collected samples continuously at a sample time of 20 seconds with the following channel sizes, in units of µm: (1) 0.3-0.5, (2) 0.5-0.6, (3) 0.6-1.0, (4) 1.0-2.0,

(5) 2.0-2.5, (6) 2.5-5.0, (7) 5.0-10.0, and (8) >10.0. The data from each OPC were relayed to a single computer over a custom radio network for storage. Inlet flows for individual OPCs were measured on-site before and after the experiment using a Gilian Gilibrator2 Calibration System, a volumetric flow meter. The average of the averages from each flow measurement period was used as the sample flow throughout the field study.

Calibration of OPC particle counts was performed for each sample day in post-campaign analysis. For this calibration, careful examination of the number concentration (number of particles/m^3) time series yielded a time period before or after the tillage operation during which no plumes were detected. Number concentration was chosen as the calibration point, as opposed to the raw particle count data, because it normalizes the raw particle counts by sample flow (see Eq. 10); sample flow varies up to 20% between OPCs. The average number concentration (N_{ij}) per bin (i) for the designated calibration time for each OPC (j) was calculated, and the mean of the averages ($\breve{N}_i$) was used as the calibration concentration. A scalar correction, Counting Correction Factor (CCF_{ij}), was applied to each bin (i) of each OPC (j) and was calculated for each collocated run based on the calibration concentration for that bin according to the following equation:

$$CCF_{ij} \quad \frac{\breve{N}_i}{N_{ij}} \tag{9}$$

Number concentration (N_{ij}) is a function of raw particle counts (p_{ij}), the measured average flow rate (q_j), the sample time (t_j), and the CCF_{ij}, as shown in Eq. 10.

$$N_{ij} \quad \frac{p_{ij} \times CCF_{ij}}{q_j \times t_j} \tag{10}$$

where the units for each variable are N number/cm^3, p_i number, q_j = cm^3/min, t minutes, and CCF is unitless. As in Eq. 9, the subscript j represents a specified OPC.

The volume concentration of aerosols based on a number concentration N is calculated based on the following assumptions: 1) the particles are spheres, 2) the maximum particle diameter measured is 20 µm, and 3) the geometric mean particle diameter per bin (GMD_i) is representative of the particles in a given bin i with the assumption of a log-normal distribution of particle numbers. The GMD_i is calculated by Eq. 11.

$$GMD_i \quad \sqrt{d_{i,upper} \times d_{i,lower}} \tag{11}$$

where $d_{i,upper}$ and $d_{i,lower}$ are the diameters of the upper and lower ranges for bin i. The assumption of a maximum measured particle diameter must be made in order to calculate the GMD for channel 8, which counts particles > 10 µm.

The cumulative volume concentration of aerosols (V_k) up to a particle diameter k may be calculated using the following equation:

$$V_k \quad \frac{\pi}{6}\int_0^{d_k} N(\mathrm{d})\mathrm{d}^3 d\mathrm{d} \tag{12}$$

where N(d) is the number concentration at diameter d. For application to the OPC data, Eq. 12 is expressed in the following terms that have been previously defined:

$$V_k \quad \frac{\pi}{6}\sum_{i=1}^{\mathrm{GMD}_i \le d_k} \mathrm{GMD}_i^3 N_i \tag{13}$$

where GMD_i is expressed in μm, N_i is in number/cm^3, and V_k is in units of μm^3/cm^3. In this case, the V_k definition is similar to PM_k concentrations: the fraction of the total volume of particles whose diameter, in μm, is ≤ k = 1, 2.5, 10, and ∞ for TSP.

By collocating PM samplers and OPCs, the data provide information about the relationship between optical and aerodynamic measurements and allow direct calibration of optical instruments (both OPC and lidar) to mass concentration instruments by estimation of the mass conversion factor (MCF) for each $\mathrm{PM_k}$ fraction. The theoretical conversion from particulate volume concentration to mass concentration is complex, and several simplifying assumptions must be made. These include a spherical particle shape approximation, *a priori* assumption of the refractive index, and neglecting multiple scattering effects. The time-resolved V_k data from each OPC as calculated in Eq. 13 are then averaged over the corresponding PM sampler sample time. The MCFs, in units of density (g/cm^3), for each PM size fraction k are calculated by dividing the mass concentrations measured by the PM samplers ($\mathrm{PM_k}$) by the time-averaged V_k. These data are averaged over several locations or instrument clusters j, where $\Sigma j = n$, and both a daily mean value and an overall mean value of the MCF_k is calculated for each PM_k fraction separately.

$$MCF_k \quad \frac{1}{n}\sum_{j=1}^{n} \frac{PM_{j,k}}{V_{j,k}} \tag{14}$$

The aerosol number size distribution ($dN/d(ln(\mathrm{d}))$) is calculated as outlined in Hinds [43] and expressed mathematically in Eq. 15.

$$dN/d(\ln(\mathrm{d})) \quad \frac{N_i}{\ln(\mathrm{d}_{i,upper}) - \ln(\mathrm{d}_{i,lower})} \tag{15}$$

where $\mathrm{d}_{i,upper}$ and $\mathrm{d}_{i,lower}$ are the diameters of the upper and lower ranges of bin i.

3.1.4.3 Organic Carbon/Elemental Carbon Analyzer

An Organic Carbon/Elemental Carbon Analyzer (OC/EC), Model 5400 from Rupprecht and Patashnick Co., Inc. (Albany, NY), was located in the Air Quality Trailer (AQT) on the downwind borders of Field 5. This instrument provides sample-averaged organic carbon and elemental carbon mass concentrations over a user-defined sample time, which was set at one hour for this study. In operation, the system alternately collects particulate matter onto one of two ceramic filters which, after the desired collection period, are heated within a closed-loop system to determine carbon content via direct thermal desorption and pyrolysis techniques developed and validated by Rupprecht and Patashnick [44]. As recommended by the manufacturer, during the analysis phases, an initial temperature plateau of 250° C for 600 seconds was used for determination of the organic carbon (OC) fraction and a final temperature

plateau of 750° C was used for quantification of the elemental carbon (EC) fraction. To account for non-carbon components of the organic compounds' mass, the OC concentrations reported by the 5400 analyzer were increased by the recommended multiplier of 1.7 [45]. A sharp-cut $PM_{2.5}$ cyclonic separator was placed at the inlet, which was located directly above the instrument on top of the trailer. A nominal flow rate of 16.7 Lpm was maintained through the system by on-board mass flow controllers and integral temperature and pressure sensors.

The 5400 instrument successfully passed the flow checks, leak checks, and CO_2 audits as prescribed by its manual the week prior to departure for the field campaign [44]. The instrument passed these same checks upon setup in the field on May 13, 2008. It passed CO_2 audits administered in the field on June 3 and June 21, 2008.

3.1.4.4 Ion Chromatographic Analysis

To more fully chemically characterize the nature of the upwind and downwind particulate matter, ion chromatographic (IC) analysis was performed on filters collected via the MiniVol systems that were collocated with the EC/OC inlet on top of the Air Quality Trailer (AQT). After final post-test weights were determined from the filters at the UWRL, the chosen filters were sonicated with triplicate rinses in 10 mL double-distilled, de-ionized water (DDI) and split into two aliquots of approximately 15 mL each for separate anion and cation analysis. The anion analysis occurred within 48 hours of sonication and the cation aliquots were stabilized with 10 µL of 0.5 M HCl acid and analyzed within 28 days of sonication. The base IC system (Dionex Corporation) utilized an AS 40 (Automated Sampler), a CD 20 (Conductivity Detector), a GP 40 (Gradient Pump), and a membrane suppressor. Cation quantification was accomplished using an IonPac® CS12A cation column, a CG12A cation guard column, and a 500 µL sample loop. The system eluent was 0.15 M H_2SO_4 with a 1.0 mL/min flow. Anion concentrations were determined using an IonPac® AS11HC anion column, a AG11HC anion guard column, and a 188 µL sample loop. For anions, the system eluent was 30 mM NaOH with a 1.0 mL/min flow. American Chemical Society (ACS) reagent grade materials were used to prepare stock standard solutions for each of the target ions, from which concentrations of 0.5, 1.0, and 5.0 mg/L (ppm) were mixed to make IC calibration curves. The ions quantified were fluoride (F^-), chloride (Cl^-), nitrite (NO_2^-), sulfate (SO_4^{-2}), nitrate (NO_3^-), sodium (Na^+), ammonium (NH_4^+), potassium (K^+), magnesium (Mg^{+2}), and calcium (Ca^{+2}). Verifications of the system calibrations were performed prior to each analysis run. Continuing calibration verification standards (CCVs) and blank samples (DDI water) were analyzed roughly every 10 samples. Peak identification and data processing were executed using Dionex PeakNet Data Chromatography software (Version 2.0).

3.1.4.5 Aerosol Mass Spectrometer

An Aerosol Mass Spectrometer (AMS) from Aerodyne Research, Inc. (Billerica, MA) was located in the sampling trailer, with a sample port on the upwind side of the trailer just below the roof level (~3 m). The AMS provides chemical composition and particle size information for volatile and semi-volatile particle components in the 0.1 - 1.0 µm size ranges in vacuum aerodynamic diameter. Hence, it is nominally considered a PM_1 instrument for the fraction of chemicals detected. An AMS size calibration was conducted on-site on May 14 using polystyrene latex spheres (PSLs). Mass calibrations were also conducted on-site on May 14 and June 4, 2008 using ammonium nitrate. The AMS vaporizer was operated at higher than normal temperature (~800 ºC vs. ~600 ºC) to detect some of the inorganic components in dust particles.

During sampling, the AMS integrated and saved particle composition and size data every ten minutes.

3.1.5 Lidar Aerosol Measurement and Tracking System

The Aglite lidar system is a monostatic laser transmitter and 28-cm receiver telescope (Figure 10). The laser is a three-wavelength, 6W, Nd:YAG laser, emitting at 1.064 (3W), 0.532 (2W) and 0.355 (1W) μm with a 10 kHz repetition rate. The lidar utilizes a turning mirror turret mounted on the top of a small trailer to direct the beam -10° to + 45° vertically and ± 140° horizontally. Lidar scan rates from 0.5° – 1°/s are used to develop the 3D map of the source(s), dependent on range and concentration of the aerosol.

The process used to retrieve aerosol mass concentration from lidar data is illustrated in Figure 11. The details of Aglite lidar calibration and the aerosol retrieval process are discussed by Marchant [46] and Zavyalov [47]. The retrieval is as follows: first, the lidar data is preprocessed. Then, the relationships between backscatter, extinction, volume concentration, and mass concentration of the aerosol components are established using *in-situ* data measured by OPCs and clusters of PM samplers with different separation heads (PM_k). After that, the inversion of the lidar data is performed using a form of Klett's solution [48] for two scatterers where extinction is proportional to backscatter. Finally, a least-squares method is used to convert backscatter values to aerosol mass concentration using the previously established relationships.

From the OPC channel counts, the particle size distribution at a single point as a function of time may be calculated according to Eq. 15. The backscatter and extinction coefficients necessary for solving the lidar equation are then calculated at the OPC reference point as a function of time. Klett's inversion is used to convert the lidar signal to the optical parameters (backscatter values in particular) of particulate emitted by the operation [48]. Having recovered backscatter values as a function of range and wavelength using the Klett inversion, these must be converted to the

Figure 10. The three wavelength Aglite lidar at dusk, scanning a harvested wheat field.

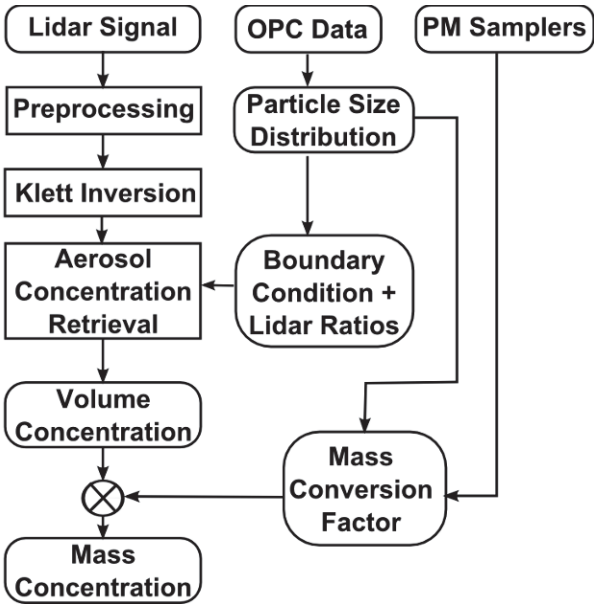

Figure 11. The Aglite lidar retrieval algorithm flow chart, showing the input locations for the in situ data.

aerosol cumulative volume concentration. Expressing the particle normalized backscatter values from the OPC ($\boldsymbol{\beta}_v$) and the lidar measured backscatter values ($\boldsymbol{\beta}_E$) in a vector form, and applying the Moore-Penrose weighted minimum least-squares solution results in the value for $n(r)$, the relative amplitude of the aerosol component to total atmospheric backscatter, at range r

$$n(r) \quad \frac{\tilde{\beta}_v^T W \beta_E(r)}{\tilde{\beta}_v^T W \beta_E} \tag{16}$$

which can be multiplied by the particle normalized volume concentration vector, resulting in the $\mathbf{V}_k(r)$:

$$V_K(r) \quad \tilde{V}_E n(r) \tag{17}$$

The term **W** is a diagonal weighting matrix, whose diagonal elements are the expected variance of the emission backscatter for the corresponding channel.

The retrieved aerosol volume concentration from the lidar return signal is multiplied by the MCF_k, which was previously calculated using *in-situ* data (Eq. 14). At this point, the kth fraction of the aerosol mass concentration of the emission component is known as a function of distance.

$$PM_K(r) \quad MCF_K \cdot V_K(r) \tag{18}$$

The concept behind our flux measurement approach is shown in Figure 12A, where the facility is treated as one would calculate the source strength in a bioreactor. In this simplified mass-balance approach, the source strength is determined using the mean flow rate through the reactor and the difference in reactive species concentration entering and leaving the vessel. The scanning lidar samples the mass concentration fields entering and leaving the facility and standard cup anemometers provide the mean wind speed profile. If we define our box large enough so that none of the emitted material escapes through the top or crosswind sides of the box, and the downwind side is far enough from the facility to minimize high frequency fluctuations, the same simple relationship found in a bioreactor applies.

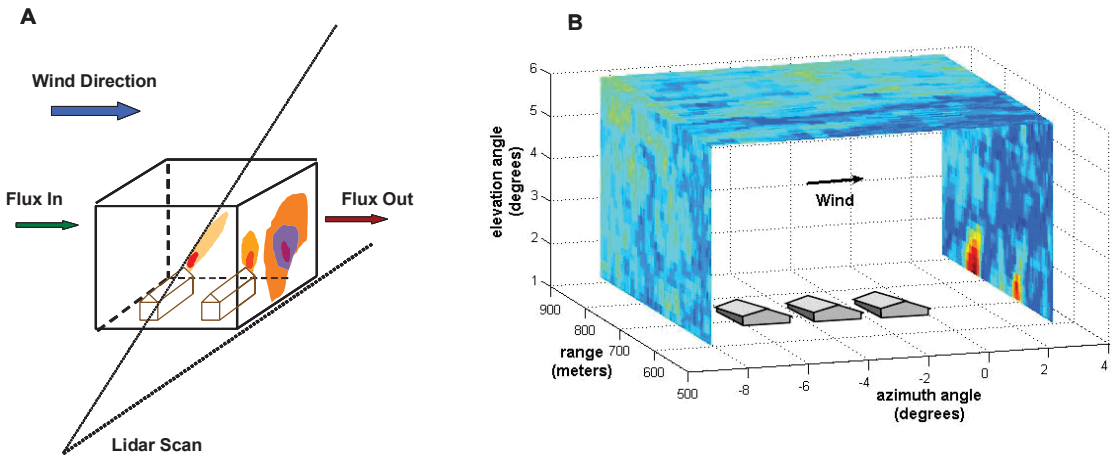

Figure 12. (A) Conceptual illustration of the method for using lidar to generate time resolved local area particulate fluxes. (B) An example of a "staple" lidar scan over the facility showing aerosol concentration on the three sides of the box.

An example of our lidar-derived concentration data is shown in Figure 12B. The concentration plot pattern from scanning up one side, across the top, and down the other looks like the common office staple (the paper fastener), and will be referred to as a 'staple' scan. The data from the top of the box is regularly examined to be sure that no significant particulate transport is passing through the top. The data for the left side panel of the 'staple' provides the background concentration entering the box, while that on the right provides the background plus facility concentrations leaving the box. The integrated mass concentration difference multiplied by the wind speed during the scan completes the flux emission calculation by yielding mass per unit time emission from the facility.

The flux calculation in the integral form for calculating facility/operation emissions (F) can be expressed as following:

$$F \quad \iint_{r,h} \bar{v}_{\perp}(r,h)\cdot\left(C_D(r,h)-C_{\bar{U}}\right)drdh \tag{19}$$

where $\bar{v}_{\perp}(r,h)$ is the average wind speed component perpendicular to the lidar scanning plane, $C_D(r, h)$ is the downwind PM_K concentration at position range r and height h, and $C_{\bar{U}}$ is the average PM_K concentration in the upwind scanning plane. $C_D - C_U$ form the mass concentration difference upwind and downwind, integrated over the range (width) and height of the sides of the staple. In our routine, Eq. 19 is discretized as:

$$F \quad \sum_{i}^{R}\sum_{R_0}^{j}\sum_{H_0}^{H}\bar{v}_{\perp ij}\left(C_{Dij}-C_{\bar{U}}\right)\cdot\Delta r\cdot\Delta h \tag{20}$$

where R_0 and R are the near and far along beam edges of the box and H_0 and H form the top and bottom of the box. (In many cases, H_0 is set above eye level and concentration is extrapolated to the ground to avoid illuminating personnel and animals.) The $\Delta r \cdot \Delta h$ term is the individual area element for which each flux component as calculated by each step in the double summation.

Figure 12B shows an example of single-scan C_U and C_D mass concentration values for PM_{10} measured along the vertical sides of the staple shape between the distances of 600 and 900 m from the lidar. Single-scan differences, of course, do not account for accumulation or depletion in the box due to wind speed variation during a scan, or from high or low concentration pulses that may still exist in the downwind sample. For a meaningful estimate of the facility emission, many scans are combined to achieve a time-averaged emission rate.

To perform the lidar calibration using the *in-situ* instruments, collocated samples are needed for the PM sampler, OPC, and lidar. In other words, the lidar beam must directly sample the same volume as an OPC/PM sampler location for at least the duration of one OPC sample collection time. When the lidar beam is held constant, usually pointing next to a sample tower, we refer to this as the 'stare' mode. The 'stare' sample mode provides not only calibration, but quality assurance of the data set as well. After data processing and PM concentrations along the beam have been calculated, successive 'stare' data are compared against data from the reference OPC and PM samplers to verify that the concentrations calculated from both instruments are similar within measurement errors.

For most of this study, the Aglite lidar was located at position L1 and used the tower T1, located at 31° as the upwind reference point. Downwind scans for Field 4 were made along the line between L1 and T2 at about 73°; downwind scans for Field 5 were made along the line between L1 and AQT at about 91°. Scanning profiles were programmed for each field and included both 'staple' scans and 'stares', with some variations as necessary according to conditions at the sample time. An example of a lidar scan profile used for each field is provided as a reference, with Figure 13 and Figure 14 presenting graphical representation of the azimuth and elevation of the beam during each sequential data averaging and archival period (averaged and archived every 0.5-1.0 seconds).

Field 4 – The scanning pattern used during the breaking borders operation on May 17 commenced with a stare at 31° for 73 seconds followed by three upwind vertical scans reaching 45° in elevation and lasting 90 seconds each. The downwind portion of the profile consisted of three vertical scans at an azimuth of 73.5°, each reaching 45° in elevation and lasting 90 seconds. These vertical scans were followed by a stare at the downwind tower for 67 seconds. The beam was then returned to 31° and began again. The total time per profile including intermittent delays to position azimuth was 758 sec. (~12.6 min.).

Field 5 – The scanning pattern used during the herbicide application operation on June 11 commenced with a stare at 31° for 33 seconds followed by two upwind vertical scans reaching 15° in elevation and lasting 29 seconds each. The downwind portion of the profile consisted of a stare for 63 seconds at azimuth angle 91° followed by four vertical scans each reaching 15° in elevation and lasting 29 seconds. The profile then moved the beam to an azimuth of 73° for a stare at T2 lasting 18 seconds. The beam was then returned to 31° and the profile was started over. The total time per profile including intermittent delays to position azimuth was 395 sec. (~6.6 min.).

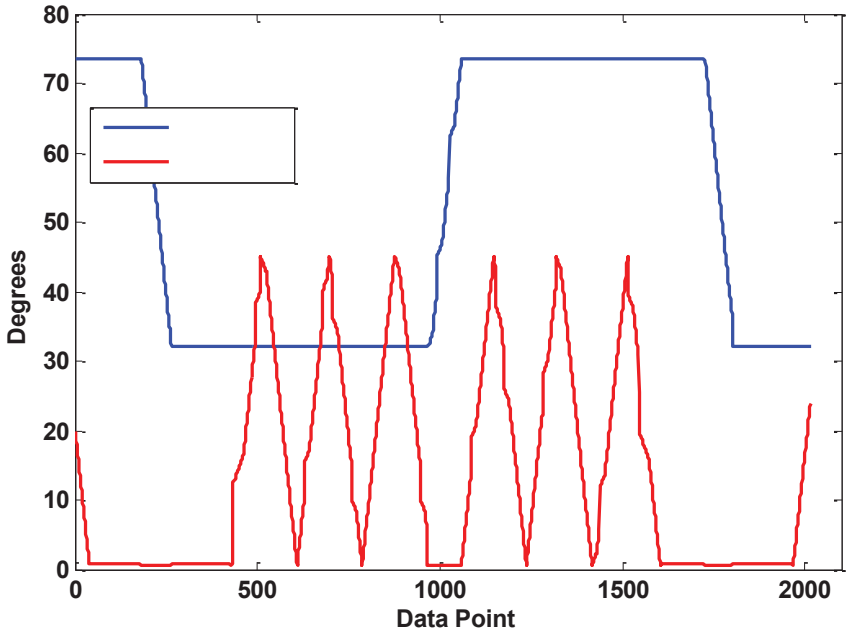

Figure 13. Example of a lidar scan profile used to monitor PM concentrations around and emissions from conventional tillage operations in Field 4. Each data point represents a 0.5 second averaging time, therefore data point 1000 was taken at time = 500 seconds.

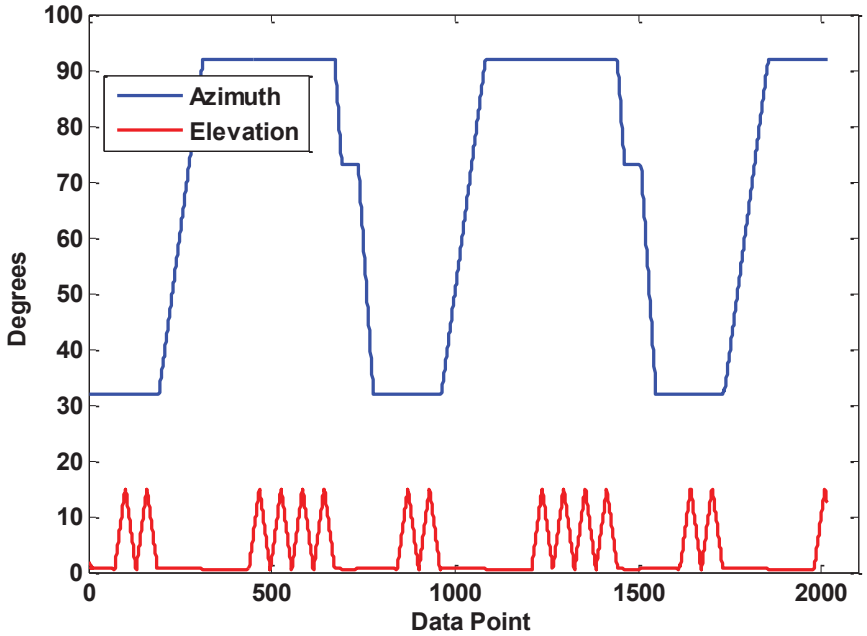

Figure 14. Example of a lidar scan profile used to monitor PM concentrations around and emissions from conservation tillage operations in Field 5. Each data point represents a 0.5 second averaging time, therefore data point 1000 was taken at time = 500 seconds.

3.2 DISPERSION MODELING SOFTWARE

The U. S. EPA has approved a number of air dispersion models for use in regulatory applications. These are listed in Appendix W of 40 CFR Part 51 [49]; included are the Industrial Source Complex Short-Term Model, version 3 (ISCST3) and the American Meteorological Society/Environmental Protection Agency Regulatory Model (AERMOD), which as of November 2005 is recommended for all regulatory applications [1][2]. Both models assume steady-state conditions, continuous emissions, and conservation of mass. The default, and minimum, time-step available for both models is one hour. Therefore, all meteorological input data represent one-hour averages.

ISCST3 assumes a Gaussian distribution of vertical and crosswind pollutant concentrations [50]. The Gaussian plume equation uses the Pasquill-Gifford horizontal and vertical plume spread parameters, σ_y and σ_z, respectively, shown in Eq. 21.

$$C_{10} \quad \frac{Q}{2u_{GM}\pi\sigma_y\sigma_z}\exp\left(-\frac{1}{2}\frac{y^2}{\sigma_y^2}\right)\left\{\exp\left(-\frac{1}{2}\frac{(z-H)^2}{\sigma_z^2}\right)+\exp\left(-\frac{1}{2}\frac{(z+H)^2}{\sigma_z^2}\right)\right\} \qquad (21)$$

C_{10} is the ten-minute average concentration (µg/m^3), Q is the emission rate (µg/s), u_{GM} is the average wind speed at release height (m/s), y is the horizontal distance of the chosen receptor from the centerline of the plume (m), z is the height of the receptor above ground level (m) and H is the effective stack height (m), which includes estimates of plume rise due to buoyancy and/or momentum [50].

ISCST3 assumes a Gaussian distribution of pollutants based on time-averaged meteorological data. It also uses stability classes to address pollution dispersion due to atmospheric mixing. Stability classes are typically determined by a combination of vertical temperature lapse rates and incoming solar radiation or methods using vertical or horizontal wind variance [51]. AERMOD requires more detailed meteorological and surface characteristic information. Because of the additional input requirements for AERMOD and the lack of an established database for these inputs, many regulatory agencies continue to use ISCST3.

The suite of meteorological instruments employed during this field study allowed us to use both models in this study. AERMOD uses continuous functions for atmospheric stability determinations, and based on stability determines the appropriate distribution: a Gaussian distribution for stable atmospheric conditions, and a bi-Gaussian distribution for unstable, or turbulent conditions. AERMOD is also better at accounting for terrain features and building downwash phenomena than ISCST3 [52]. The commercial interface used to run the models was ISC-AERMOD View packaged by Lakes Environmental, Inc. (Waterloo, Ontario, Canada).

Final emission rates were determined using inverse modeling coupled with observed facility-derived pollutant concentrations. In inverse modeling, the downwind impact on pollutant concentrations by a source is known while the emission rate is unknown. To solve for the source emission rate, a model such as ISCST3 or AERMOD is run with the following inputs: on-site collected meteorological data, the facility layout, the locations of pollutant sources and receptors (samplers), and an estimated or "seed" emission rate, which can be obtained from literature. Observed facility-derived concentrations are calculated by subtracting measured background levels from concentrations measured at locations impacted by the source plume. Modeled concentrations are then compared to the facility-derived concentrations from both MiniVols and OPCs at each sampler location. The location-specific ratio of the measured concentration

($C_{measured}$) to the modeled concentration ($C_{modeled}$) is multiplied by the seed emission rate (E_{seed}) and an average across all valid locations is calculated to yield the source emission rate corresponding to the measured facility-derived concentrations ($E_{estimated}$) as shown in Eq. 22.

$$E_{estimated} \quad E_{seed}\left(\frac{C_{measured}}{C_{modeled}}\right) \tag{22}$$

A seed emission rate of 8.6 μg/s-m^2 was used in the dispersion models. This value was an average of preliminary emission rates found through inverse modeling in the 2007 fall tillage CMP study that is a companion to the current study [7].

It should be noted that evaluations of air dispersion model accuracy have shown that models are better at predicting concentrations over longer averaging times than shorter time periods at a specific location; such models were developed and optimized to predict longer-term averages and do not incorporate all of the many temporally and spatially variable factors that may affect dispersion in the atmosphere. Models can predict the magnitude of the highest concentration reasonably well, with a typical range of error of ±10% to 40%, but do not reliably predict the exact location and time of the highest value. Measured and modeled concentrations at the same location are usually poorly correlated, which is likely due to a combination of uncertainties in the input data and unquantifiable uncertainties within the model. The uncertainty of the input data (e.g., meteorological data, emission rates, source and receptor locations, topography) potentially may be reduced through careful collection and screening. In addition, the deposition and particle removal mechanisms are limited in the ISCST3 and AERMOD models herein employed. Insufficient correction within a given model for these and other processes that decrease downwind pollutant concentrations will lead to an underestimation of emission rates based on measured downwind impacts.

An example of errors due to uncertainty in the input parameters is that concentration errors between 20% and 70% can result from an uncertainty of 5° to 10° in the wind direction that directly affects plume location, depending on atmospheric stability and the sampler/receptor location. Uncertainty within air dispersion models, called “inherent uncertainty,” is mostly due to the simplification of complex and highly variable processes affecting dispersion in the atmosphere. If atmospheric conditions that are used as inputs into the model (e.g., wind speed, wind direction, mixing height) are consistent across multiple sample periods, the model would predict the same concentration, while measured concentrations could vary significantly due to variability in the complex processes that are not directly accounted for in the model. These inherent uncertainties can produce predicted ground level concentration errors of up to 50%. A more detailed discussion of air dispersion model uncertainty and accuracy is presented in Appendix W, 40 CFR 51 [49]. The report “Air Emissions from Animal Feeding Operations: Current Knowledge, Future Needs” by the National Research Council of the National Academies states that due to the assumptions required with Gaussian dispersion models, the uncertainty associated with predicted concentrations are not smaller than ±50%. Additional uncertainty is introduced by stability classification and sample instruments [53]. However, the placement of near ground-level receptors along the downwind side of large, ground-level area sources, such as the setup in this study, potentially may reduce the inherent uncertainty of the predicted concentrations due to both the vertical and horizontal proximity of the receptor to the source. Unfortunately, no discussion of uncertainty in dispersion models under such conditions is available.

Based on the issue of potentially reducible uncertainty, all of the input data for both models were very carefully screened to reduce uncertainty in the output to the maximum extent possible, as is subsequently described. Even with such efforts, the error in the model predicted concentrations for this study is expected to be ±50% according to the above sources, which, when combined with a ±20% sampling error of the difference between upwind and downwind MiniVol PM samplers (±10% each) in Eq. 22, yields a range of error about the calculated emission rate at a single location between -46% and +140%. Averaging valid emission rates per sample period may reduce the potential error range to -33% to +100% by removing instrument sampling error.

The meteorological data were carefully screened and corrected for errors prior to preprocessing for the dispersion models. It was this same screening process that uncovered the erroneous wind direction averaging code for the meteorological towers in the analysis of the 2007 fall tillage CMP study [7]. As previously described, we have instead employed the horizontal, one-minute averaged wind directions from sonic anemometers. The meteorological inputs for the models generated by the preprocessing programs were also screened for consistency with input measured values; adjustments were made as necessary. The effects of the uncertainty associated with the meteorological input, however small, combined with the inherent uncertainty within the model most greatly impacts model-predicted concentrations at receptor locations that are near the edges of the predicted plume, which in turn may greatly impact the calculated emission rates. Arya (1998) suggests that the plume edge be defined as 10% of the maximum modeled concentration to minimize these effects [54]. Therefore, emission rates calculated at locations with predicted concentrations less than 10% of the maximum predicted concentration were not used in calculating the average emission rate.

AERMET, the preprocessor of meteorological data for AERMOD, requires that the surrounding land use and land cover be categorized to quantify the Bowen ratio, surface roughness, and midday albedo. For this study, the land use on all sides of the site was classified as cultivated land and the default spring time values of midday albedo (0.14), Bowen ratio (0.30), and surface roughness (0.03 m) were used because the summer values for cultivated land assume vegetation cover, which was not the situation for the majority of measurement periods. During each of the sample runs, the sky was clear of clouds, so the amount of cloud cover was set to 0.0 for all hours. The mixing height for input into RAMMET and AERMET was set at 1000 m because all samples were started at least two hours after sunrise and ended before sunset. In addition, all the receptor locations of interest were on the southern edge of the field so the exact depth of the mixing layer during daylight hours over such a short distance at ground level was not considered to be a significant factor. Based on the measured incoming solar radiation, vertical temperature lapse rates, and surface wind speed, stability classes for ISC during all sample periods were determined to be slightly unstable to very unstable. The Upper Air Estimator in AERMET View was used to calculate required upper air parameters based on observed surface conditions.

Digital elevation model files based on 7.5 minute topographical maps were used to calculate receptor and source elevations. The terrain was not considered to be a significant factor in the modeled concentrations as the change in elevation over the entire modeled domain (~2 km x 2 km) was gradual and no greater than 2 meters. The areas tilled during the sample periods were represented in the dispersion models by ground level area sources that varied in size and shape. The readings of the handheld GPS tracking device located on Tractor 1 for each tillage operation, mentioned in Section 2.2 were used to develop the source areas and shapes. The GPS readings of sample locations were used to specify discrete receptors for comparison between modeled and

measured concentrations at specific locations. In addition, a receptor grid with 15 m x 15 m spacing and a flagpole height of 2.0 m above ground level was set up slightly upwind of, over, and downwind of the area source to provide a visualization of the modeled particulate matter concentrations resulting from the area source emissions. Elevations for receptors and source areas were calculated and assigned by AERMAP. Table 30 in Appendix A provides more details about the settings used in each model. All concentrations used for emission rate calculations and presented in this report are averages over the modeled periods.

3.3 STATISTICAL ANALYSIS OF DATA

The goal of this investigation is to determine if there are statistical differences between the conventional and conservation tillage practices. Many different instruments and techniques were used during this experiment; some techniques exhibit Gaussian distributions and some instruments exhibit Poisson distributions. Instruments that count events (photons or particles) exhibit Poisson statistics. The specific "Poisson" instruments are the OPC and Aglite. All other instruments exhibit Gaussian statistics. Regardless of the kind of statistics a particular instrument might use, the same general principle is employed, which is based on comparison of the maximum error (as computed through confidence intervals and T-values) for conservation and non-conservation tillage processes. The respective maximum errors for two tillage processes are compared using a simple T-test for the two time intervals. The null hypothesis is "there are no differences in the particulate emissions between conventional and conservation management practices."

Soil samples were collected over the entire field of study and analyzed using Gaussian statistics. The respective averages and confidence intervals were calculated for each region of the field. Since no statistical difference was found among regions of the field, global statistics for the whole field were calculated and used to describe the entire field. In the case of the OPC instruments, the OPCs generate a particle size distribution every 20 seconds for a tillage operation lasting several hours. These data were first manually examined to remove data artifacts such as unrealistic high particle counts or partial distributions. Then, all of the particle size distributions for the entire tillage process were averaged and the variance and confidence intervals calculated according to their corresponding Poisson definitions.

The process of extracting particle volume and mass concentrations from the Aglite lidar return signal is an iterative process that involves several linear least squares regressions. Our process for retrieval is to average the returns for an entire tillage process, then run the concentration extraction regression. Typically, several million laser shots are averaged prior to calculation of concentrations.

A challenge in dealing with highly variable discrete events, such as agricultural tillage operations is that PM emissions from each tractor/implement pass can – and does – vary considerably from the previous tractor pass across the field. This leads our raw data to appear "noisy," though in fact the error bars on any given measurement are typically much smaller, usually by a factor of five or more, than the natural variability in the instantaneous emissions from the tillage process.

The aggregation of the particulate data, lidar and meteorology data provide an estimate of the particulate flux within a field. This data will be expressed as cumulative particulate emission for a specific portion of the tillage operation. Then, differences between systems will be compared using Gaussian mean comparison methods.

4. RESULTS AND DECISIONS

4.1 GENERAL OBSERVATIONS

4.1.1 Soil Characteristics

The average bulk density and soil moisture values, with 1σ and the number of samples collected (*n*), are presented in Table 13. Figure 15 provides a map of soil sample locations in both fields. The average bulk densities (± 1σ) for Fields 4 and 5 were 1.57 ± 0.05 g/cm^3 and 1.57 ± 0.08 g/cm^3, respectively. Similarly, the soil moisture did not differ significantly between the two fields. Soil moisture generally did not change with increasing number of tillage operations. The largest in-field differences expectedly were recorded after the irrigation event at the end of May 2008 (see Table 13).

Analysis performed on samples from Field 4 yielded an average soil composition of 62% sand, 29% silt, and 9% clay. For Field 5, the composition was 67% sand, 23% silt, and 10% clay. Stable aggregate results are presented in Table 14 and show that the mass of stable aggregates decreased after the first tillage operation with the greatest decrease in the largest sieve. Since the bulk density and the soil moisture data from the two fields are essentially the same within the error of the measurement, we expect these fields to have similar characteristics for aerosol/dust generation. Similarly, as has been shown in the literature [10][11][12][16], we expect the soil moisture content to strongly influence the amount of aerosol/dust production from any given tillage operation.

Table 13. Statistics of soil characteristics measured for both fields.

Bulk Density Data Summary	**Mean (g/cm^3)**	**σ (g/cm^3)**	***n***	**95% CI**
Field 4 (Conventional Tillage)	1.57	0.05	10	0.03
Field 5 (Conservation Tillage)	1.57	0.08	10	0.05
Soil Moisture Data Summary (Date)	**Mean (%)**	**σ (%)**	***n***	**95% CI**
Field 5 (5/17/08)	1.3	0.5	10	0.3
Field 4 (5/17/08)	1.0	0.6	10	0.4
Field 4 (5/19/08)	1.7	0.7	10	0.4
Field 4 (5/20/08)	3.3	1.6	10	1.0
Field 4 (6/5/08)	6.1	2.2	12	1.2
Field 5 (6/7/08)	8.1	1.6	10	1.0

Table 14. Stable aggregate analysis results for both fields.

Sample collection	Sieve Size (mm)	Mass per sieve pan (g)	Total Stable Aggregate Mass out of 100 g analyzed (g)
Conventional Tillage, Field 4			
Prior to tillage	4	31.41	
	2	11.38	
	1	9.67	
	0.5	10.48	
	0.25	12.16	75.1
After Disc 1	4	4.1	
	2	6.25	
	1	5.2	
	0.5	15.74	
	0.25	19.51	50.8
After Disc 2	4	12.92	
	2	8.75	
	1	15.64	
	0.5	11.62	
	0.25	9.27	58.2
After flood irrigation	4	12.88	
	2	11.55	
	1	6.16	
	0.5	14.28	
	0.25	12.02	56.89
Conservation Tillage, Field 5			
Prior to tillage	4	24.84	
	2	10.63	
	1	6.57	
	0.5	12.58	
	0.25	11.68	66.3
After flood irrigation	4	7.23	
	2	10.87	
	1	8.64	
	0.5	13.87	
	0.25	16.72	57.33

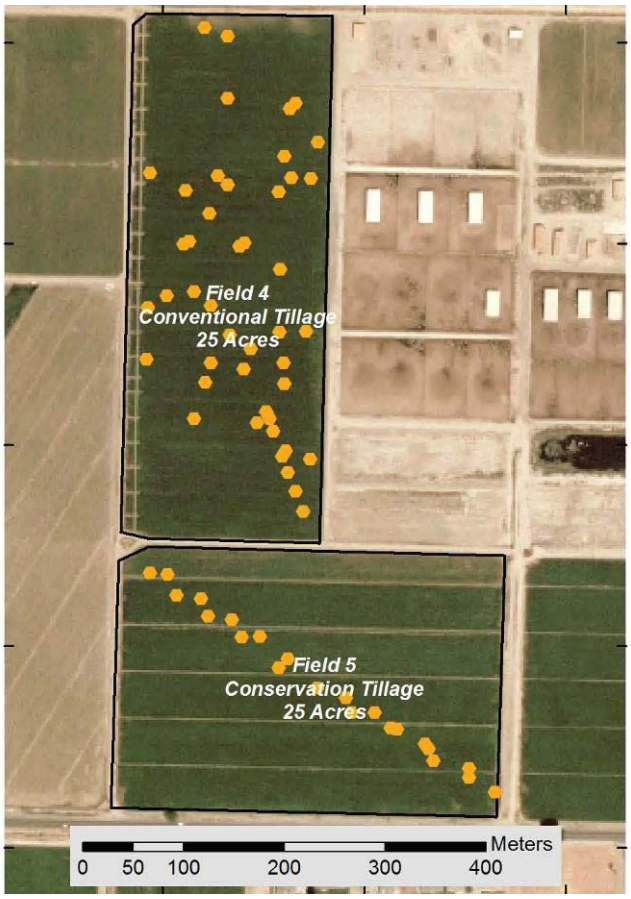

Figure 15. Soil sample collection locations in fields under study.

4.1.2 Meteorological Measurements

A summary of the meteorological characteristics recorded during the study period are presented in this section with some examples.

4.1.2.1 Precipitation Event

One precipitation event occurred during the break in measurement periods from May 20th to June 5th to allow for flood irrigation of both fields. The proximity in time of the precipitation event to flood irrigation of the fields suggested that the effects of flood irrigation on soil conditions and PM emissions would mask any effect of the precipitation event. A minimum of ten days passed between the completion of irrigation on the study fields and any tillage activity.

4.1.2.2 Hourly Wind Data

One-minute averaged wind data collected at the meteorological tower at the WM location from May and June 2008 were averaged again to hourly values in order to create a wind rose of actual conditions during the field experiment (see Figure 16) for comparison with the wind rose created for May and June 2005-2007 (see Figure 6) from the CIMIS station located near Stratford, CA. The wind speed measured at 2.5 m agl on the tower was used because the wind measurement for the CIMIS station appeared to be at the 2-3 m agl level. The wind rose in Figure 16 closely resembles the data collected by the CIMIS station for the previous three years. Wind conditions were very favorable for the designed sample layout throughout the duration of the field study.

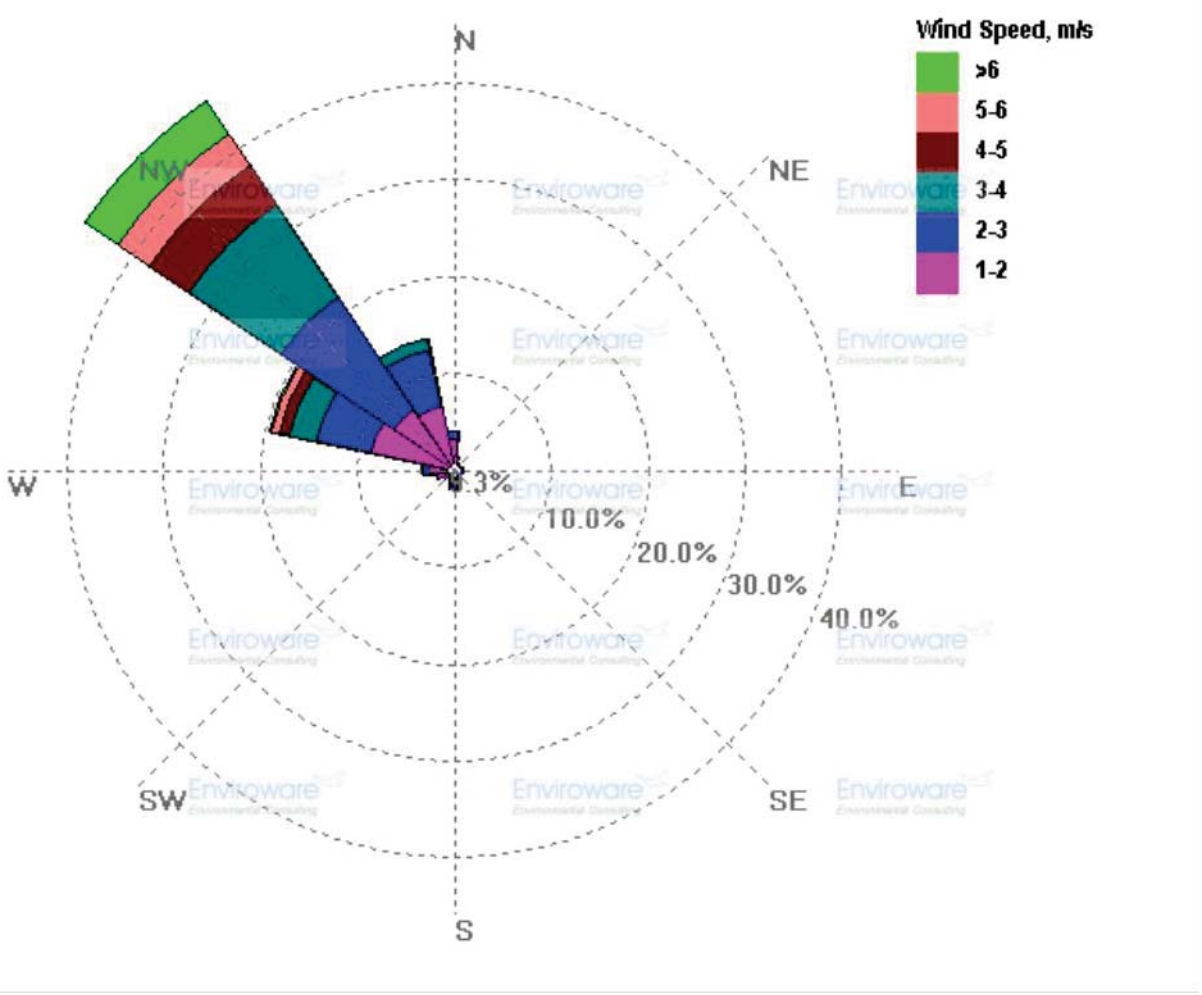

Figure 16. Wind rose of wind speed and direction measured during the May-June 2008 campaign

4.1.2.3 Period-Average Meteorological Conditions

Meteorological characteristics were monitored on-site throughout the field study. Sample period average conditions were calculated and are presented in Table 15 based on measurements taken at the WM and EM locations. As can be seen from these data, all measurements were made during warm and dry conditions. Winds were consistently out of the northwest with average speeds between 2 and 6 m/s.

Table 15. Average ± 1σ temperature, relative humidity, wind speed, and wind direction for each sample period as measured at the WM tower. Temperature, relative humidity, and wind speed were measured at 9.7 m agl and wind direction was measured at 11.3 m agl.

Sample	Ambient Temperature (C)	Relative Humidity (%)	Wind Speed (m/s)	Wind Direction (°)
5/17 Run 1	32.3 ± 2.1	33 ± 4	3.6 ± 0.6	321 ± 15
5/17 Run 2	36.8 ± 0.2	24 ± 0.3	4.3 ± 0.6	321 ± 8
5/18	33.8 ± 2.8	29 ± 4	4.3 ± 1.2	325 ± 16
5/19 Run 1	31.4 ± 2.5	27 ± 3	2.9 ± 0.8	318 ± 22
5/19 Run 2	35.3 ± 1.5	21 ± 3	3.3 ± 0.5	319 ± 16
5/20 Run 1	29.1 ± 2.2	30 ± 10	5.1 ± 1.1	320 ± 10
5/20 Run 2	32.5 ± 0.4	23 ± 1	5.9 ± 0.8	317 ± 8
6/5 Run 1	24.7 ± 2.6	34 ± 7	3.3 ± 1.3	320 ± 30
6/5 Run 2	27.6 ± 0.5	26 ± 2	4.0 ± 0.9	315 ± 7
6/7	22.5 ± 2.7	40 ± 9	4.0 ± 1.0	335 ± 20
6/11*	29.1 ± 0.1	19 ± 1	3.8 ± 0.6	326 ± 17
6/18	34.1 ± 0.3*	16 ± 1*	5.6 ± 0.7	326 ± 4
6/25*	30.2 ± 2.5	29 ± 5	1.9 ± 0.8	328 ± 29

* Data taken from EM tower due to missing data at WM tower

4.1.2.4 Wind Profile Calculations

The wind profiles used in calculating the PM mass fluxes through the vertical lidar beam planes were determined by fitting the power law wind speed equation (Eq. 5) to cup anemometer data from the meteorological tower located at location WM. In fitting the measured data, calculated p values ranged from the minimum to the maximum designated limits of 0.1 and 0.6, respectively, and followed a diurnal cycle similar to that of atmospheric stability class; the mean value of p throughout the field study ± 1σ was 0.25 ± 0.13.An example of a calculated wind speed profile based on tower-mounted cup anemometer data and a power-law fitting model is presented in Figure 17.

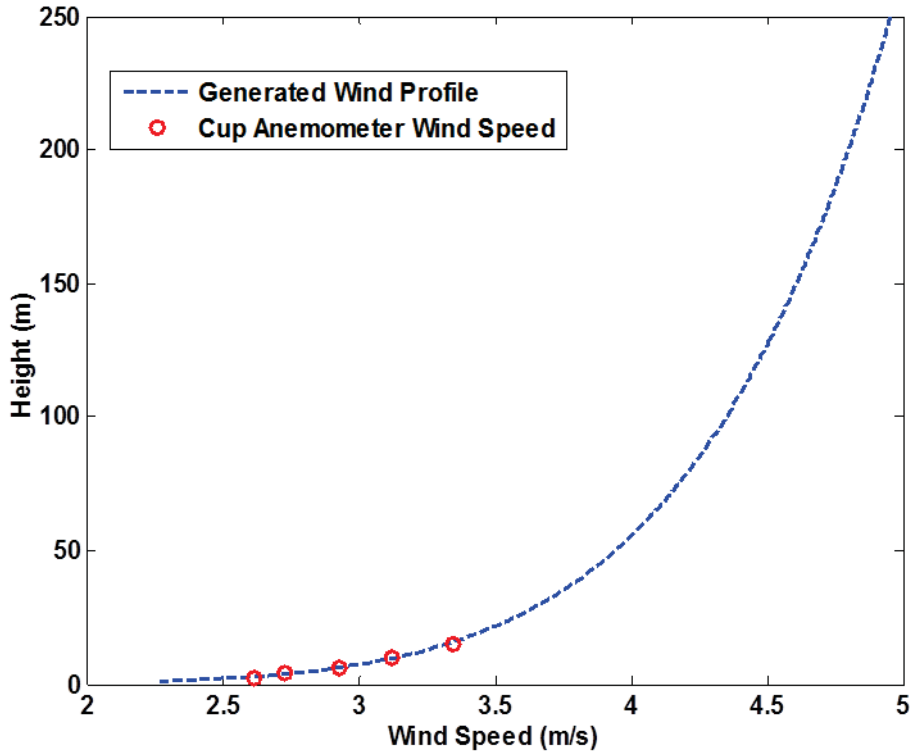

Figure 17. Cup anemometer measurements shown with the wind speed profiled calculated using the measured wind speed.

4.2 AEROSOL CHARACTERIZATION DATA

The following section contains the aerosol data collected using both the filter and optical sampler methods.

4.2.1 Minivol Filter Sampler Data

As mentioned in Section 3.1.4.1, an array of Airmetrics MiniVol samplers was positioned to characterize the upwind/background and downwind PM concentrations. A total of 296 samples were collected: 116 (39%) $PM_{2.5}$, 116(39%) PM_{10}, and 64 (22%) TSP. Calculated $PM_{2.5}$ concentrations based on filter catch ranged from 23.2 to 3244.9 µg/m^3; PM_{10} concentrations ranged from 38.1 to 1458.4 µg/m^3; TSP concentrations ranged from 73.6 to 2276.9 µg/m^3. The MDL for each sample period was calculated based on the average run time of the MiniVols, the targeted flow of 5.0 L/min, and the minimum filter catch that could be measured in the difference between the pre- and post-test filter weights of 5 µg. The MDL for each run varied based on different sample times; the average MDL ± 1 σ (n = 13) was 6.6 ± 4.9 µg/m^3 and the median was 4.3 µg/m^3, with a range of 2.3 for a run length of 7.3 hours to 17.3 µg/m^3 for a run length of 1.0 hour. The calculated PM concentrations measured at all sample locations during May 2008 may be found in Table 31 and during June 2008 may be found in Table 32 in Appendix A. Figure 18 presents a contour plot of the measured PM_{10} concentrations at 2 m agl for the June 25 sample period across the field of study. Sample locations are shown by (+) markers and the field edges are approximated by the black lines. Note the background PM_{10} concentrations were around 100 µg/m^3.

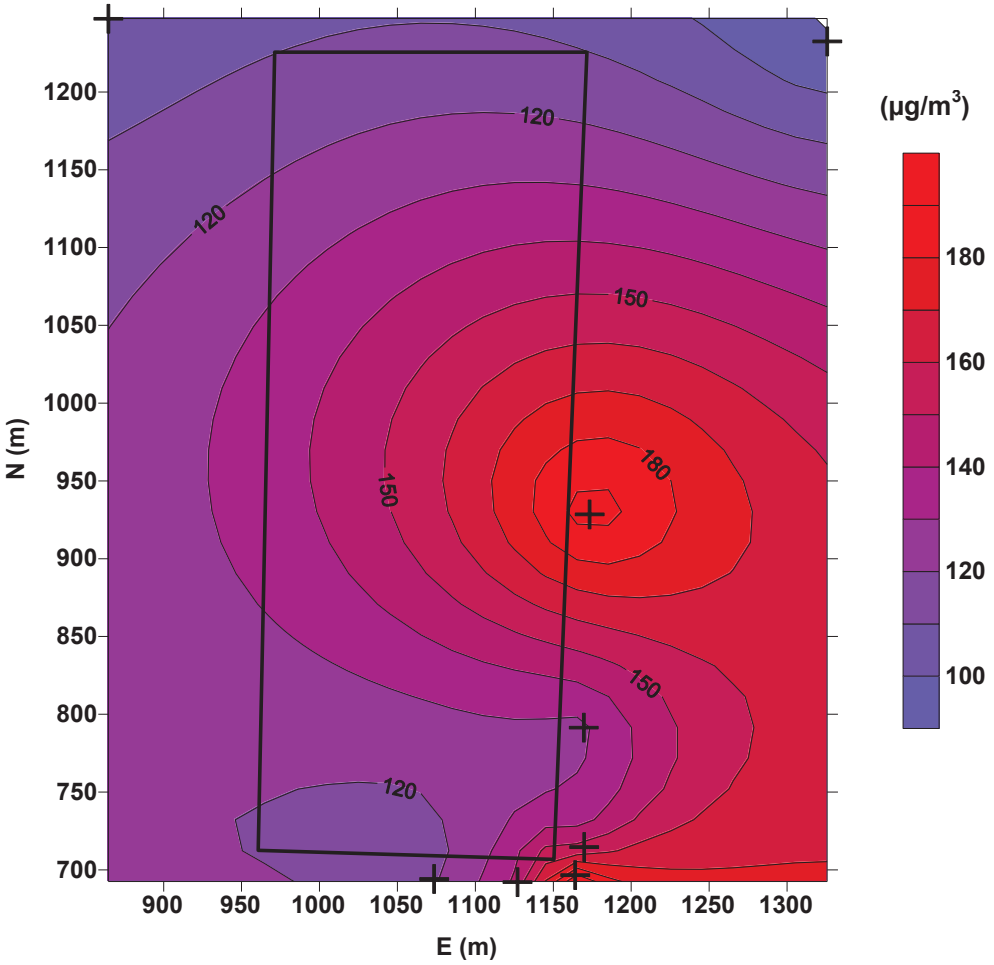

Figure 18. Contour plot of measured PM_{10} concentration for the June 25 sample period.

Of the 296 filter samples collected, 165 did not pass quality analysis/quality control (QA/QC) steps applied to the dataset, leaving 131 for use in calculating emission rates using inverse modeling. An investigation into this high rate of failure was conducted and a detailed description is provided in Appendix B. In summary, filters that did not pass QA/QC were suspected to have been contaminated either during sampling or during storage and handling. Evidence of "particle bounce" was found on many $PM_{2.5}$ and PM_{10} samples collected during May sample periods. Particle bounce occurs when particles that collide with the impactor plate, the mechanism used by the MiniVols to exclude particles larger than the design size, are re-entrained in the airstream and collected on the filter downstream and result in higher measured levels than actually existed. This issue is most likely due to exposing the MiniVol samplers to dust plumes exceeding the maximum recommended exposure level and improper instrument maintenance and cleaning through the May sample periods. Corrective action was taken during the June sample periods and no issues associated with particle bounce were observed in the second portion of the study.

Additionally, some particles were observed on top of and imbedded into the plastic annular ring around the Teflon filter material – the plastic ring is covered by the filter holder assembly during deployment. This was likely due to contamination during on-site filter storage or handling. Efforts were made to minimize this issue throughout, especially during the June sample periods. However, windblown dust did impact the handling and storage area during the last sample

periods in May. The size fraction distribution of approved filters was nearly identical to the total sample set: 51 (39%) were $PM_{2.5}$, 50 (38%) were PM_{10}, and 30 (23%) were TSP. These finalized concentrations are given in Table 33 and Table 34 in Appendix A. See Appendix B for a detailed discussion of the QA/QC steps, filter inspection failure, possible causes of the failures, and preventative solutions for future sampling.

4.2.2 PM Chemical Analysis

4.2.2.1 Organic Carbon/Elemental Carbon Analyzer

As mentioned previously, the organic carbon/elemental carbon analyzer passed the manufacturer's suggested in-field audits and after completion of the field project the data were manually screened for completeness and potential outliers. During the two distinct periods of sampling, May 13-20 and June 3-21, 2008, the EC/OC instrument operated continually except for brief periods for QA/QC checks, servicing of the system generator, or significant breaks in the producer operations. An unanticipated consequence of the one hour sample times, coupled with the dual channel operation of the R P 5400 EC/OC Analyzer, was that the sampling/analysis/cleaning cycles extended beyond the planned two hours. The net result was a sampling profile wherein every third hour of data was missing (66% sample collection efficiency over the entire deployment). However, because the actual farm practice periods varied from one to eight hours, the actual, observed data periods ranged from one to eight hours, the data coverage was from 50-100%, averaging 78.2% ± 10.3%.

The $PM_{2.5}$ OC/EC time series data collected at the downwind Air Quality Trailer (AQT) are shown in Figure 19, with the shaded sections indicating the discrete sampling periods for the observed tillage practices. As can be seen, the $PM_{2.5}$-associated EC was typically quite low, ranging from 0.3 $\mu g/m^3$ to 0.7 $\mu g/m^3$ and averaging 0.4 $\mu g/m^3$ ± 0.1 $\mu g/m^3$ (at the 95% confidence interval) during the concurrent tillage sampling periods and demonstrated relatively little variability. During these same sample periods, the total $PM_{2.5}$ at the AQT, measured by the filter-based MiniVol systems, ranged from 30.8 $\mu g/m^3$ to 141.6 $\mu g/m^3$ and averaging 64.1 $\mu g/m^3$ ± 26.3 $\mu g/m^3$ (at the 95% confidence interval). For further comparisons, during the non-test periods the EC $PM_{2.5}$ concentrations averaged 0.8 $\mu g/m^3$ ± 0.1 $\mu g/m^3$ (at the 95% confidence interval). This would suggest that the EC fraction of the $PM_{2.5}$ at the site was not greatly impacted by the examined tillage practices or by typical EC sources such as biomass or diesel combustion and is more likely of a regional phenomenon.

The observed OC $PM_{2.5}$ concentrations, derived by multiplication of the raw OC concentrations by 1.7 (refer back to Section 3.1.4.3), were approximately an order of magnitude greater than the EC concentrations, ranging from 2.8 $\mu g/m^3$ to 9.2 $\mu g/m^3$ and averaging 5.6 $\mu g/m^3$ ± 1.3 $\mu g/m^3$ (see Figure 20). Although the $PM_{2.5}$ organic component seemed to vary more and occasionally show greater concentration spikes than the EC, these episodes generally occurred during non-test events, when the OC $PM_{2.5}$ averaged 6.0 $\mu g/m^3$ ± 1.3 $\mu g/m^3$, statistically indistinguishable from the tillage test periods.

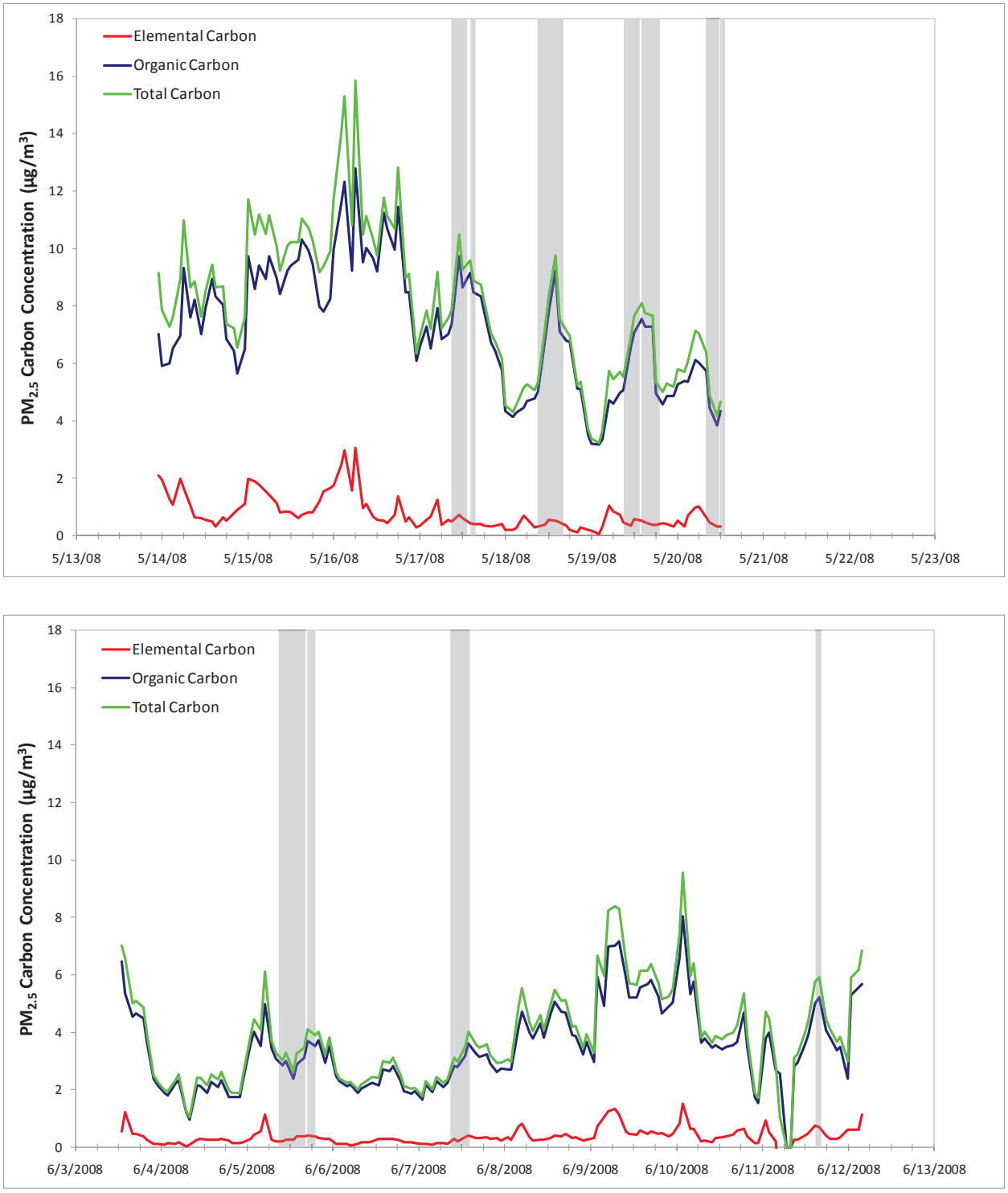

Figure 19. $PM_{2.5}$ OC/EC time series concentrations as collected at the downwind AQT location. The shaded sections indicate the observed agricultural practices. It should also be noted that the raw instrument OC concentrations have been multiplied by 1.7 to account for potential non-carbon functional groups.

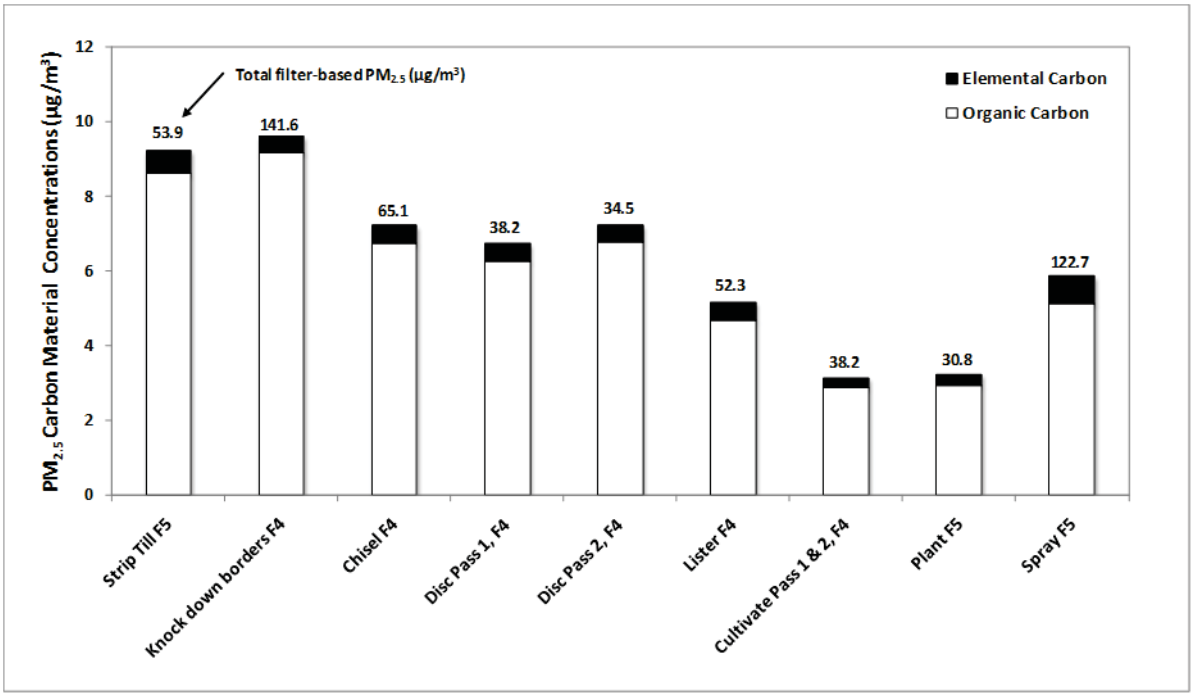

Figure 20. $PM_{2.5}$ organic matter and EC concentrations during specific sampling periods (parallel to filter-based sampling).

As can be derived from Figure 21, on average, the total carbon-related material accounted for around 11.7% ± 3.7% of the $PM_{2.5}$ mass observed at the AQT (downwind). Furthermore, as also shown in Figure 21, the operations on the two different fields, Field 4 (conventional) versus Field 5 (CMP), showed no statistical difference at the 95% confidence level in the percentage of $PM_{2.5}$-based OC or EC. Field 4 (conventional) operations averaged 11.5% ± 4.2% and 0.8% ± 0.3% OC and EC $PM_{2.5}$, respectively, while Field 5 (CMP) operations averaged 9.9% ± 6.7% and 0.9% ± 0.3% OC and EC $PM_{2.5}$, respectively.

4.2.2.2 Ion Chromatographic (IC) Analysis

In addition to the near-real time $PM_{2.5}$ carbon compositional analysis described above, soluble ionic analyses were performed on selected $PM_{2.5}$ filters collected at the AQT. The sample collection and ion chromatographic analyses were described previously in Section 3.1.4.4. The filters analyzed for soluble anions and cations were from most of the discrete sample periods described above in the carbon fraction analysis (Section 4.2.2.1). The AQT sample location was far enough downwind from conventional tillage operations in Field 4 (~ 250 m) that the samplers were not overloaded like the other downwind samplers during the chisel (May 18), disc 1 (May 19 R1), disc 2 (May 19 R2), and lister (May 20 R1) passes. The collocated OPC time series supports this conclusion. As such, a total of nine filters were analyzed for soluble ions. However, two of these filters, from 5/20/08 and 6/5/08, were subsequently suspected as potentially having contamination issues (see Section 4.2.1) and were discarded from further analysis.

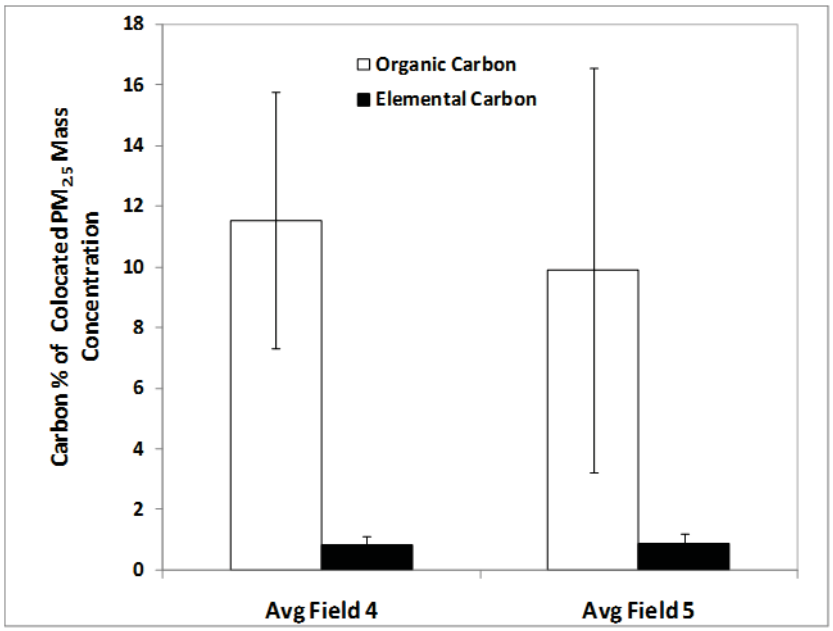

Figure 21. $PM_{2.5}$ organic matter and elemental carbon concentrations during specific sampling periods (parallel to filter-based sampling).

The cations observed included sodium (Na^+), ammonium (NH_4^+), potassium (K^+), magnesium (Mg^{2+}), and calcium (Ca^{2+}). The resolved anions included fluoride (F^-), chloride (Cl^-), nitrite (NO_2^-), and nitrate (NO_3^-). It should be noted here that sulfate (SO_4^{2-}) is often an expected anion present in common ambient particulate; unfortunately, chromatographic failures prevented clear resolution of the sulfate peak so no values for SO_4^{2-} were obtained. However, similar studies by the project investigators found central California tillage dust contained low levels of SO_4^{2-}, averaging less than 4% of the total observed soluble ions and around 0.5% of the total $PM_{2.5}$ mass [7]. Aside from the sulfate, all of the expected ions where observed with the exception of fluoride, which was not detected (n.d.) in any of the samples. As can be derived from Figure 22, the observed soluble ions contributed around 10% of the total filter $PM_{2.5}$ mass. On average, chloride was the most common anion and ammonium and magnesium were the most common cations. It should be noted that these dominances were not always significant at the 95% confidence level. Table 16 presents the average ion concentrations across the seven analyzed filters (uncertainty represents the 95% confidence interval).

Figure 23 shows the average mass percentages for the individual ions, along with the 95% confidence interval. As can be seen, the average individual ionic species concentrations rarely approached 2% of the total $PM_{2.5}$. Although not explicitly shown in either Figure 22 or Figure 23, the total observed ionic percentage can be derived and averaged 10.3% ± 3.8%.

As might be expected, if the presumed sources of the combustion and secondary particles are more regional in nature, the ionic species would show very little mass concentration differences across the samples. When the ionic contributions observed within this study are combined with the EC and OC contributions, the bulk of the particulate material, 81.8% ± 6.1%, was still contributed by unknown (unanalyzed) constituents (see Figure 24). These unaccounted for compounds are most likely insoluble crustal elements associated with the background aerosol and expected soil disturbance emissions during the tillage processes.

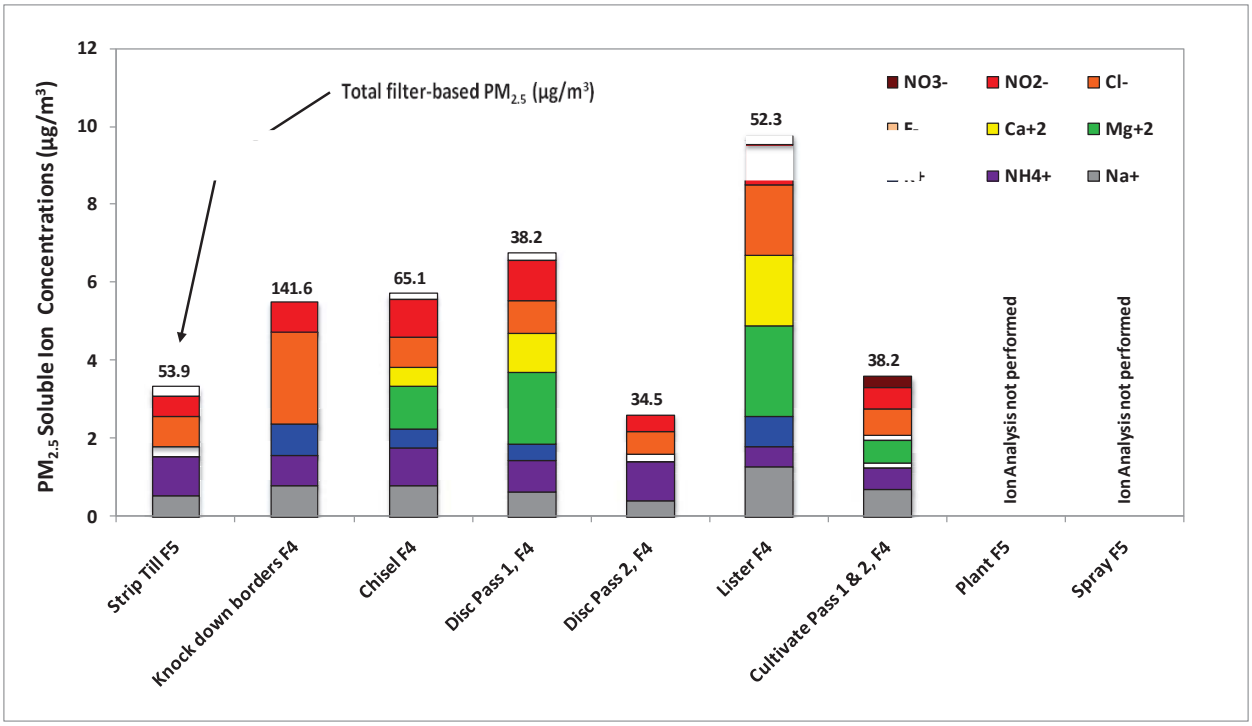

Figure 22. Soluble ionic mass concentrations of AQT downwind $PM_{2.5}$ filters.

Table 16. $PM_{2.5}$ filter ion concentrations averaged over seven downwind samples collected at AQT (uncertainty represents the 95% confidence interval).

Analyzed Ion	F^- ($\mu g/m^3$)	Cl^- ($\mu g/m^3$)	NO_2^- ($\mu g/m^3$)	NO_3^- ($\mu g/m^3$)	Na^+ ($\mu g/m^3$)	NH_4^+ ($\mu g/m^3$)	K^+ ($\mu g/m^3$)	Mg^{+2} ($\mu g/m^3$)	Ca^{+2} ($\mu g/m^3$)
Mass Concentration	n.d.	1.1 ± 0.5	0.8 ± 0.2	0.2 ± 0.1	0.7 ± 0.2	0.8 ± 0.1	0.4 ± 0.2	0.8 ± 0.6	0.5 ± 0.3

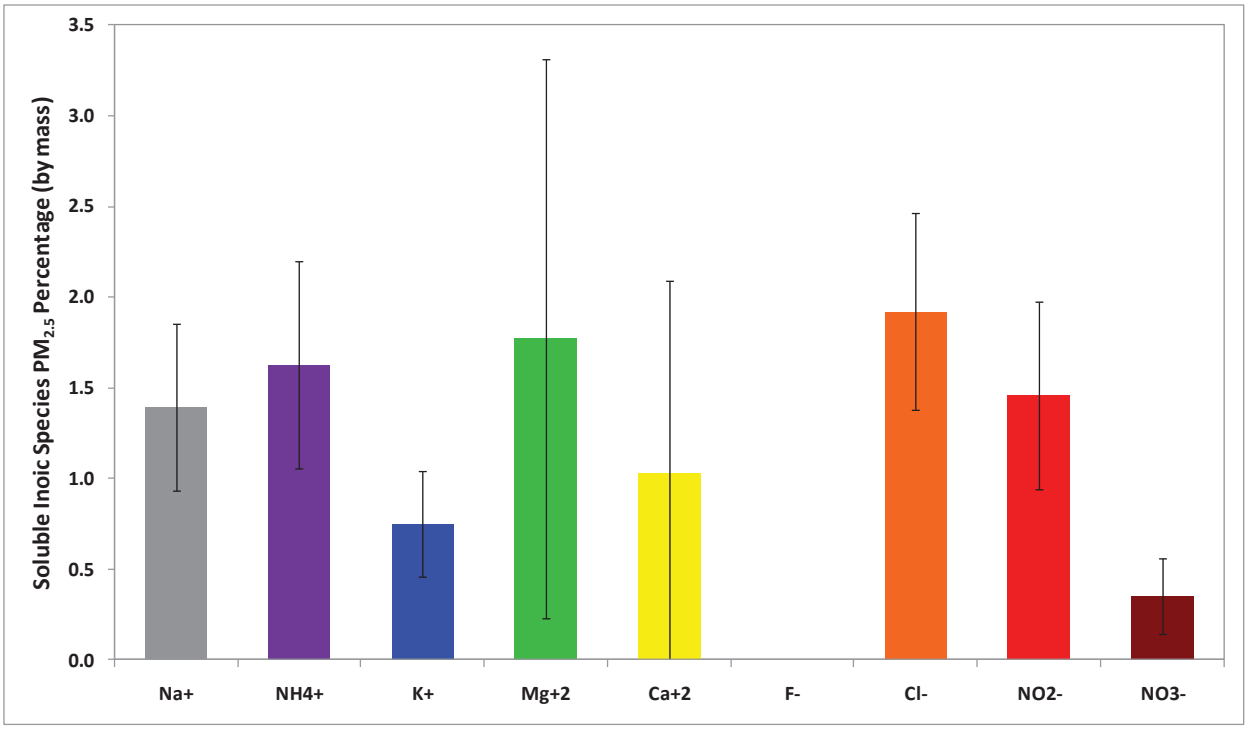

Figure 23. Average soluble ionic mass percentage composition of the AQT downwind $PM_{2.5}$ filters. The error bars represent the 95% confidence interval.

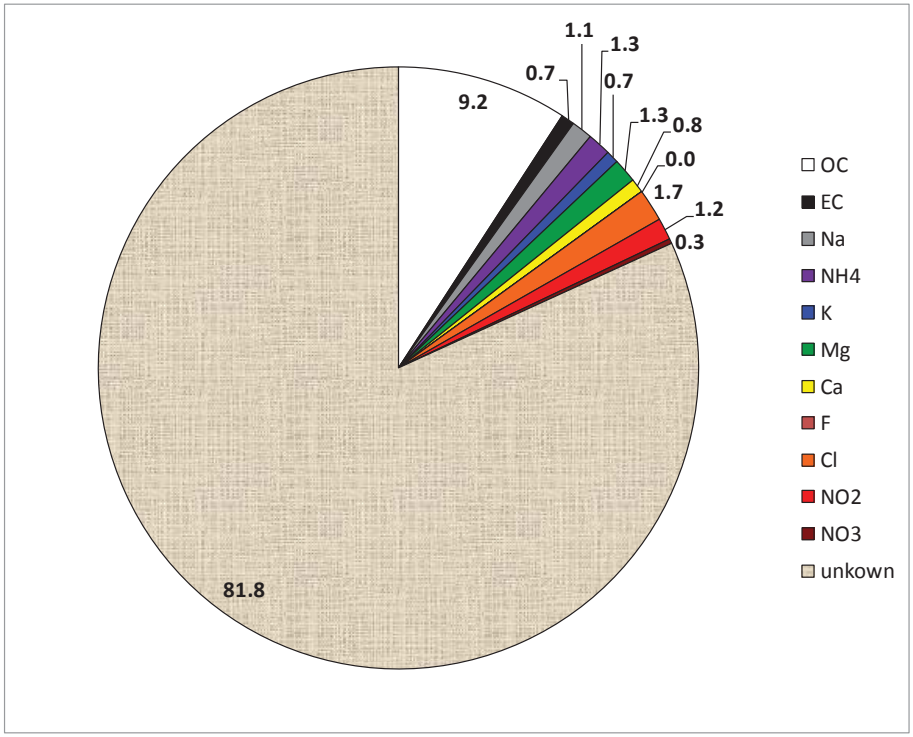

Figure 24. Average compositional mass percentage of the AQT downwind $PM_{2.5}$ filters.

4.2.3 Aerosol Mass Spectrometer

During the tillage experiment, the AMS acquired chemical composition data from May 14-May 19 with some significant gaps in the data due to mass spectrometer malfunctioning. This required manual screening of the AMS data. Approximately 35% of data over the time period was found to be valid. Large gaps occurred throughout the sampling period with, for example, no data acquired on May 17. Similar to the AMS data acquired in the companion experiment in Los Banos the previous year [7], the OC fraction dominated the detected particle chemical composition (Figure 25). The mass spectrum shows that PM_1 is mostly dominated by the presence of photochemical regional pollutants, such as ammonium nitrate (NH_4NO_3) and ammonium sulfate ($(NH_4)_2SO_4$) salts and OC, as in Figure 26. Particle size information was obtained (Figure 27 a and b) and is indicative of photochemical production of particles with the size distributions showing a mode at approximately 0.6 μm (600 nm).

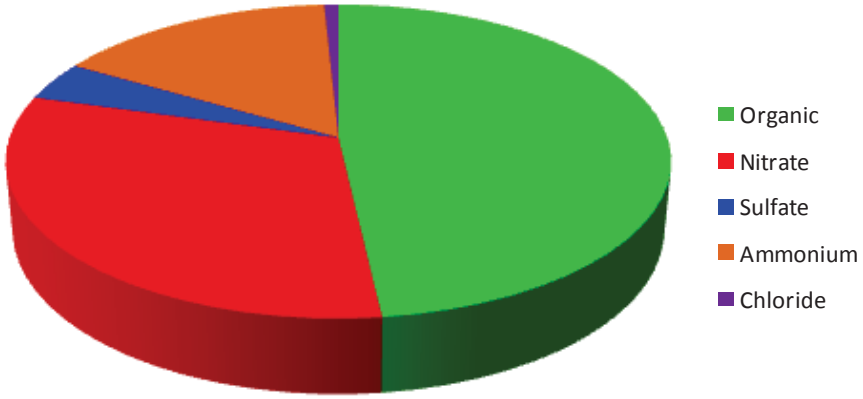

Figure 25. Average chemical composition of particles detected by the AMS from May14-15.

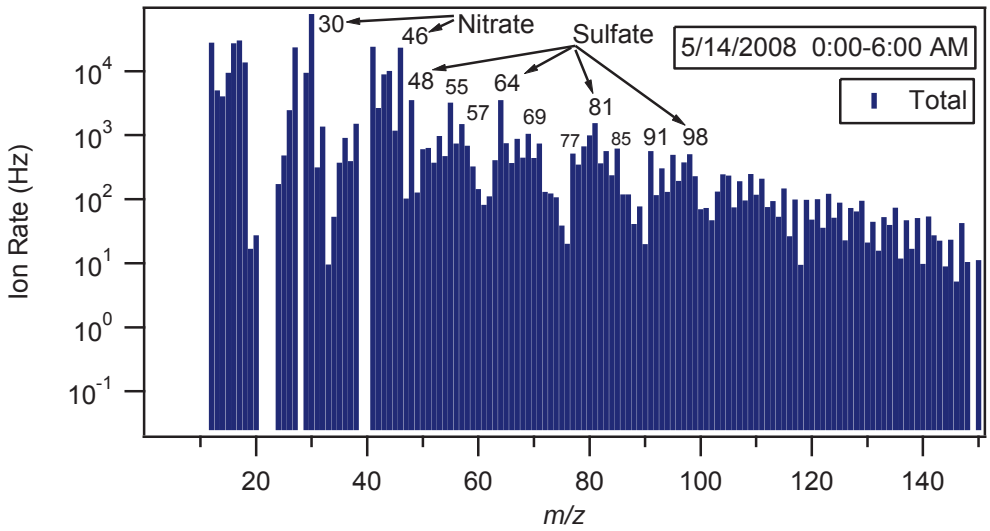

Figure 26. Representative AMS mass spectrum of particles detected during the study. Mass-to-charge (*m/z*) ion assignments include nitrate (*m/z* 30 NO^+ and *m/z* 46 NO_2^+), sulfate (m/z 48 SO^+, 64 SO_2^+, 81 HSO_3^+, and 98 $H_2SO_4^+$), and carbon (*e.g.* *m/z* 55 $C_4H_7^+$, 57 $C_4H_9^+$, 77 $C_6H_5^+$, 91 $C_7H_7^+$).

Because of the major gaps in the AMS data, there were few and limited time periods where the AMS and Met One OPC data overlap. A brief six-hour overlap period is shown in Figure 28 where AMS mass concentration data accounts for ~80% of the converted mass concentrations for the 1 µm size bin of the OPC at the AQT sampling site. Since the AMS does not detect refractory components of the aerosol (e.g., inorganic oxides and black/elemental carbon) and it measures vacuum aerodynamic diameter versus the OPC that measures optical diameter, it is expected that the AMS would detect less mass concentration than the OPC. The overall trend, however, for the time period is consistent between the two instruments.

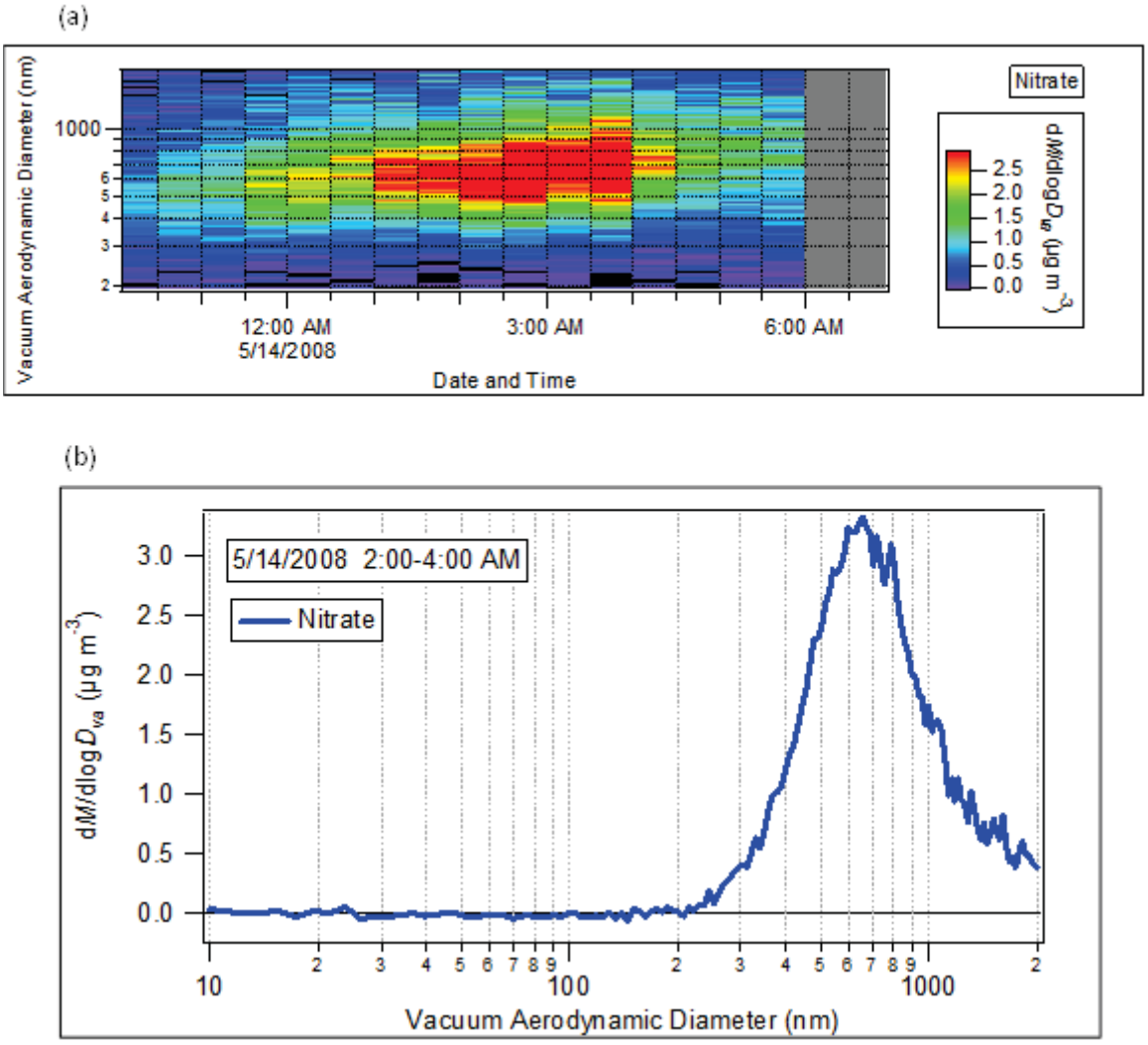

Figure 27. (a) Image plot of nitrate particles on May 14, 2008 using m/z 30 (NO+). This shows the formation of a mode of nitrate particles in the early morning hours of 5/14/2008, with peak mass concentration at ~3:00 AM Pacific Standard Time. (b) Integrated size distribution of nitrate particles from 2:00-4:00 AM on May 14, 2008 showing the peak in the mass distribution at ~0.65 µm.

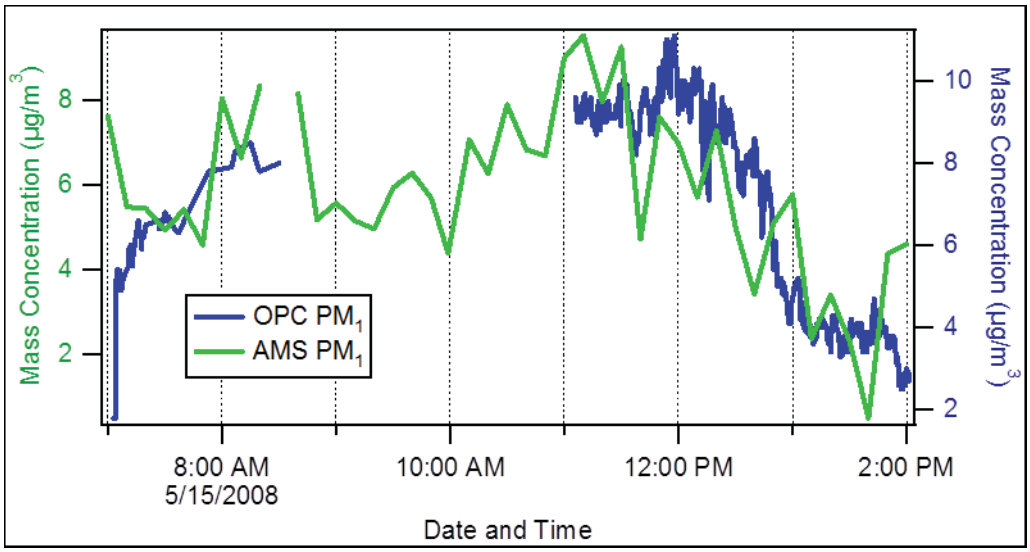

Figure 28. Comparison of AMS PM_1 and OPC PM_1 (assuming a MCF of 1.0 g/cm^3) data for the morning of May 15, 2008

4.3 OPTICAL CHARACTERIZATION DATA

Several different optical instruments were used to characterize the airborne particles, both background and those emitted by the operations under study. Samples of the results from each instrument are presented below, with emphasis on the lidar results.

4.3.1 Met One Optical Particle Counter

The collected OPC data were analyzed for particle size distribution, particle volume concentrations, and converted to particle mass concentration through multiplication with the MCF, as described in Section 3.1.4.2. Table 35 and Table 36 present the $PM_{2.5}$, PM_{10}, and TSP concentrations as reported by the OPCs. Three to four OPCs were in positions immediately downwind of the field under study in each sample period, with between one and four OPCs in upwind locations. Unlike the downwind MiniVol samplers, the downwind OPCs were not overwhelmed by the dust plumes from the tillage activities – the manufacturer specified range of the OPC of 0 to 318,000,000 particles/m^3 was never exceeded – and thus provided usable data throughout all sample periods. Upwind OPC time series data were examined for contamination from activities upwind of the site, such as unpaved road traffic. Contamination was found in six of the 12 sample periods, with five of those occurring at the 10.0 sample site that was immediately downwind of an unpaved road (see Figure 7). Large spikes indicative of contamination were removed from the upwind OPC time series data in these instances to estimate the background aerosol concentration; the estimated background levels were in very good agreement with those measured by an OPC at a different, uncontaminated upwind location (see Table 37 and Table 38).

Data completeness for the OPC datasets was calculated as a ratio of the number of valid samples per sample period over the possible number of valid samples and expressed as a percentage. Data completeness was less than 100% due to communication errors between the OPCs and the computer logging the data, resulting in lost packets of 20 second sample data. Communication error frequency was variable between OPCs and across time. Data completeness per sample period ranged from 81.8% to 100.0%, and averaged (± 1σ) 97.4 ± 3.7%.

The distribution of Met One optical particle counters surrounding the fields of interest at two heights provided the ability to examine particle emissions by number and size at several locations, as well as to monitor the PM concentration time series. Examples of particle volume size distributions measured during tillage operations, in units of $\mu m^3/cm^3/\mu m$, are presented in bar graph form in Figure 29 (dV/dd is the change in aerosol volume concentration normalized by the change in particle diameter). Each graph shows the background particle volume distribution, the volume distribution of aerosols downwind of the source, and the difference between the two that is the volume distribution of the emitted particles. Examining these data based on volume concentration causes the large particles to have a more visible effect than if number concentrations were examined. However, viewing the data in this way is advantageous because it is analogous to mass: the relative shape of and difference between the curves remains the same while the scale changes as the transition to mass concentration is made. Therefore, the given graphs show that the greatest volume (and mass) of emitted aerosols is in the large particle range above a diameter of about 2.5 μm. As seen in the reported PM sampler levels, the greatest contribution by tillage activities was in the PM_{10} and TSP measurements.

Examples of PM time series are shown in Figure 30 from both upwind and downwind elevated locations during the May 19 R2 period. This example was chosen because it demonstrates that downwind samplers were exposed to extremely high PM concentrations in the tillage plumes, supporting the conclusion that downwind filter-based samplers adjacent to the activity were overloaded during this and other sample periods. OPC time series from other periods in which the filter-based samplers were determined to have been overloaded also show extremely high concentrations over very short durations of time. Applying contouring software to OPC number and PM_{10} concentrations measured around the field under study yields the graphs in Figure 31. Data from the June 25 sample period were chosen for direct comparison with the filter-based PM_{10} concentrations (Figure 18). The number concentration contour plot presents the number of particles larger than 1 μm per liter of air; this is the particle size range containing the greatest volumetric contribution from agricultural tillage. The OPC PM_{10} concentrations were calculated by multiplying the V_{10} concentrations by the MCF_{10} for that sample period. Sample locations are shown by the (+) markers; there were fewer OPC sample locations than MiniVol locations, leading to a coarser contour map for OPCs. Field edges are approximated by the solid black lines.

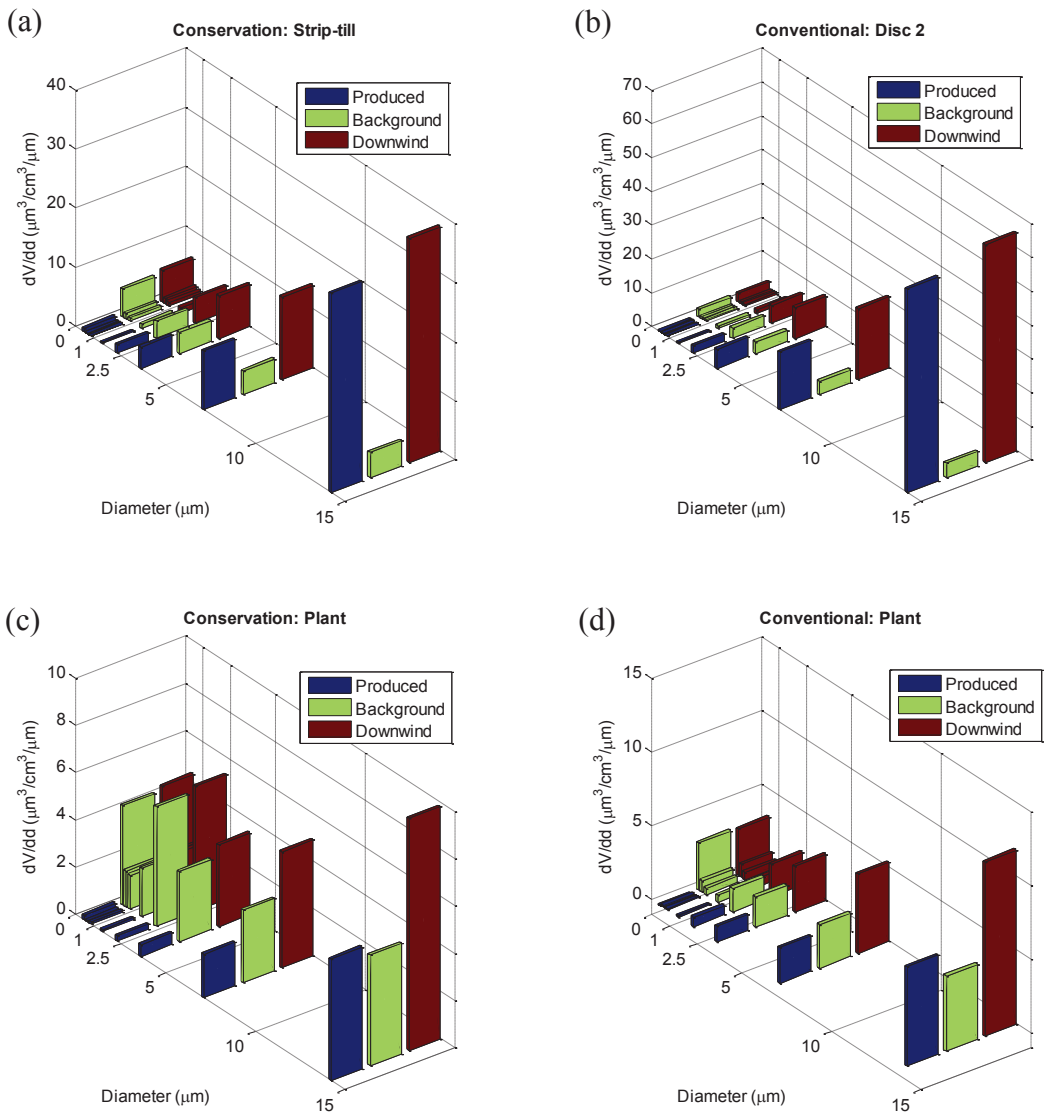

Figure 29. Particle volume size distributions measured from upwind (background) and downwind (background plus emissions) locations, with the difference being the aerosol emitted by the tillage activity: (a) strip-till operation, conservation tillage method; (b) disc 2 operation, conventional tillage method, (c) plant operation, conservation tillage method; and (d) plant operation, conventional tillage method.

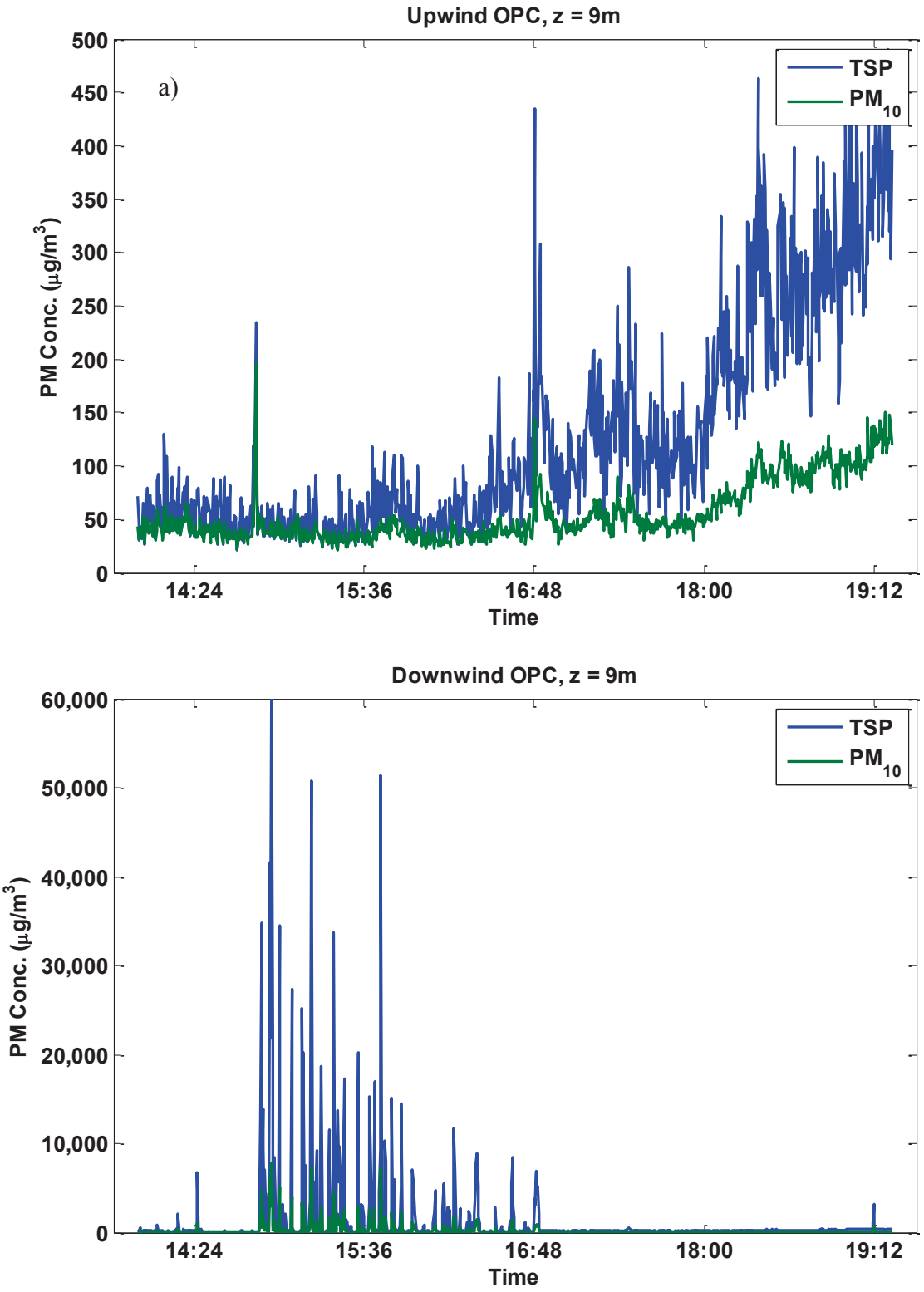

Figure 30. OPC PM time series, created by multiplying the volume concentrations (V_k) by the daily MCF, as measured at elevated locations in a) an upwind and b) a downwind positions during the May 19 R2 sample period.

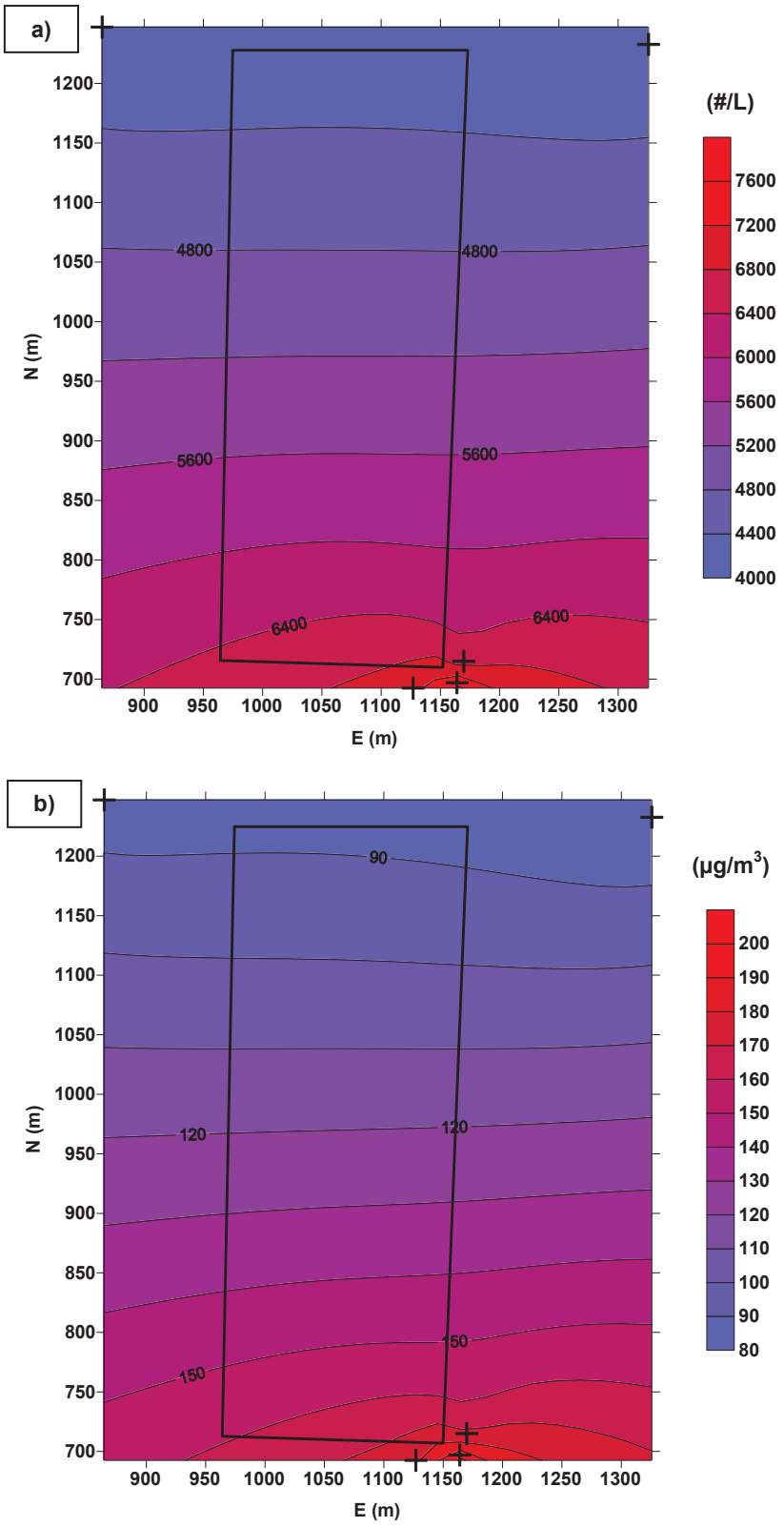

Figure 31. Contour plots of average OPC a) number concentration (#/L) for particles larger than 1 µm and b) PM_{10} concentration (µg/m^3) across the field for the third cultivator pass on June 25.

4.3.2 Optical To PM Mass Concentration Conversion

A key factor in converting the OPC and lidar data from number density (volume) data to mass concentration is the derivation of the MCF, which was described in Eq. 14. The daily average MCF from all locations with valid collocated OPC and MiniVol samples are shown in Figure 32 with the corresponding 95% confidence interval (CI) about the mean. As OPC data collected at each site and during each sample period passed QA/QC, the calculation of MCF values was dependent solely on the presence of a valid filter-based PM measurement. While the near-source downwind filter-based samples for sample periods May 18 through May 20 R2 were determined to have been overloaded, and thus prevented emission rates being calculated for those operations, the upwind and far-source downwind samples were not compromised and were used in calculating the daily MCF values.

Day-to-day variation in the MCF is not well understood. Potential factors leading to this variation include, but are not limited to: 1) changes in background aerosol sources, composition, and particle shape that affect the OPC/MiniVol relationship between particle detection/separation; 2) different treatments of particles larger than the sampled PM size k by the two methods. If a particle larger than the cut-off size k is present on the filter at the time of the post-sample weighing, its mass is included and, with sufficient numbers of large particles, would lead to higher-than-actual PM_k concentrations. The collocated OPC counts particles larger than k in their respective size bins; therefore, they are not integrated into the V_k value like in the PM_k concentration calculation. Thus, a higher-than-actual PM_k concentration would be divided by the actual Vk, leading to a higher-than-actual MCF value. The second potential factor would be most influential in cases where the PM samplers had been overloaded. However, previous efforts have removed filter-based samples known or suspected to have been overloaded from emission rate and MCF calculations.

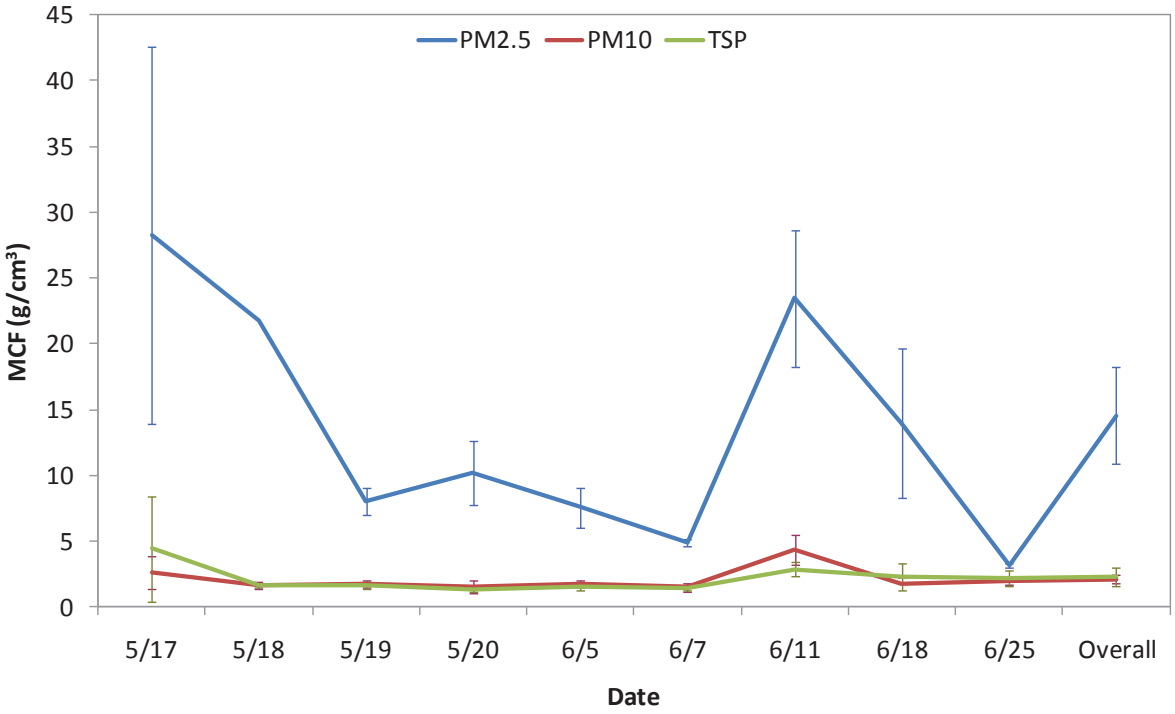

Figure 32. Average daily measured MCF values with error bars representing the 95% confidence intervals.

Most of the PM_{10} and TSP MCF values were within the expected range of 1.0 to 2.5 g/cm^3. However, the $PM_{2.5}$ MCF values were much larger than expected, with individual values ranging from 3.2 g/cm^3 to 28.2 g/cm^3. The mean ± 1σ was 14.6 ± 3.7 g/cm^3 and the median was 10.1 g/cm^3 with 25% and 75% quartiles of 6.1 and 17.7 g/cm^3. As previously stated, calculating the MCF is a simplified method to account for several complex and possibly interdependent variables that affect how an aerosol mixture is measured/detected based on both optical and aerodynamic properties. Some of the known aerosol property relationships that are incorporated into the single MCF value are particle density (ρ), dynamic shape factor (χ), index of refraction (n), and porosity. In past field campaigns, $PM_{2.5}$ MCF values have generally been slightly higher than PM_{10} and TSP values, but the $PM_{2.5}$ MCF values calculated from the MiniVol and OPC data collected during this field campaign are generally much higher than those seen before in our own unpublished work. Due to the non-physically large MCF values for $PM_{2.5}$, the calculated $PM_{2.5}$ MCF values were not used to convert the lidar volume concentrations to mass concentrations. By way of example, the density of Ni is 8.9 g/cm^3 and Hg is 13.5 g/cm^3, while the average observed $PM_{2.5}$ MCF value during this campaign is 14.6 g/cm^3. There is no conceivable way that this number is correct. Instead, the average soil particle density of 2.65 g/cm^3 given in the NRCS National Soil Survey Handbook was used as a constant $PM_{2.5}$ MCF for all sample periods [56]. Table 17 presents the MCF values (± 95% confidence interval where applicable) used to convert OPC and lidar volume concentration data to mass concentration for this study.

Table 17. Mass conversion factors (g/cm^3) used to convert optical particle measurements to mass concentrations for each day and averaged for the whole campaign. Error values represent the 95% confidence interval for *n*≥3.

	$PM_{2.5}$		PM_{10}		TSP	
Date	**Avg**	***n***	**Avg ± 95% CI**	***n***	**Avg ± 95% CI**	***n***
May 17	2.65	---	2.6 ± 1.3	9	4.4 ± 4.0	7
May 18	2.65	---	1.6 ± 0.3	2	1.6 ± 0.1	3
May 19	2.65	---	1.7 ± 0.3	5	1.6 ± 0.3	8
May 20	2.65	---	1.6 ± 0.5	5	1.4 ± 0.2	4
June 5	2.65	---	1.8 ± 0.3	5	1.5 ± 0.2	2
June 7	2.65	---	1.5 ± 0.3	5	1.4 ± 0.2	4
June 11	2.65	---	4.3 ± 1.2	4	2.9 ± 0.5	4
June 18	2.65	---	1.8 ± 0.5	6	2.3 ± 1.0	4
June 25	2.65	---	2.0 ± 0.3	6	2.2 ± 0.6	5
All	**---**	**---**	**2.1 ± 0.3**	**49**	**2.3 ± 0.7**	**44**

A possible correlation with the high $PM_{2.5}$ MCF values was found when sample period averages were compared against the length of each sample period, as seen in Figure 33. The highest average MCFs for all size fractions were found during the shortest sample periods. It is unclear what this correlation may mean, but it is not likely a cause as sampler operation is assumed to be independent of sample period length.

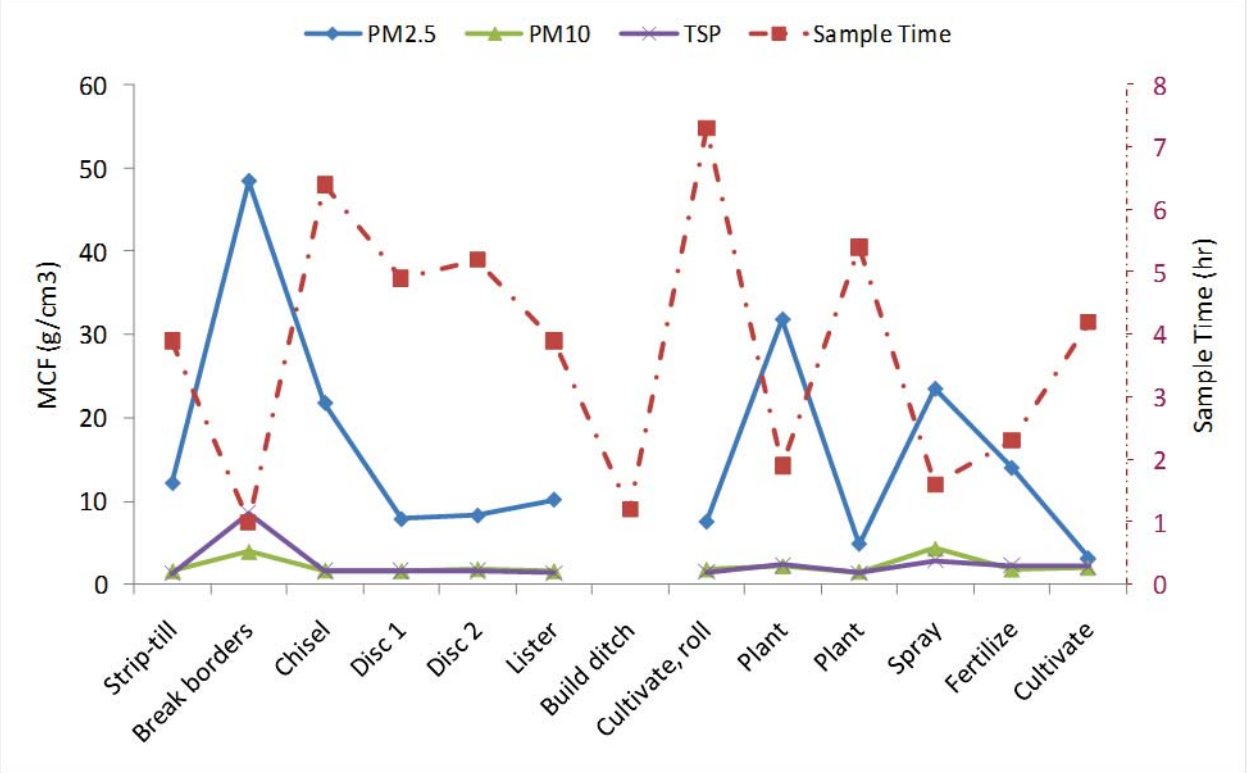

Figure 33. Sample period MCF values compared with the length of each sample period

The particle size distributions measured by OPCs upwind and downwind of the source were used in lidar retrievals to estimate the range dependent V_k (see Eq. 17). Collocated OPC and PM sampler data were used to estimate the MCF. This in turn was used to convert lidar-measured particle concentration to mass concentration units, which can be compared with the PM sampler measurements.

After lidar and OPC measurements were converted to PM concentrations, a quality-assurance step of comparing collocated PM sampler, OPC, and lidar concentrations during 'stare' modes was performed. The time series of routine lidar stares were plotted with the time series data from the calibration OPC to ensure that trends and concentrations are the same in both data sets (Figure 34). It should be noted that lidar measurements were taken every 0.5-1.0 s while the OPCs recorded 20 s samples. Therefore, 20-40 lidar measurements are presented for every OPC measurement when the lidar beam was at the calibration point.

To compare lidar and OPC retrievals with collocated PM sampler measurements, the lidar and OPC time series were averaged and a 95% confidence interval was calculated over the corresponding MiniVol sampling time. Results from these calculations for June 18 are presented in Table 18. Large differences in the reported MiniVol $PM_{2.5}$ measurements and those calculated from optical measurements are likely due to the use of an MCF value of 2.65 g/cm^3 instead of the unusually high values calculated during this campaign. The OPC (20 s) and lidar (0.5 s) collect data at a much higher rate than the MiniVols (2.17 h for this sample run) and are able to capture the temporal variability of the background aerosols that in many cases exceed the uncertainty of lidar retrievals (20-25%) [47].

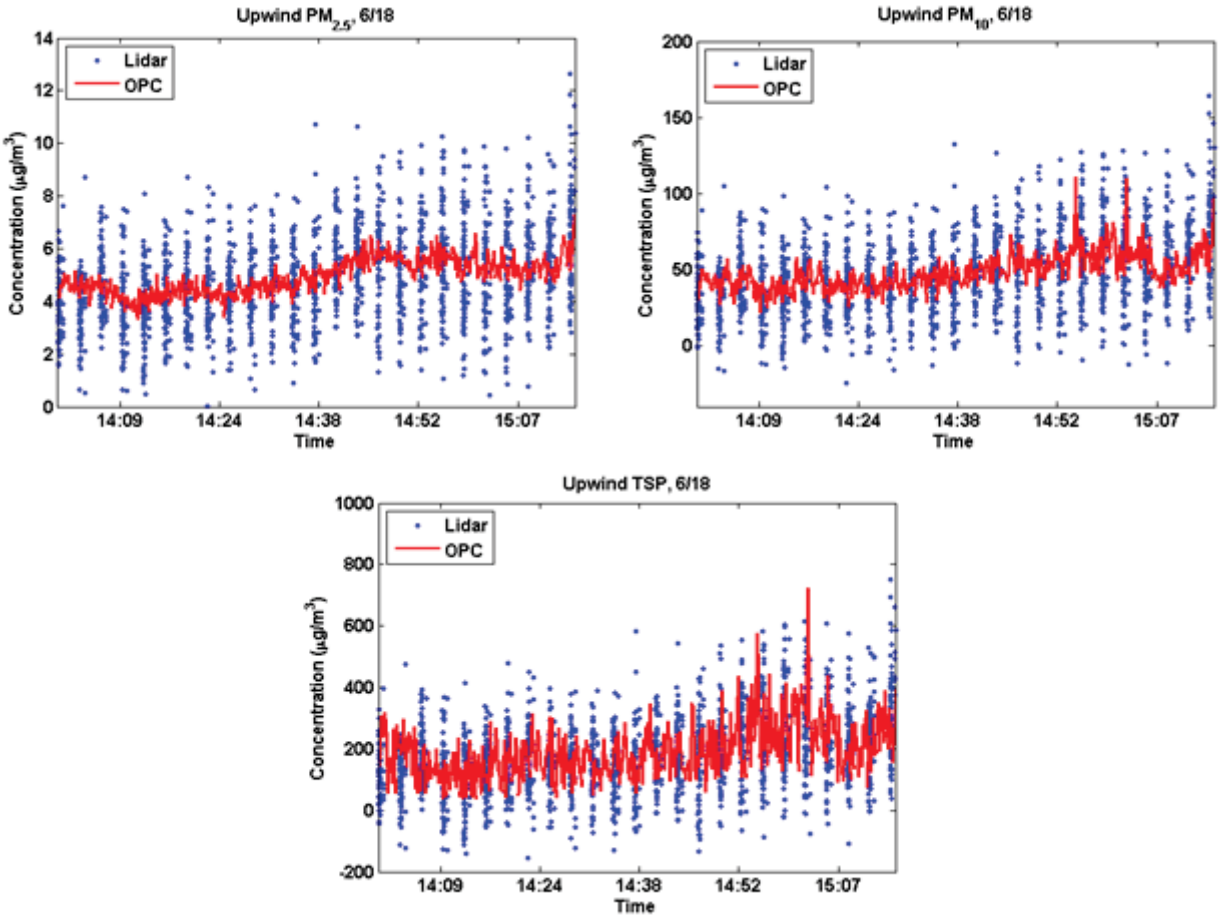

Figure 34. $PM_{2.5}$, PM_{10}, and TSP mass concentrations retrieved from collocated lidar and OPC during the 'stare' time series for 6/18. Data acquisition time of the lidar data is 0.5 s while OPCs were set to 20 s accumulation time. Measurements were done on the upwind side of facility (location T1)

Table 18. Comparison of PM mass concentrations (µg/m3) as reported by MiniVol samplers and mean values measured by collocated OPCs and lidar at T1 (upwind) and T2 (downwind) for 6/18/2008.

Upwind	**$PM_{2.5}$ (µg/m^3)**	**PM_{10} (µg/m^3)**	**TSP (µg/m^3)**
PM sampler (T1)	30.1	56.5	195.4
Upwind PM sampler average ± 1σ	29.1 ± 1.3 (n = 2)	62.6 ± 8.5 (n = 2)	214.5 ± 27.0 (n = 2)
OPC (T1) ± 95% CI	4.9 ± 0.06	48.2 ± 1.1	185.4 ± 8.5
Lidar ± 95% CI	5.1 ± 0.09	50.8 ± 1.3	200.0 ± 6.7
Downwind			
PM sampler (T2)	63.2	87.5	---
Downwind PM sampler average ± 1σ	48.1 ± 12.8 (n = 5)	262.6 ± 153.9 (n = 5)	1696.0 ± 284.1 (n = 2)
OPC (T2) ± 95% CI	6.4 ± 0.5	93.0 ± 15.1	442.3 ± 95.2
Lidar ± 95% CI	6.3 ± 0.1	68.1 ± 2.1	284.5 ± 10.2

A similar comparison of OPC and lidar time series data measured from downwind of the tillage field is shown in Figure 35. The spikes of the concentrations (especially of PM_{10} and TSP) are due to the dust plume generated by tillage operations crossing this OPC. Spikes are rarely observed on the upwind side of the field (upwind spikes are associated with road traffic). As a quality check, comparison analysis of collocated lidar, OPC, and MiniVol data was done for all days of the campaign. In general, the OPC and lidar data averaged for the PM sampler acquisition time are in agreement with mass concentrations measured by the collocated PM samplers. Discrepancies between point-source instruments (PM samplers and OPC) and lidar are due to inherently different measurement techniques. Point instruments capture particle concentration at a single point (a few cm^3) with a small volumetric flow (1.6×10^{-5} to 8.3×10^{-5} m^3/s). The lidar acquires information in a volume of ~ 3 m^3 for each bin along the laser beam for each sample (1-2 samples per second in this experiment), and thus can capture a spatially variable plume while the plume may miss the point sensors. The best agreement is observed when the lidar is compared with PM sampler data averaged over several locations along the up- or down-wind side of the tillage field. For similar reasons, using MCF values averaged over the whole campaign yields larger discrepancies between collocated lidar and OPC/PM sampler PM concentration data than daily averaged MCF values. Based on these observations, a daily averaged MCF is used for conversion of lidar 'staple' data used for flux and emission rate calculations.

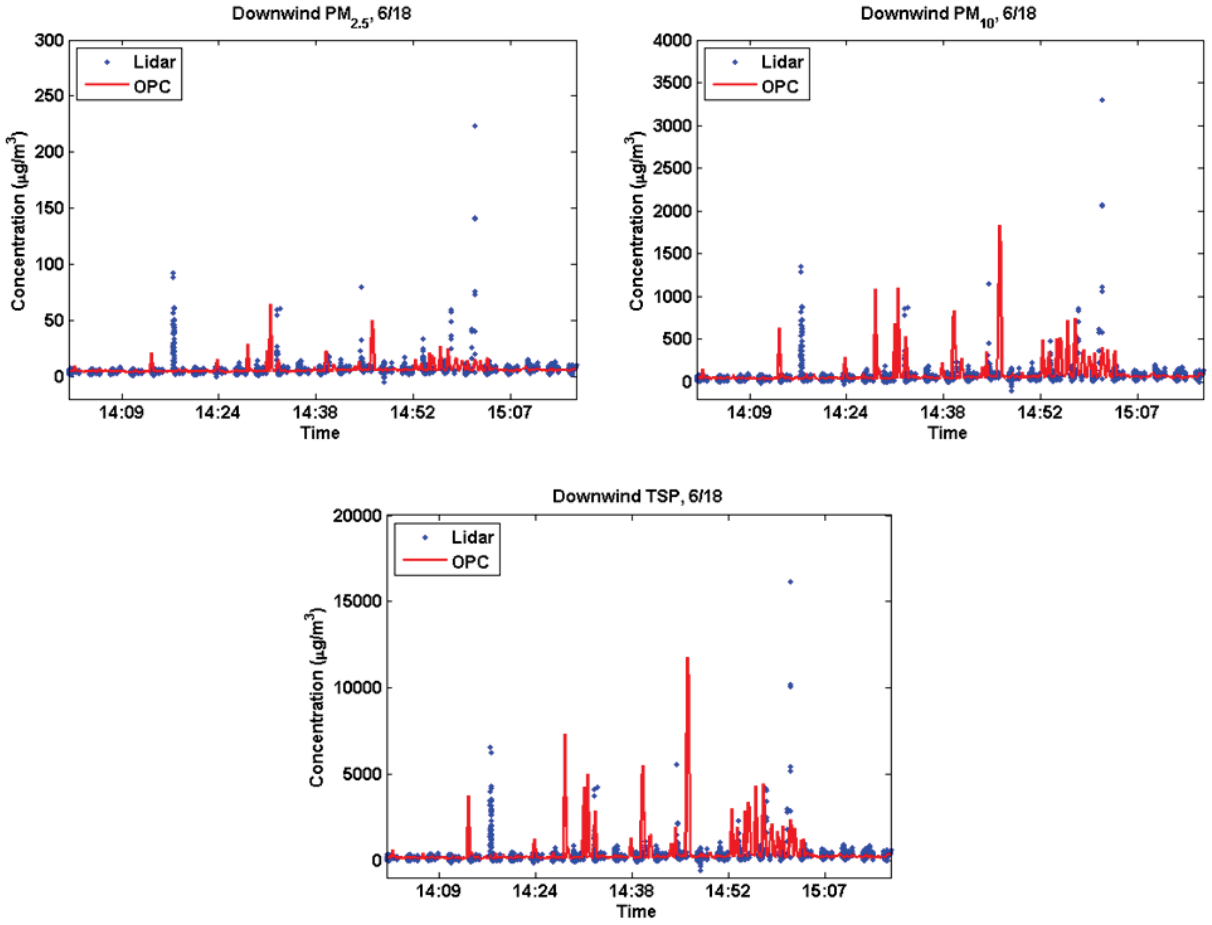

Figure 35. $PM_{2.5}$, PM_{10}, and TSP mass concentrations retrieved from collocated lidar and OPC during 'stares' at downwind locations. Data acquisition time of the lidar data point is 0.5 sec while OPCs were set to 20 sec accumulation time. Measurements were done on the downwind side of field (location T2) on 6/18/2008.

4.3.3 Lidar Aerosol Concentration Measurements

Lidar data was collected throughout all sample periods, except for the Cultivator 3 pass monitored on June 25 due to an equipment failure after the previous measurement. All lidar scans collected during times when no tillage activity was occurring, based on detailed field notes, were removed from further calculations. The remaining scans were visually checked to remove scans with data acquisition errors and to prevent the use of data that was contaminated by other sources; sources of observed contamination were vehicular traffic on unpaved roads, agricultural activities immediately upwind, activities associated with the adjacent dairy, and windblown dust. Contaminated upwind scans, as well as the corresponding downwind scans, were removed from further emission rate calculations. In most cases two or more downwind scans use the same upwind scan as a reference because multiple downwind scans were made for each upwind scan. Downwind scans were not used in further calculations if the corresponding wind direction was outside of ± 70° from perpendicular to the downwind lidar beam path; if the lidar scan contained apparent plumes from an outside source (such as from unpaved road traffic or the dairy); if no plumes were detected; or if the tillage plume had a potentially significant portion crossing the lidar beam closer than 500 meters down beam. In addition, upwind scans were invalidated if none of the associated downwind scans were usable. Light wind speeds (< 1 m/s) were recorded during portions of some measurement periods. Light winds challenge the measurement system and resulted in additional invalidation of some lidar scans. The total number of lidar scans made along both upwind and downwind planes is presented in Table 19, along with the number of valid scans, i.e. those that passed all quality checks, and the percent of valid scans compared to the total number of scans.

Table 19. Total number of upwind and downwind vertical lidar scans and the number of those scans determined to be valid for emission rate calculations. No lidar data exists for the 6/25 run because of instrument problems after the 6/18 run.

Date	Operation	Field	Upwind Scans			Downwind Scans		
			Total	Valid	% Valid	Total	Valid	% Valid
5/17 Run 1	Strip-till	5	62	22	35.5	118	86	72.9
5/17 Run 2	Break down borders	4	20	6	30.0	60	14	23.3
5/18	Chisel	4	122	92	75.4	366	276	75.4
5/19 Run 1	Disc 1	4	103	20	19.4	130	56	43.1
5/19 Run 2	Disc 2	4	150	19	12.7	148	31	20.9
5/20 Run 1	Lister	4	126	17	13.5	126	53	42.1
5/20 Run 2	Build ditches	4	42	5	11.9	42	15	35.7
6/5 Run 1	Break down ditches, Cultivator, Roller	4	90	56	62.2	259	169	65.3
6/5 Run 2	Plant	4	36	25	69.4	114	73	64.0
6/7	Plant	5	58	33	56.9	162	86	53.1
6/11	Herbicide Application	5	24	0	0.0	48	0	0.0
6/18	Fertilizer Application	4	20	10	50.0	40	14	35.0
6/25	Cultivator	4	---	---	---	---	---	---

In several cases, the percent of valid scans was very low. Although wind and background conditions were good during the herbicide application on 6/11, none of the scans taken were deemed valid because the mass difference between the upwind and downwind scans was below the minimum detection level (MDL). This means that the operation didn't produce plumes significant enough to be detected by the lidar; this operation was performed by a very small

tractor pulling a small spraying apparatus – the only disturbance of the ground was due to moving tires. Plumes of insufficient concentration differences from background levels led to downwind scan invalidation in many other instances also. The dairy pen areas adjacent to Field 4 proved to be sufficient PM sources such that lidar scans showing dust plumes passing over the pens prior to crossing the scanning plane were nearly always invalidated. Additionally, windblown dust was entrained off of both Field 4 and upwind field surfaces during both the May 20 sample periods. All of these factors combined to significantly decrease the number of valid lidar scans available for emissions estimation from most operations.

Examples of the lidar-derived PM concentration have been presented in Figure 34, Figure 35, and Table 18. Additionally, upwind and downwind plume area average volume concentrations used in the flux calculations are shown in Figure 36 and Figure 37. The two top panels show the profile-averaged wind speed and direction values used in the flux calculation, with the third and fourth panels showing the area-averaged volume concentrations measured upwind (C_U) and downwind (C_D) in $\mu g^3/cm^3$ (see Eq. 17). It was assumed that the upwind PM concentrations would be more uniform than the downwind PM, therefore, more downwind scans were made than those of the upwind conditions. In Figure 36 and Figure 37, the gaps in the upwind concentration are due to this sampling plan.

4.4 FLUXES AND EMISSIONS RATES

Emission rates for the observed tillage operations were calculated using lidar measurements and measured PM concentrations coupled with model-predicted concentrations via inverse modeling. During the May 20 R2 sample period, strong ground-level winds were measured throughout the entire 1-hr sample time; wind-blown dust plumes originating from the field of study were visible, often impacting both ground-level and elevated downwind samplers, and recorded by field personnel. Due to the size and frequency of these wind-blown dust plumes in comparison to the strength of the monitored operation (building irrigation ditches and field edge borders), any emission rate derived from data collected during this sample period does not accurately represent the operation's actual impact on downwind PM concentrations. In addition, the same operations of building and breaking down of the ditch and field-edge borders around Field 5, the conservation tillage field, were carried out but not measured. Therefore, the emission rate for building ditches and field-edge borders before irrigation and breaking them down after irrigation and before planting was omitted from summations of the emission rates within each investigated tillage method.

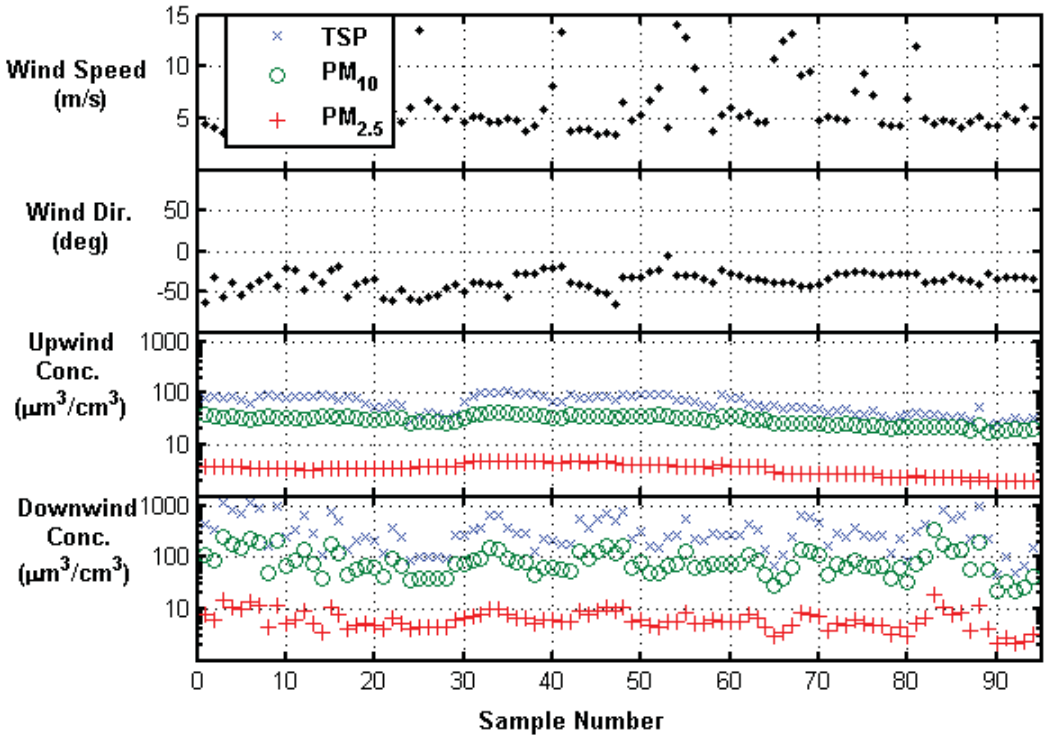

Figure 36. Wind speed, wind direction, upwind and downwind plume area average particulate volume concentrations, for the May 17, 2008 strip-till pass of the conservation tillage method.

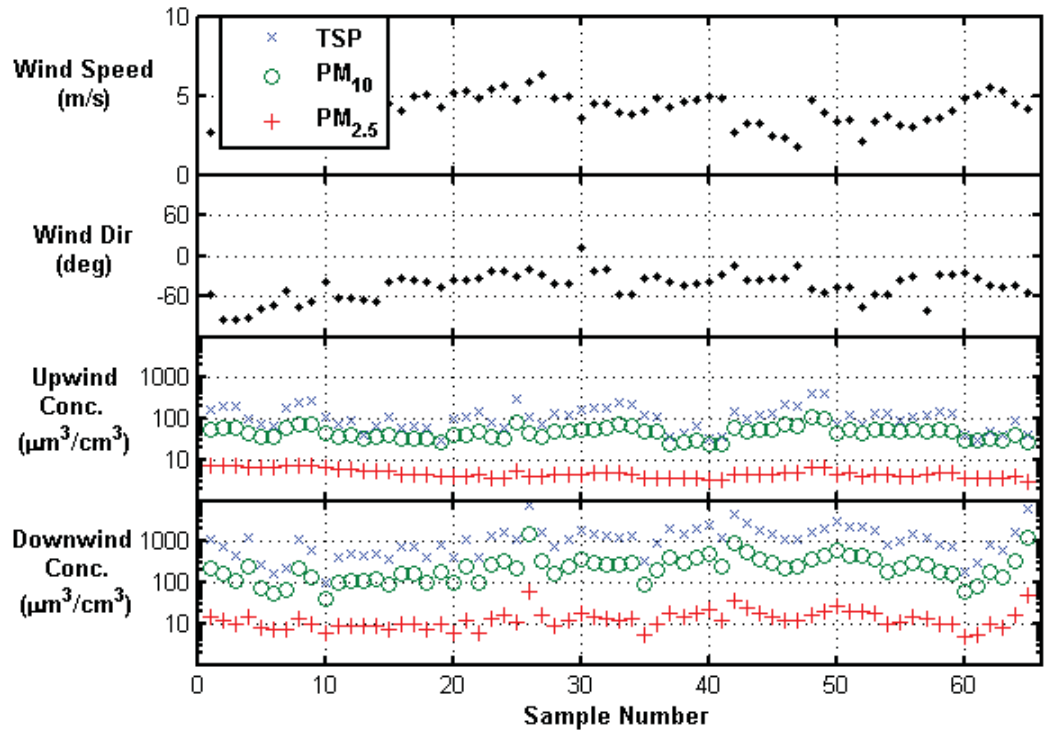

Figure 37. Wind speed, wind direction, upwind and downwind plume area averaged particulate volume concentrations for the May 19, 2008 first disc pass of the conventional tillage operation.

4.4.1 Lidar Based Fluxes and Emission Rates

The combination of 'staple' and 'stare' measurements from the upwind and downwind sides of the field, as described in Section 3.1.5, were performed continuously during each tillage operation of the field campaign except the last one. A critical component failure prevented us from further using the lidar during the June 25 sample period. Figure 38 and Figure 39 show calculated net fluxes for sequential lidar measurements taken during the strip-till pass in the conservation tillage method on 5/17/2008 and the initial discing pass of the conventional tillage operation on 5/19/2008, respectively. The net mass flux through the lidar's vertical scan is the product of the plume area averaged volume concentration difference (C_D-C_U) multiplied by the daily average MCF and the component of the wind velocity that is perpendicular to the lidar beam. It is then normalized by the total area tilled and the ratio of the sample time to total tractor time to yield the emission rate per unit area tilled per unit of operation time.

Net fluxes were calculated using up- and downwind concentration measurements averaged over each vertical scan with average wind information for the time of the individual scan. Single-scan differences do not account for accumulation or depletion in the measurement box due to wind speed variation during a scan, incoming background variation, or storage in/flushing of the flux box due to the existing large scale wind eddy structure (i.e. we do not attempt to measure the same air mass at the upwind and downwind scans). The process is assumed to be a continuous emission source, requiring several scans to achieve a meaningful mean estimate of the facility emission. For calculation efficiency, the net flux was calculated through the downwind surface first and then the upwind flux, using the difference in upwind/downwind fluxes rather than difference in concentrations.

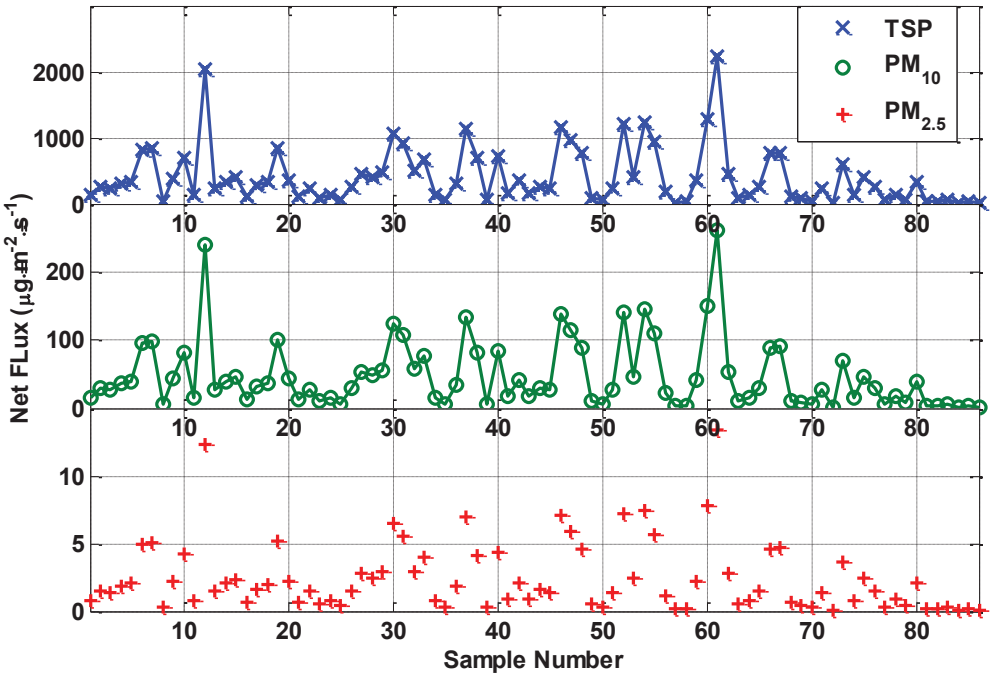

Figure 38. Lidar-derived fluxes (µg/m^2/s) of $PM_{2.5}$, PM_{10}, and TSP for the May 17, 2008 strip-till pass of the conservation tillage method.

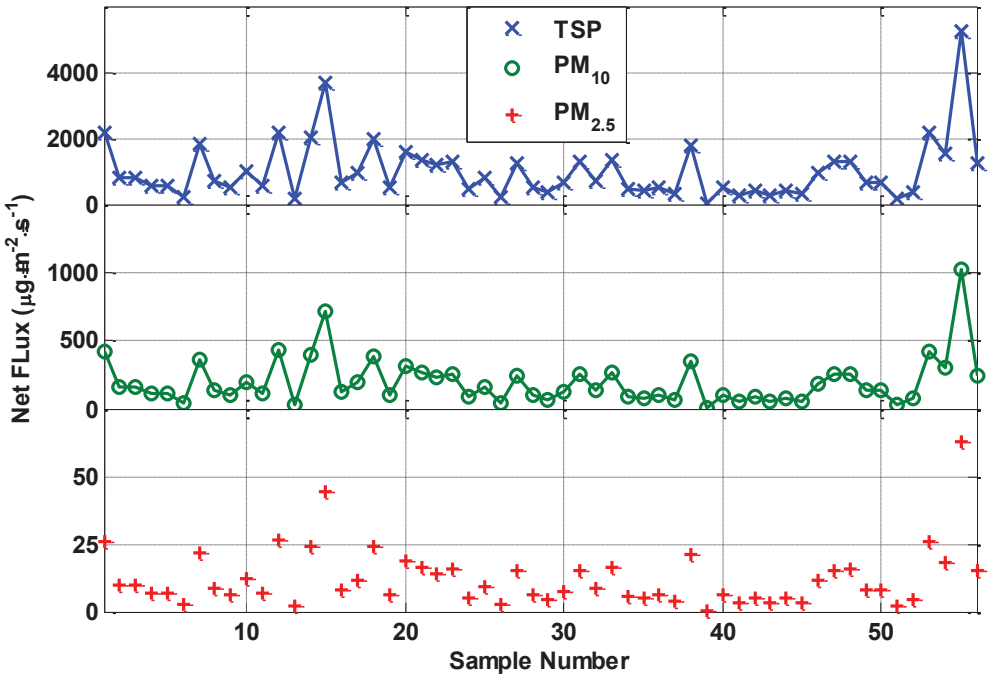

Figure 39. Lidar derived fluxes (µg/m^2/s) of $PM_{2.5}$, PM_{10}, and TSP for the May 19, 2008 first disc pass of the conventional tillage operation.

The plume area was chosen manually by observing each downwind scan and highlighting the area to be included in the calculation. Choosing an area that fully includes the source plume but not a lot of extra area has two advantages: the primary is that portions of the upwind/downwind scans that would clutter the plume can be removed; secondarily, it minimizes the required computational resources used by not calculating flux values for pixels which do not contribute significantly to the overall tillage process.

Using the series of flux measurements collected during each tillage operation, similar to those in Figure 38 and Figure 39, the mean emissions of PM per unit area tilled per second of tillage operation were calculated for all days and are shown in Table 20 with respective 95% confidence intervals. Emission rates reported for multiple operations occurring in the same run are the average amount of PM emitted per tillage pass and does not represent measured a emission rate from individual operations. The breaking down of borders and ditches operation in the June 5 R1 sample tilled the same 4% of the total field area each pass, so the effects of the greater number of passes is spread over a much smaller area than the majority of other tillage operations. The summed emission rate for the conventional tillage method includes the following thirteen implement passes listed in order of occurrence: two break down in-field borders passes (emission rate spread over entire field area, not just the area tilled), a chisel pass, two disc passes, a lister pass, two cultivator passes, a roller pass, a planter pass, a fertilizer injection pass, and two additional cultivator passes. The summed emissions do not include the emissions calculated for the building of ditches and borders on May 20. While the last two cultivator passes were not monitored using the lidar, they have been included in the summed emissions because they are standard weed control operations in the conventional tillage sequence at this production site. The measured emission rate from the June 5 R1 sample period with the plant, cultivator 1 2, and roller operations was used for the emission rate of the cultivator 3 and 4 passes. Each of the cultivator and roller passes were assumed to have the same emissions and variance as was

reported for the June 5 R1 sample period. Likewise, the planter and lister were assumed to have the same emissions as reported for the June 5 R2 and May 20 R1 periods, respectively.

Table 20. Mean fluxes (µg/m2/s) ± 95% confidence interval from quality controlled samples for each tillage operation.

Operation (date)	Valid lidar samples with detectable Δmass (*n*)	$PM_{2.5}$ (µg/m^2/s)	PM_{10} (µg/m^2/s)	TSP (µg/m^2/s)
Conservation Tillage Method				
Strip-till	86	2.5 ± 0.6	47.7 ± 10.7	405.3 ± 91.2
Plant	86	3.6 ± 1.1	12.8 ± 3.8	41.3 ± 12.4
Herbicide Application	0	< MDL	< MDL	< MDL
Summed Emissions		**6.1 ± 1.2**	**60.5 ± 11.4**	**446.6 ± 92.0**
Conventional Tillage Method				
Break down in-field borders (over entire field area)	14	0.9 ± 0.6	10.2 ± 6.3	46.0 ± 28.5
Chisel	276	4.5 ± 0.5	50.9 ± 5.6	224.6 ± 24.6
Disc 1	56	12.1 ± 2.8	196.2 ± 46.0	1,003.0 ± 235.2
Disc 2	30	3.5 ± 1.0	62.6 ± 17.2	353.7 ± 97.2
Lister	51	16.6 ± 7.0	252.5 ± 106.3	1280.7 ± 539.4
Build up ditch and field-edge borders (over entire field area)	15	12.0 ± 5.6	151.6 ± 70.1	686.6 ± 317.5
Break down ditch and field-edge borders, Cultivator, Roller	160	0.9 ± 0.2	4.1 ± 0.8	13.2 ± 2.6
Plant, Cultivator 1 & 2, Roller	74	0.6 ± 0.2	5.8 ± 1.5	20.7 ± 5.3
Fertilizer Injection	14	2.4 ± 1.6	35.8 ± 23.6	176.0 ± 116.1
Cultivator 3	---	---	---	---
Summed Emissions		**45.8 ± 7.8**	**644.5 ± 120.0**	**3,217.0 ± 609.5**

The error values used here for the lidar data denote our confidence in the mean due to the scan-to-scan variability due to the wind transport process occurring on that day, and not to the precision of the accuracy of the individual measurements. Measurement precision, as reported by Bingham et al. [57] show measurement accuracy on the order of 0.1 g/s passing through a lidar scanning plane. This is evident in the last scans shown in Figure 38, where transport across the downwind plane was at or below the lidar system detection limit. Standard deviations of the measurement sequences can be of the same magnitude as the fluxes under light and variable wind conditions, with some scans showing very light, diffuse plumes crossing the lidar plane followed by very dense ones.

The 95% confidence intervals of the individually calculated emission rates were calculated by using the sample statistics (standard deviation and number count) for each day. The 95% confidence interval for the total emission, on the other hand, was derived using the assumption that the average emission rate of each day can be treated as a random variable. The variance of the average emission rate of each day was assumed to equal the variance of the sample set divided by the number of samples for that day. The 95% confidence interval for the daily mean was calculated by assuming a Gaussian distribution and calculating the interval in which the daily mean falls with a 95% probability. The variance of the total emission from each tillage

technique, conventional or CMP, was calculated as the sum of the variances of each operation. The 95% confidence interval was then calculated, again assuming a Gaussian distribution.

The flux data presented in Table 20 were multiplied by the total tractor operation time to yield a total mass emitted per unit area of the field for each operation to calculate emission rates presented in Table 21. The same thirteen passes in an identical configuration were used to calculate the summed emissions for the conventional tillage method.

Table 21. Aerosol mass transfer (± 95% confidence interval) from each field (flux normalized by operation duration and area tilled) as calculated from lidar data for all tillage operations.

Sample	Operation	# of passes	$PM_{2.5}$ (mg/m^2/ operation)	PM_{10} (mg/m^2/ operation)	TSP (mg/m^2/ operation)
Conservation Tillage Method					
May 17 R1	Strip-till	1	26.9 ± 6.1	523.8 ± 117.8	4450.5 ± 1000.9
June 7	Plant	1	50.2 ± 15.0	175.6 ± 52.6	567.6 ± 169.9
June 11	Herbicide Applications	1	< MDL	< MDL	< MDL
Summed Emissions		**3**	**77.1 ± 16.2**	**699.4 ± 129.0**	**5,018.1 ± 1,015.2**
Conventional Tillage Method					
May 17 R2	Break down in-field border (over entire field area)	2	3.0 ± 1.8	33.6 ± 20.8	152.3 ± 94.4
May 18	Chisel	1	101.1 ± 11.1	1132.8 ± 123.9	4997.9 ± 546.8
May 19 R1	Disc 1	1	210.1 ± 49.3	3410.7 ± 799.9	17440.2 ± 4090.4
May 19 R2	Disc 2	1	58.9 ± 16.2	1066.4 ± 293.2	6023.4 ± 1655.8
May 20 R1	Lister + Disc	1, 1.5	302.8 ± 127.5	4608.1 ± 1940.8	23375.6 ± 9845.2
May 20 R2	Build up ditch and field-edge borders (over entire field area)	4, 2	36.0 ± 16.6	453.1 ± 209.5	2051.7 ± 948.6
June 5 R1	Break down ditch, break down field edge borders, Cultivator, Roller	12, 4, 2, 1	22.9 ± 4.5	109.4 ± 21.3	354.0 ± 69.0
June 5 R2	Planter, Cultivator 1 & 2, Roller	1, 2, 1	8.3 ± 2.1	79.5 ± 20.2	285.3 ± 72.4
June 18	Fertilizer Injection	1	9.4 ± 6.2	139.4 ± 91.9	684.1 ± 451.3
June 25	Cultivator Pass 3	1	---	---	---
Summed Emissions		**13**	**811.1 ± 138.7**	**11,051.2 ± 2,126.0**	**54,881.3 ± 10,814.4**

4.4.2 Inverse Modeling Calculations

4.4.2.1 ISC/AERMOD dispersion models

The ground level area source dimensions used in the dispersion models were based on the GPS readings of field perimeter measurements and from the tractor while performing the operation. The seed emission rate of 8.6 μg/s-m^2 per operation, calculated by averaging across preliminary emission rates for all operations derived in the 2007 tillage CMP study [7], was applied to all sources on a per pass basis. In some measurement periods there were multiple passes over the same area by either the same implement or different implements. The seed emission rate was therefore adjusted by multiplying by the number of passes to account for the actual total emissions per operation and sample period. Table 22 lists the tillage operations carried out during each measurement period, the number of passes performed per operation, the area tilled per pass per sample period, the percent of the field that was tilled per pass during the measurement period, and the resulting seed emission rate used in the dispersion models. To compare the modeled concentrations to field measurements, the measured background PM concentration must be subtracted from the measured downwind concentration results to yield the concentration resulting from the source activity.

Note that the area worked by some of the operations was much smaller than the entire area of the field, with the building and breaking down of borders and ditches on May 20 and June 5 working less than 4% of the field each. However, these operations required more passes over the same area to accomplish the task. The total area tilled (area/pass times the number of passes) for breaking down ditches and borders passes of the June 5 R1 period was 31,008 m^2, just 13% of the total area tilled during the sample period. Therefore, the contribution of this operation to the average emission rate per pass is thought to be small compared to the other two operations.

In situations in which multiple passes were monitored in the same sample period, the emission rates were calculated on a single-pass basis and all applications of the emission rates herein derived should take into account the total number of passes performed over the same area. While the seed emission rates for operations with multiple passes over the same area are significantly higher than other operations in the same measurement period that involve just one pass, as found in the first June 5 sample, the low percentage of the total area tilled combined with lower active time for such sources, results in the period-averaged, model predicted concentration being dominated by the longer term, more ubiquitous operation. As the individual effects of each of the three operations in the June 5 R1 sample on measured concentrations could not be distinguished in the period-averaged filter sample, the derived emission rates for each measurement period, using the three seed emission rates shown, represents a conglomerate emission rate. However, for the June 5 R2 sample period, the derived emission rates are for planting only; the cultivator and rolling operations were performed in the northern third of the field and, coupled with meteorological conditions, did not impact most downwind samplers. Therefore, source impacts at all but one downwind location are due strictly to the planting operation.

Table 22. Tillage operations, number of passes, area tilled per pass during monitoring period, and the seed emission rate used for modeling particle dispersion using ISCST3 and AERMOD for each sample period.

Sample Period	Tillage Method	Tillage Operation	# of passes	Area tilled/pass (m^2)	Field portion tilled/pass (%)	Seed emission rate (µg/s-m^2)
May 17 R1	Conservation	Strip-till	1	90,484	100.0	8.6
May 17 R2	Conventional	Breaking down borders	2	10,112	10.0	17.2
May 18	Conventional	Chisel	1	85,116.1	84.7	8.6
May 19 R1	Conventional	Disc	1	100,482.5	100.0	8.6
May 19 R2	Conventional	Disc	1	100,482.5	100.0	8.6
May 20 R1	Conventional	Lister	1	100,482.5	100.0	8.6
		Disc	3	8,121	8.1	25.8
May 20 R2	Conventional	Build ditches and borders	N,W,S sides – 2; E side – 4	N,W,S – 1,795; E – 1,034	N,W,S – 1.8; E – 1.0	N,W,S sides – 17.2; E side – 34.4
June 5 R1	Conventional	Break down ditches/borders	W – 4; E – 12	W – 1,548; E – 2,068	W – 1.5; E – 2.1	W – 34.4; E – 103.2
		Cultivate	2	69,953.5	69.6	17.2
		Roll	1	67,644	6.5	8.6
June 5 R2	Conventional	Plant	1	48,175	47.9	8.6
		Cultivate	2	25,741	25.6	17.2
		Roll	1	32,404	32.2	8.6
June 7	Conservation	Plant	1	90,484	100.0	8.6
June 11	Conservation	Herbicide application	1	90,484	100.0	8.6
June 18	Conventional	Fertilizer application	1	38,126.5	37.9	8.6
June 25	Conventional	Cultivate	1	100,482.5	100.0	8.6

ISCST3 concentrations for modeled sample periods ranged from 0.0 to 194.8 µg/m^3, with the highest concentrations typically modeled at a height of 2 m on the southern and western edges of the tillage area, although the exact location varied slightly with differing wind directions. Figure 40 shows an example of ISCST3-modeled concentrations for the third pass with the cultivator on June 25, 2008 of the conventional tillage method with northwest winds. It should be noted that a 10 m x 10 m grid of receptors at 2 m agl were employed throughout the near-field modeling domain, which produces a much smoother and more detailed contour plot than the measured PM_{10} concentration contour plot seen in Figure 18 and the OPC PM_{10} concentration plot in Figure 31.

AERMOD modeled concentrations for sample periods besides the May 20 R1 and June 5 R2 samples ranged from 0.0 to 205.1 µg/m^3, with the highest concentrations typically modeled at a height of 2 m on the southern and western edges of the tillage area and at different locations depending on wind direction. Figure 41 shows an example of AERMOD modeled concentrations for the same cultivator third pass shown in Figure 40 for ISCST3, with the same 10 m x 10 m grid spacing.

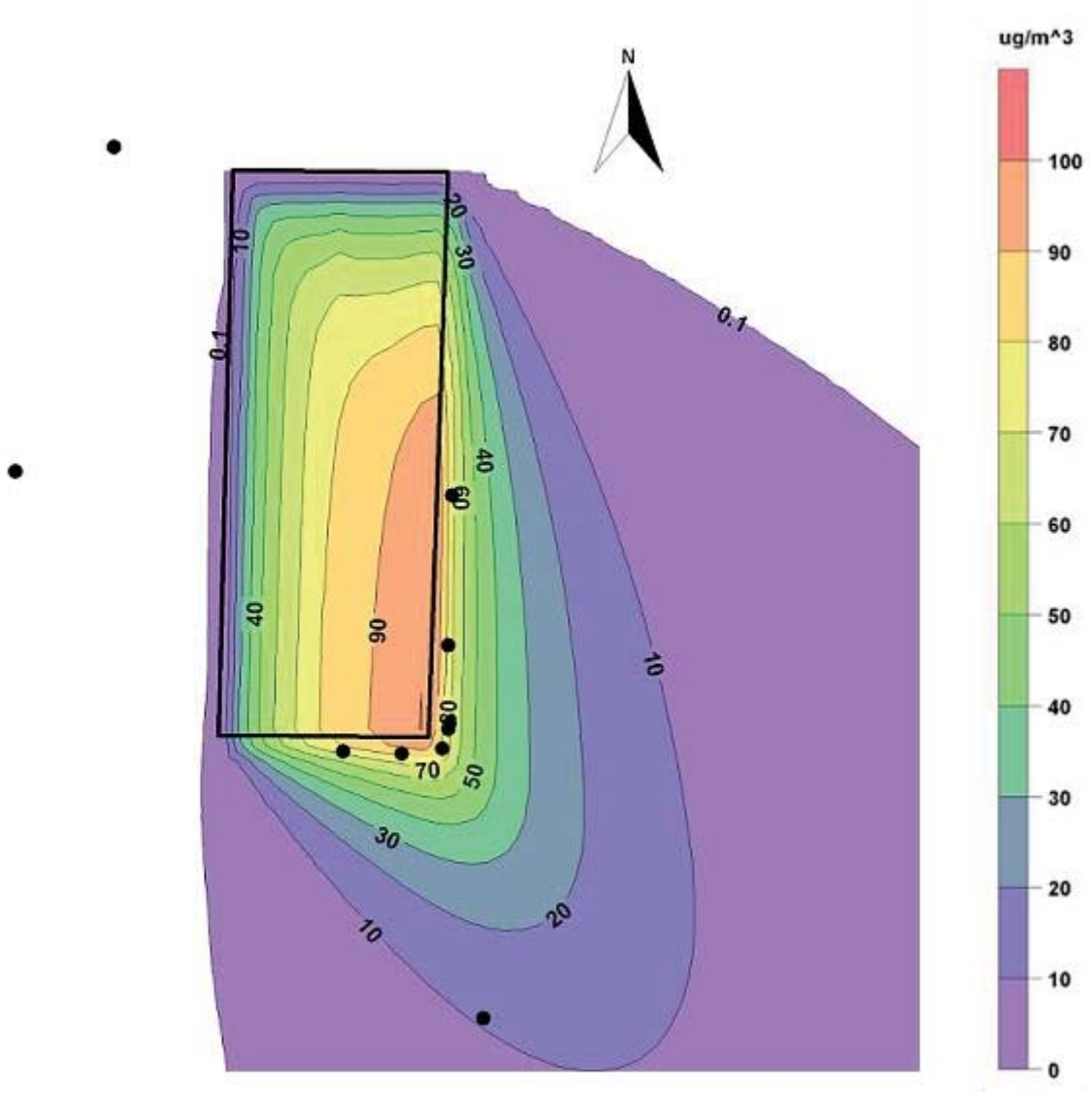

Figure 40. ISCST3-modeled results for the third cultivator pass of the conventional tillage operations on June 25, 2008 with northwest winds. The area of operations and sampler locations are denoted in black and contour line numerical values are in µg/m^3.

4.4.2.2 ISCST3-Based Emission Rates

The MiniVol $PM_{2.5}$, PM_{10}, and TSP concentrations were evaluated for use in calculating emission rates based on inverse modeling as described in Appendix B, with the verified PM concentrations shown in Table 33 and Table 34 in Appendix A. OPC mass concentrations were calculated by multiplying the V_k by the MCF_k for each sample period for use in emission rate calculations and are presented in Table 35 and Table 36. The OPC data were evaluated for impacts to upwind concentrations and whether intense plumes from the tillage operations overwhelmed the downwind OPCs or not for the May 18 through May 20 R2 sample periods. Manufacturer specifications state the range of the OPC is 0 to 318,000,000 particles/m^3.

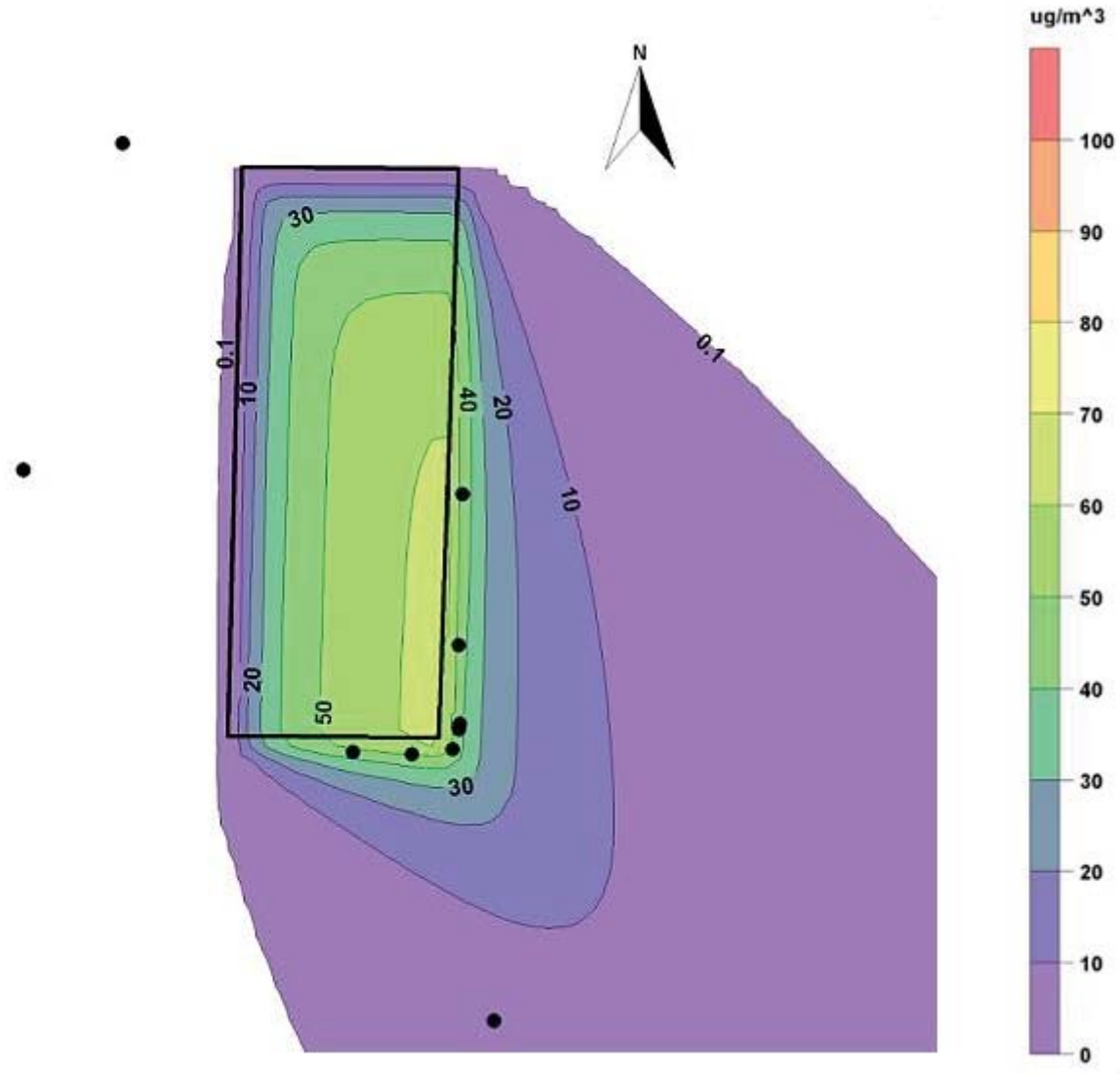

Figure 41. AERMOD modeled results for third cultivator pass of the conventional tillage operations on June 25, 2008 with northwest winds. The area of operations and sampler locations are denoted in black and contour line numerical values are in µg/m3.

Examination of the downwind May 18 through May 20 OPC data found that there were no significant problems with overloading, allowing these data to be used in emission rate calculations. Potential contamination of both OPC and MiniVol upwind samples from nearby activities was investigated using OPC time series data. Some significant events were found. Upwind filter samples affected by these events had already been removed in the QA/QC investigation detailed in Appendix B. Measured upwind OPC PM concentrations were adjusted to represent solely background concentrations by removing high values identified as potential contamination from background concentration average calculations. OPC PM concentrations used in emission rate calculations are given in Table 37 and Table 38.

Sample period average upwind MiniVol and OPC PM concentrations in each size fraction for were subtracted from downwind concentrations to calculate PM concentrations produced by the tillage activity, with only downwind concentrations greater than the average upwind plus the

calculated 67% confidence interval used to calculate emission rates. These operation-produced PM concentrations were then compared with the model-predicted concentrations as shown in Eq. 22 and multiplied by the seed emission rate to calculate the observed emission rate at each location. Emission rates were then averaged across all valid sample locations for each sample period and are presented in Table 23 in units of mass per unit area tilled per tractor operation time with 95% confidence intervals when three or more samples were available. Emission rates presented in Table 24 are in units of mass per unit area tilled, representing the total emissions per unit area per operation. The 95% confidence intervals reported for the summed emissions per tillage method were calculated the same way as those for the lidar emission rates.

Emission rates were not calculated using filter data for the following sample periods due to the near-source downwind samplers being overloaded: May 18, May 19 R1, May 19 R2, May 20 R1, and May 20 R2. Additionally, $PM_{2.5}$ and PM_{10} filter-based emission rates for May 17 R2 and PM_{10} emission rates for June 5 R2 were not calculated because the upwind samples were compromised. All of these sample periods were operations in the conventional tillage field; therefore, a summation of emissions based on MiniVol data across all conventional tillage operations was not possible. In addition, some emission rates based on the MiniVol data set are based on one or two data points, preventing further statistical calculations. However, emission rates were able to be calculated using at least three OPC PM data points for all of these sample periods. The emission rates reported for the June 5 R2 sample in the conventional field are for planting only: the first and second cultivator passes and the roller pass that were being performed at the same time were shown to impact only one downwind sampler location through examination of tractor location, average wind direction (320° ± 4), OPC data, and model predicted concentrations. Data at this location were removed from emission rate calculations.

4.4.2.3 AERMOD-based Emission Rates

Sample period averaged emission rates based on concentrations predicted by AERMOD were determined using the same techniques described for the calculations of ISCST3-based emission rates. Emission rates on a mass per unit area tilled per unit time of operation are found in Table 25 and emission rates on a mass per unit area tilled are found in Table 26, with the 95% confidence intervals calculated the same way as those for the lidar emission rates for periods with three or more valid downwind samples of each size.

Table 23. Mean emission rates per unit area per unit time (± 95% CI for $n \geq 3$) for each operation as determined by inverse modeling using ISCST3.

Sample	Operation	# of passes	$PM_{2.5}$ ($\mu g/m^2/s$)		PM_{10} ($\mu g/m^2/s$)		TSP ($\mu g/m^2/s$)	
			MiniVol	OPC	MiniVol	OPC	MiniVol	OPC
Conservation Tillage Method								
May 17 R1	Strip-till	1	2.7 ± 0.5	1.0 ± 0.1	21.8 ± 4.9	30.7 ± 4.5	108.3 ± 54.1	147.9 ± 33.0
June 7	Plant	1	6.5	0.3 ± 0.2	6.7	8.5 ± 1.8	41.9 ± 25.7	43.3 ± 11.4
June 11	Herbicide Application	1	12.1	0.2 ± 0.1	16.5	10.4 ± 4.1	31.6 ± 14.9	30.0 ± 16.9
Summed Emissions		**3**	**21.3**	**1.5 ± 0.2**	**45.0**	**49.7 ± 6.3**	**181.7 ± 61.7**	**221.2 ± 38.8**
Conventional Tillage Method								
May 17 R2	Break down in-field borders (spread over entire field area)	2	---	0.3 ± 0.1	---	24.0 ± 5.3	3.2	288.8 ± 51.6
May 18	Chisel	1	---	0.4 ± 0.1	---	12.7 ± 6.3	---	79.5 ± 27.2
May 19 R1	Disc 1	1	---	0.8 ± 0.3	---	30.7 ± 12.4	---	203.2 ± 86.1
May 19 R2	Disc 2	1	---	1.1 ± 0.3	---	53.1 ± 18.1	---	310.7 ± 75.8
May 20 R1	Lister	1	---	1.0 ± 0.1	---	42.5 ± 4.8	---	245.2 ± 42.0
May 20 R2	Build up ditch and borders	4, 2	---	---	---	---	---	---
June 5 R1	Break down ditch, break down borders, Cultivator 1 & 2, Roller	12, 4, 2, 1	1.5 ± 0.6	0.2 ± 0.1	3.1 ± 1.6	3.7 ± 1.6	---	18.7 ± 11.3
June 5 R2	Plant	1	6.1 ± 0.6	0.4 ± 0.2	---	10.0 ± 3.9	33.1	52.7 ± 19.3
June 18	Fertilizer Injection	1	12.6 ± 11.4	3.9 ± 2.9	102.9 ± 63.1	116.8 ± 61.0	682.7	841.5 ± 387.2
June 25	Cultivator 3	1	0.9 ± 0.1	0.3 ± 0.1	6.6 ± 3.1	9.9 ± 3.8	55.1 ± 8.1	65.9 ± 22.1
Summed Emissions		**13**	**---**	**9.4 ± 2.9**	**---**	**344.8 ± 66.1**	**---**	**2498.2 ± 415.5**

Table 24. Mean emission rates per unit area (± 95% CI for $n \geq 3$) for each operation as determined by inverse modeling using ISCST3.

Sample	Operation	# of passes	$PM_{2.5}$ (mg/m^2/ operation)		PM_{10} (mg/m^2/ operation)		TSP (mg/m^2/ operation)	
			MiniVol	OPC	MiniVol	OPC	MiniVol	OPC
Conservation Tillage Method								
May 17 R1	Strip-till	1	29.9 ± 5.9	10.7 ± 1.6	239.2 ± 54.1	337.6 ± 49.0	1189.1 ± 593.9	1623.7 ± 362.0
June 7	Plant	1	89.6	4.5 ± 2.1	92.5	117.2 ± 24.8	575.6 ± 353.3	595.9 ± 157.4
June 11	Herbicide Application	1	40.5	0.6 ± 0.3	55.3	34.8 ± 13.7	105.8 ± 50.0	100.4 ± 56.7
Summed Emissions		**3**	**159.9**	**15.9 ± 2.7**	**386.9**	**489.6 ± 56.6**	**1870.4 ± 692.8**	**2320.0 ± 398.7**
Conventional Tillage Method								
May 17 R2	Break down in-field borders (spread over entire field area)	2	---	1.1 ± 0.3	---	79.5 ± 17.7	10.5	956.6 ± 170.8
May 18	Chisel	1	---	9.5 ± 2.3	---	282.9 ± 140.4	---	1767.8 ± 605.0
May 19 R1	Disc 1	1	---	13.7 ± 5.6	---	533.3 ± 215.9	---	3533.4 ± 1497.6
May 19 R2	Disc 2	1	---	18.3 ± 5.5	---	904.5 ± 308.3	---	5290.4 ± 1291.0
May 20 R1	Lister	1	---	17.7 ± 1.2	---	775.1 ± 87.1	---	4475.3 ± 766.8
May 20 R2	Build up ditch and borders	4, 2	---	---	---	---	---	---
June 5 R1	Break down ditch, break down borders, Cultivator 1 & 2, Roller	12, 4, 2, 1	40.2 ± 16.4	5.6 ± 3.3	84.1 ± 42.8	100.2 ± 42.2	---	498.9 ± 301.7
June 5 R2	Plant	1	84.0 ± 8.6	5.1 ± 2.8	---	137.6 ± 53.5	454.6	724.6 ± 265.0
June 18	Fertilizer Injection	1	48.8 ± 44.3	15.1 ± 11.2	400.1 ± 245.2	454.3 ± 237.0	2654.3	3271.6 ± 1505.5
June 25	Cultivator 3	1	12.7 ± 2.0	4.4 ± 1.7	94.8 ± 45.5	142.9 ± 54.8	796.7 ± 117.6	954.4 ± 320.3
Summed Emissions		**13**	**---**	**107.1 ± 15.5**	**---**	**3833.0 ± 489.9**	**---**	**24381.5 ± 2781.5**

Table 25. Mean emission rates per unit area per unit time (± 95% CI for $n \geq 3$) for each operation as calculated by inverse modeling using AERMOD.

Sample	Operation	# of passes	$PM_{2.5}$ ($\mu g/m^2/s$)		PM_{10} ($\mu g/m^2/s$)		TSP ($\mu g/m^2/s$)	
			MiniVol	OPC	MiniVol	OPC	MiniVol	OPC
Conservation Tillage Method								
May 17 R1	Strip-till	1	2.7 ± 0.5	1.2 ± 0.2	25.1 ± 7.0	36.2 ± 7.3	131.9 ± 74.0	174.6 ± 49.8
June 7	Plant	1	6.5	0.4 ± 0.2	6.8	9.2 ± 1.8	46.3 ± 27.1	47.0 ± 12.1
June 11	Herbicide Application	1	12.1	0.2 ± 0.1	15.6	10.2 ± 3.1	33.8 ± 19.8	28.3 ± 14.2
Summed Emissions		**3**	**21.3**	**1.7 ± 0.3**	**47.5**	**55.6 ± 8.1**	**212.1 ± 81.3**	**249.9 ± 53.2**
Conventional Tillage Method								
May 17 R2	Break borders (spread over entire field area)	2	---	0.4 ± 0.1	---	25.0 ± 4.6	4.0	301.7 ± 42.0
May 18	Chisel	1	---	0.5 ± 0.2	---	18.4 ± 6.9	---	93.7 ± 36.2
May 19 R1	Disc 1	1	---	1.0 ± 0.6	---	40.5 ± 21.4	---	269.0 ± 143.4
May 19 R2	Disc 2	1	---	1.2 ± 0.6	---	56.2 ± 33.1	---	325.7 ± 179.1
May 20 R1	Lister	1	---	0.9 ± 0.1	---	39.2 ± 4.7	---	226.3 ± 41.9
May 20 R2	Build up ditch and borders	4, 2	---	---	---	---	---	---
June 5 R1	Break down ditch, break down borders, Cultivator 1 & 2, Roller	12, 4, 2, 1	1.5 ± 0.6	0.2 ± 0.2	3.4 ± 1.7	4.4 ± 1.7	---	21.6 ± 12.0
June 5 R2	Plant	1	6.1 ± 0.6	0.4 ± 0.2	---	10.4 ± 3.0	40.4	54.9 ± 14.1
June 18	Fertilizer Injections	1	12.6 ± 11.4	3.9 ± 2.9	102.7 ± 64.5	115.9 ± 60.9	692.4	829.6 ± 376.4
June 25	Cultivator 3	1	0.9 ± 0.1	0.5 ± 0.2	10.7 ± 4.9	16.5 ± 5.7	90.3 ± 13.7	110.5 ± 32.0
Summed Emissions		**13**	**---**	**10.4 ± 3.0**	**---**	**376.8 ± 73.9**	**---**	**2688.5 ± 451.2**

Table 26. Mean emission rates per unit area (± 95% CI for $n \geq 3$) for each operation as calculated by inverse modeling using AERMOD.

Sample	Operation	# of passes	$PM_{2.5}$ (mg/m^2/ operation)		PM_{10} (mg/m^2/ operation)		TSP (mg/m^2/ operation)	
			MiniVol	OPC	MiniVol	OPC	MiniVol	OPC
Conservation Tillage Method								
May 17 R1	Strip-till	1	31.7 ± 5.6	12.7 ± 2.8	275.8 ± 76.7	397.2 ± 80.4	1448.3 ± 812.5	1917.1 ± 547.0
June 7	Plant	1	91.5	4.9 ± 2.2	93.5	126.9 ± 25.1	636.8 ± 372.8	645.9 ± 166.2
June 11	Herbicide Application	1	36.7	0.6 ± 0.3	52.1	34.1 ± 10.3	113.3 ± 66.2	94.7 ± 47.5
Summed Emissions for Conservation Tillage		**3**	**159.9**	**18.1 ± 3.5**	**421.4**	**558.2 ±84.9**	**2198.4 ± 896.4**	**2657.7 ± 573.7**
Conventional Tillage Method								
May 17 R2	Break borders (spread over entire field area)	2	---	1.2 ± 0.3	---	83.0 ± 15.4	130.6	999.1 ± 139.2
May 18	Chisel	1	---	11.3 ± 4.2	---	409.5 ± 154.2	---	2085.4 ± 804.5
May 19 R1	Disc 1	1	---	18.0 ± 9.9	---	704.7 ± 372.4	---	4677.8 ± 2492.6
May 19 R2	Disc 2	1	---	20.2 ± 9.9	---	957.7 ± 564.2	---	5545.3 ± 3049.5
May 20 R1	Lister	1	---	16.3 ± 1.7	---	714.8 ± 86.3	---	4131.1 ± 764.0
May 20 R2	Build up ditch and borders	4, 2	---	---	---	---	---	---
June 5 R1	Break down ditch, break down borders, Cultivator 1 & 2, Roller	12, 4, 2, 1	43.8 ± 11.1	6.6 ± 4.1	90.3 ± 45.6	116.5 ± 46.0	---	578.0 ± 320.8
June 5 R2	Plant	1	86.9 ± 13.5	5.2 ± 2.5	---	142.6 ± 40.7	555.6	754.5 ± 193.6
June 18	Fertilizer Injections	1	50.3 ± 46.7	15.0 ± 11.2	399.4 ± 250.7	450.5 ± 236.9	2692.1	3225.5 ±1493.4
June 25	Cultivator 3	1	21.0 ± 3.4	7.5 ± 2.8	155.5 ± 71.6	239.3 ± 82.3	1307.3 ± 198.0	1599.8 ± 462.7
Summed Emissions for Conventional Tillage		**13**	**---**	**123.1 ± 20.4**	**---**	**4374.0 ± 752.6**	**---**	**27,351.4 ± 4438.3**

4.5 DERIVED EMISSION RATE COMPARISON

Two emission rate determination approaches were employed to calculate three different sets of emission rates in order to quantify differences between conventional tillage methods and a conservation tillage method using strip-till technology. Problems with filter-based PM measurements prevented emission rate calculations for all size fractions over five consecutive sample periods and some size fractions during two other periods, preventing the summation of ISCST3- and AERMOD-based emission rates for MiniVol data across the conventional tillage

method operations. The OPC-based PM measurements passed QA/QC and were used to calculate emission rates through inverse modeling for all size fractions for all sample periods. The lidar system effectively sampled the vertical downwind plane and measured time-resolved plume characteristics for each operation at each particulate size fraction, except for when a critical component failure in the lidar system prevented it from collecting data for the last tillage operation. Sample period average emission rates, with their respective error estimates, are shown in Figure 42 for comparison when values from all methods are available.

A summary table of the PM_{10} emission rates calculated from each approach is given in Table 27 for comparison. The calculated PM_{10} emission rates demonstrate that for total mass of PM_{10} per unit area per unit time of operation ($\mu g/m^2/s$), the conservation tillage method produced about 10% as much as the conventional method based on lidar measurements. PM_{10} emission rates calculated by the lidar and the inverse modeling method are within the extent of their 95% confidence intervals for the May 19 R2, June 5 R1, and June 18 samples, while differences between them are statistically significant for the May 17 R1, May 18, May 19 R1, and June 5 R2 samples. Another difference is that the filter and OPC-based inverse modeling did report emission rates for the herbicide application in the conservation tillage field while the lidar reported upwind and downwind concentration differences less than the MDL. A potential explanation for this is that the lidar beam was only able to come down to 6-8 m agl for safety reasons, while most filter and OPC samplers were located below this level. If a plume stayed close to the ground, the lidar may have been unable to detect it.

The largest difference in derived emission rates is between the model-derived values and the lidar. This is likely due to the fact that ISCST3 and AERMOD are very similar numerical models and the lidar measures actual fluxes. The models are limited to the types and configuration of sources that can be used (point source, volume source, area source, or line source), which means that a compromise must be made when dealing with a small, moving area source such as is the case in agricultural tillage. Also, the temporal and spatial resolution of the lidar allows it to see micro-scale variations in plume characteristics and movement such as plume strength, frequency, lofting and detachment from the surface, wind direction and wind speed effects.

The models must assume a constant emission from the entire emitting surface area, while the lidar sees the plume movement as the tractor moves across the field. This kind of microstructure cannot be captured by the long-term sampling required for implementation of ISCST3 and AERMOD. Consequently, ISCST3 and AERMOD are incapable of generating fine levels of spatial and temporal detail. As discussed previously [7], examples of such differences in technique are evident when comparing single-scan and sample period average PM concentrations measured by the lidar with average modeled concentrations in a vertical plane. In this work, it is obvious that the plumes measured by lidar were detected at much higher elevations than predicted by the models, as observed by the greater than background concentrations measured at heights up to and exceeding 100 m. Since the point sensors were deployed near the surface (at 2 and 9 m) downwind of the source, these higher plumes were only sampled by the lidar.

Another factor to consider is the exhaust emissions from the tractor engines. The report detailing the comparison of fall CMP and conventional tillage method measurements and findings [7], the companion study to the study herein described, calculated exhaust PM_{10} emissions based on fuel usage information provided by the cooperating producer and a fuel use-based PM_{10} exhaust emission rate given by Kean et al. [30]. Exhaust emissions in the fall tillage report were

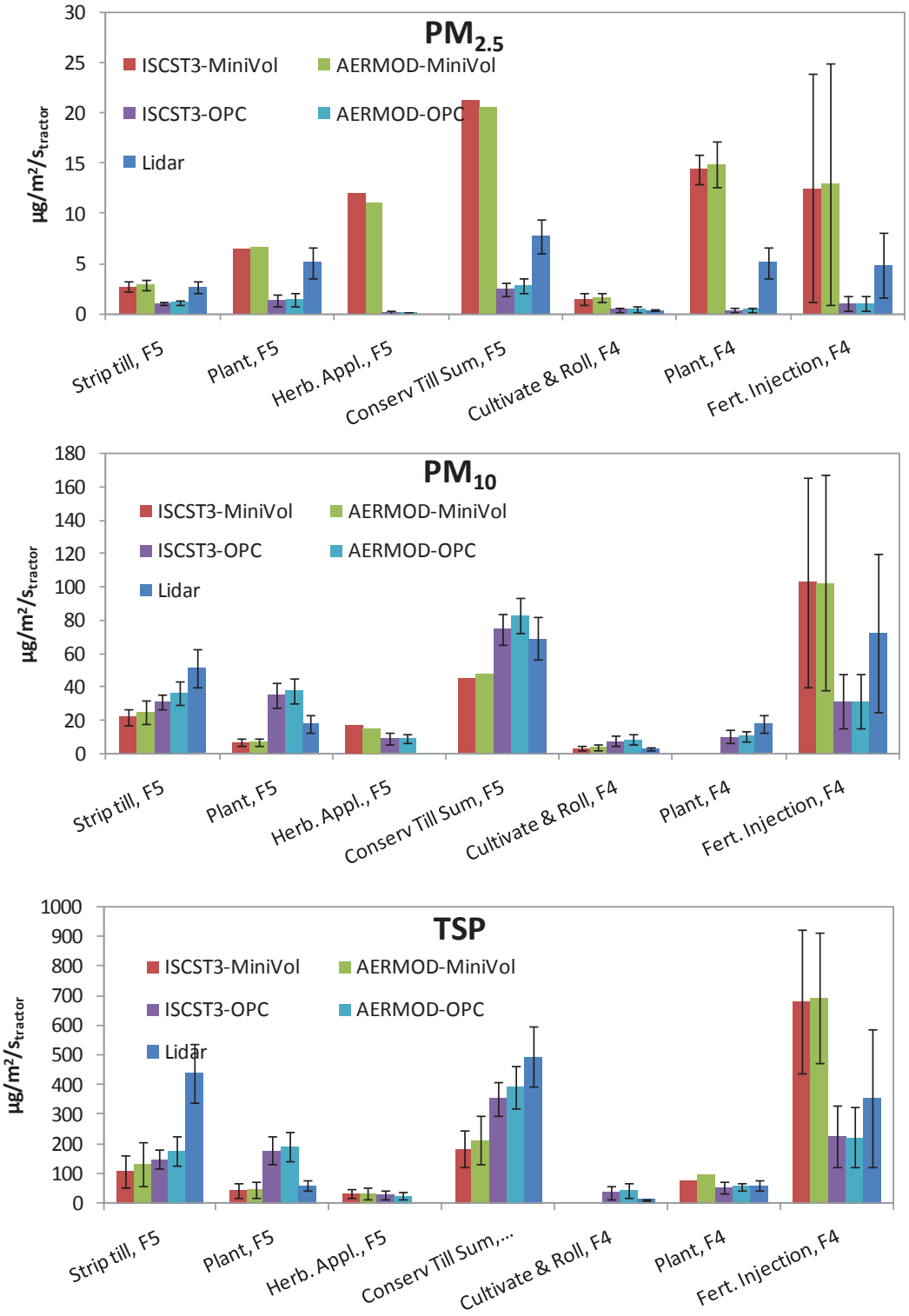

Figure 42. A comparison of $PM_{2.5}$, PM_{10}, and TSP emission rates ± 95% confidence intervals derived through lidar scanning techniques and inverse modeling using ISCST3 and AERMOD dispersion models and measured PM concentrations.

Table 27. Calculated PM_{10} emission rates (± 95% confidence interval) from the lidar and inverse modeling using two dispersion models.

Sample	Operation	Emission Rates (µg/m²/s)				
		Lidar	ISCST3		AERMOD	
			MiniVol	OPC	MiniVol	OPC
Conservation Tillage Method						
May 17 R1	Strip-till	47.7 ± 10.7	21.8 ± 4.9	30.7 ± 4.5	25.1 ± 7.0	36.2 ± 7.3
June 7	Plant	12.8 ± 3.8	6.7	8.5 ± 1.8	6.8	9.2 ± 1.8
June 11	Herbicide Application	< MDL	16.5	10.4 ± 4.1	15.6	10.2 ± 3.1
Sum for Conservation Tillage (mg/m²)		**60.5 ± 11.4**	**45.0**	**49.7 ± 6.3**	**47.5**	**55.6 ± 8.1**
Conventional Tillage Method						
May 17 R2	Bread down in-field borders	10.2 ± 6.3	---	24.0 ± 5.3	---	25.0 ± 4.6
May 18	Chisel	50.9 ± 5.6	---	12.7 ± 6.3	---	18.4 ± 6.9
May 19 R1	Disc 1	196.2 ± 46.0	---	30.7 ± 12.4	---	40.5 ± 21.4
May 19 R2	Disc 2	62.6 ± 17.2	---	53.1 ± 18.1	---	56.2 ± 33.1
May 20 R1	Lister	252.5 ± 106.3	---	42.5 ± 4.8	---	39.2 ± 4.7
May 20 R2	Build ditch and field edge borders	151.6 ± 70.1	---	---	---	---
June 5 R1	Break down ditch and field edge borders, Cultivator Passes 1 2, Roller	4.1 ± 0.8	3.1 ± 1.6	3.7 ± 1.6	3.4 ± 1.7	4.4 ± 1.7
June 5 R2	Plant	5.8 ± 1.5	---	10.0 ± 3.9	---	10.4 ± 3.0
June 18	Fertilizer Injection	35.8 ± 23.6	102.9 ± 63.1	116.8 ± 61.0	102.7 ± 64.5	115.9 ± 60.9
June 25	Cultivator Pass 3	---	6.6 ± 3.1	9.9 ± 3.8	10.7 ± 4.9	16.5 ± 5.7
Sum	**Conventional**	**644.5 ± 120.0**	**---**	**344.8 ± 66.1**	**---**	**376.8 ± 73.9**

predicted to generally be lower than 10% of the derived lidar-based tillage emission rates, and therefore were not considered to be significant contributors to produced particulate matter. Fuel usage was not monitored during this comparison study for spring CMP and conventional tillage methods reported herein, therefore prohibiting the calculation of PM_{10} exhaust emissions. However, similar percent-based contributions to the total measured PM emissions were expected to apply. Therefore, it was assumed that the tractor exhaust emissions during the spring tillage comparison study were not significant contributors to the derived emission rates.

5. SUMMARY AND CONCLUSIONS

A project to determine the control effectiveness of Conservation Management Practices (CMPs) for agricultural tillage was funded by the San Joaquin Valleywide Air Pollution Study Agency and carried out in the San Joaquin Valley of California in May and June of 2008. The study was conducted to quantify particulate emissions ($PM_{2.5}$, PM_{10}, and TSP) from conventional agricultural tillage methods and a conservation tillage CMP utilizing an Orthman 1-tRIPr, a strip-till implement. The Orthman 1-tRIPr is a tillage implement that incorporates multiple conventional tillage implements into one piece of equipment and applies these to narrow strips across the field, as opposed to the conventional tillage method which applies more operations to the entire surface area of the field. The objective of this study was to address three fundamental research questions:

1) What are the magnitude, flux, and transport of PM emissions produced by agricultural practices for row crops where tillage CMPs are being implemented vs. the magnitude, flux, and transport of PM emissions produced by agricultural practices where CMPs are not being implemented?
2) What are the control efficiencies of equipment being used to implement the "conservation tillage" CMP? If resources allow assessing additional CMPs, what are the control efficiencies of the "equipment change/technological improvements" CMP?
3) Can these CMPs for a specific crop be quantitatively compared, controlling for soil type, soil moisture, and meteorological conditions?

The study was carried out from May 15 until June 25, 2008 in the San Joaquin Valley of California on a commercial production farm. Two adjacent fields with the same crop and similar soil properties were selected for observation. The study investigated conventional 13-pass spring tillage sequence for a field going from winter wheat to corn was: in-field irrigation border breakdown (x2), chisel, disc (x2), lister, cultivate (x2), top roll, plant, fertilizer injection, and cultivate (x2). The conservation tillage CMP sequence consisted of three passes: strip-till, plant/fertilize, and herbicide spray. Both fields also required passes over very small areas (<5% of total field area) to build and break down ditches and field-edge borders, but this step was only measured in the conventional tillage application. Particulate emissions were determined using arrayed filter and optical-based sampling coupled with inverse modeling, using both ISCST3 and AERMOD, as well as advanced scanning lidar techniques. Supporting operation characteristics (operation time, number of tractors in operation, potential contamination issues, etc.) were recorded and meteorological, soil characteristic, and particle chemical composition measurements were made and are reported in this document.

Overloading of downwind filter-based samplers and contaminated upwind samplers prevented emission rates from being calculated through inverse modeling for some or all PM size fractions during seven sample periods. The collocated OPCs were found to have not been overloaded, thus allowing emission rates to be calculated from mass converted OPC data for all sample periods. The scanning lidar technology employed was able to calculate emissions for all but one measurement period.

Table 28 summarizes PM_{10} aerosol emission values found during this study along with results from previous studies found in the literature in units of mass emitted per unit area tilled. The summed emissions for the conventional tillage method based on lidar data includes the following

13 passes in order: two break down in-field border passes, chisel, two disc passes, lister, two cultivator passes, roll, plant, fertilizer injection, and two more cultivator passes. The summed conservation tillage sequence consists of the following three passes: strip-till, plant, and herbicide application.

Some of the values herein reported are in agreement with those reported by Flocchini et al. (2001) and Madden et al. (2008), as well as the PM_{10} emission factors used by CARB, such as the strip-till and plant passes in the conservation tillage method and the cultivate and roll passes in conventional tillage [12][16][13]. Other emission rates are different and larger than previous values reported in the literature, especially the discing 1 and 2, chisel, and lister passes of the conventional tillage, though those derived through inverse modeling are below the estimated 95% level for their respective distributions as presented in the uncertainty calculations in this report. The lidar-derived emission rates for the disc 1, disc 2, chisel, and lister passes are high when compared to values found by inverse modeling coupled with OPC PM data, values in the literature for the same operations, and values reported in the 2007 fall CMP tillage study which used the same lidar methodology. These relatively high emission rates provide indirect support for the conclusion that downwind PM samplers were likely overloaded during those sample periods by high aerosol concentrations. While the values from listed published studies are generally not in close agreement, they are relatively well fit by lognormal or Weibull distributions, which have previously been shown to represent emissions factors datasets well [31]. In addition, they are within the range of the variability expected from measurements made under different meteorological and soil conditions, as demonstrated by the wide range of values from Flocchini et al. (2001) [12] summarized in Table 2. The results from this campaign are not in as good agreement as previous results have been [7]. In general our results are larger than their corresponding literature values.

Emission rates for $PM_{2.5}$, PM_{10}, and TSP from both lidar data and inverse modeling coupled with OPC data by operation are presented in Table 29 in units of mass emitted per unit area tilled per operation pass, along with the average tillage rate in hours per hectare where the hour represents total tractor operation time. In the case where two tractors were operating at the same time for the duration of the sample period, the total tractor operation time would be twice that of the elapsed time of the operation. Comparisons were made between the conventional and CMP tillage practices based on these variables and are shown in the same table. The conservation tillage method produced 9.5% as much $PM_{2.5}$, 6.3% as much PM_{10}, and 9.1% as much TSP as the conventional method according to the lidar data and 14.7% as much $PM_{2.5}$, 12.8% as much PM_{10}, and 9.7% as much TSP as the conventional method according to the AERMOD-OPC combination. Therefore, the control efficiency of the CMP for particulate emissions from these three data sets was as follows: lidar – 0.91, 0.94, and 0.91 for $PM_{2.5}$, PM_{10}, and TSP, respectively; and AERMOD-OPC – 0.85, 0.87, and 0.90 for $PM_{2.5}$, PM_{10}, and TSP, respectively.

The control efficiency (η) was calculated according to Eq. 23, which was based on a collection efficiency equation found in Cooper and Alley (2002)

$$\eta = \frac{E_{CT} - E_{ST}}{E_{CT}} \tag{23}$$

where E_{CT} is the calculated emission rate for the conventional tillage method and E_{ST} is the calculated emission rate for the strip-till conservation tillage method [58]. These differences in

total emissions per tillage treatment are significant at the 99.99% level for $PM_{2.5}$, PM_{10}, and TSP for both emissions calculation methodologies employed.

Table 28. A comparison of PM_{10} emission rates herein derived and found in literature.

Operation	Flocchini et al. (2001) [12] *	Madden et al. (2008) [16] *	CARB (2003a) [13]	Previous SDL CMP Study: Lidar [7] *	This study				
					Lidar	ISCST3		AERMOD	
						MiniVol	OPC	MiniVol	OPC
	(mg/m^2)	(mg/m^2)	(mg/m^2)	(mg/m^2)	(mg/m^2)	(mg/m^2)	(mg/m^2)	(mg/m^2)	(mg/m^2)
Conservation Tillage Method									
Strip-till		180.5			523.8 ± 117.8	239.2 ± 54.1	337.6 ± 49.0	275.8 ± 76.7	397.2 ± 80.4
Plant		233.8			175.6 ± 52.6	92.5	117.2 ± 24.8	93.5	126.9 ± 25.1
Herbicide Application					< MDL	55.3	34.8 ± 13.7	52.1	34.1 ± 10.3
Conservation Method Sum					**699.4 ± 129.0**	**386.9**	**489.6 ± 56.6**	**421.4**	**558.2 ±84.9**
Conventional Tillage Method									
Break down in-field borders					33.6 ± 20.8	---	79.5 ± 17.7	---	83.0 ± 15.4
Chisel	512.2		134.5	74.3	1132.8 ± 123.9	---	282.9 ± 140.4	---	409.5 ± 154.2
Disc 1	166.1	161.8		99.7	3410.7 ± 799.9	---	533.3 ± 215.9	---	704.7 ± 372.4
Disc 2	58.5	612.5		80.7	1066.4 ± 293.2	---	904.5 ± 308.3	---	957.7 ± 564.2
Lister		540.5	134.5		4608.1 ± 1940.8	---	775.1 ± 87.1	---	714.8 ± 86.3
Cultivate 1& 2 and Roll		302.4	89.7		109.4 ± 21.3	84.1 ± 42.8	100.2 ± 42.2	90.3 ± 45.6	116.5 ± 46.0
Plant		235.8			79.5 ± 20.2	---	137.6 ± 53.5	---	142.6 ± 40.7
Fertilizer Injection					139.4 ± 91.9	400.1 ± 245.2	454.3 ± 237.0	399.4 ± 250.7	450.5 ± 236.9
Cultivate 3		236.5	89.7		---	94.8 ± 45.5	142.9 ± 54.8	155.5 ± 71.6	239.3 ± 82.3
Conventional Method Sum					**11,051.2 ± 2,126.0**	**---**	**3833.0 ± 489.9**	**---**	**4374.0 ± 752.6**

* Average of available data per operation when applicable

Table 29. Particulate emissions, from Lidar data and inverse modeling with OPC data, and tillage rate comparison between conventional and conservation tillage.

	Average Emission Rates ± 95% CI (mg/m^2)						Average Tillage Rate (hr/hect.)
	$PM_{2.5}$		PM_{10}		TSP		
	Lidar	AERMOD-OPC	Lidar	AERMOD-OPC	Lidar	AERMOD-OPC	
Conservation Tillage Method							
Strip-till	26.9 ± 6.1	12.7 ± 2.8	523.8 ± 117.8	397.2 ± 80.4	4,450.5 ± 1,000.9	1,917.1 ± 547.0	0.337
Plant	50.2 ± 15.0	4.9 ± 2.2	175.6 ± 52.6	126.9 ± 25.1	567.6 ± 169.9	645.9 ± 166.2	0.422
Herbicide Application	< MDL	0.6 ± 0.3	< MDL	34.1 ± 10.3	< MDL	94.7 ± 47.5	0.103
Sum	**77.1 ± 16.2**	**18.1 ± 3.5**	**699.4 ± 129.0**	**558.2 ± 84.9**	**5,018.1 ± 1,015.2**	**2,657.7 ± 573.7**	**0.862**
Conventional Tillage Method							
Break down in-field borders	3.0 ± 1.8	1.2 ± 0.3	33.6 ± 20.8	83.0 ± 15.4	152.3 ± 94.4	999.1 ± 130.6	0.455
Chisel	101.1 ± 11.1	11.3 ± 4.2	1132.8 ± 123.9	409.5 ± 154.2	4,997.9 ± 546.8	2,085.4 ± 804.5	0.726
Disc 1	210.1 ± 49.3	18.0 ± 9.9	3410.7 ± 799.9	704.7 ± 372.4	17,440.2 ± 4,090.4	4,677.8 ± 2,492.6	0.481
Disc 2	58.9 ± 16.2	20.2 ± 9.9	1066.4 ± 293.2	957.7 ± 564.2	6,023.4 ± 1,655.8	5,545.3 ± 3,049.5	0.471
Lister	302.8 ± 127.5	16.3 ± 1.7	4608.1 ± 1940.8	714.8 ± 86.3	23,375.6 ± 9,845.2	4,131.1 ± 764.0	0.406
Break down ditches, Cultivator passes 1 and 2, & Roller	22.9 ± 4.5	6.6 ± 4.1	109.4 ± 21.3	116.5 ± 46.0	354.0 ± 69.0	578.0 ± 320.8	0.311
Plant	8.3 ± 2.1	5.2 ± 2.5	79.5 ± 20.2	142.6 ± 40.7	285.3 ± 72.4	754.5 ± 193.6	0.289
Fertilizer Injection	9.4 ± 6.2	15.0 ± 11.2	139.4 ± 91.9	450.5 ± 236.9	684.1 ± 451.3	3,225.5 ± 1,493.4	0.283
Cultivator Passes 3 & 4	---	7.5 ± 2.8	---	239.3 ± 82.3	---	1,599.8 ± 462.7	0.400
Sum	**811.1 ± 138.7**	**123.1 ± 20.4**	**11,051.2 ± 2,126.0**	**4,374.0 ± 752.6**	**54,881.3 ± 10,814.4**	**27,351.4 ± 4,438.3**	**5.30**
Comparison of Methods							
Control Efficiency, η	**0.905**	**0.853**	**0. 937**	**0.872**	**0.909**	**0.903**	**---**
Percent Reduction	90.5	85.3	93.7	87.2	90.9	90.3	83.7
Statistically Significant Difference (α 0.0001)	Yes	Yes	Yes	Yes	Yes	Yes	Unknown

The time per hectare required to perform the CMP work was 16.3% of the conventional method, similar to the percent difference between PM emissions of the two treatments. It is interesting to note that while the absolute values of calculated emissions are different between the two techniques, the control efficiencies are very close to each other. Also, the control efficiencies are similar across the three size fractions. It should be noted that other reductions in emissions between the two tillage management practices are likely to have occurred, mainly due to decreased fuel usage in tractor engines. Unlike the previously conducted companion study, fuel usage was not quantified in this study and prevented accounting for the associated reductions in emissions. However, these reductions are expected to be similar to the reduction in tractor operation time (~85%).

Our lidar measurements indicate comparable levels of suspended particulate as is predicted by our modeling. Previous results supported the use of lidar measurements as an important complement to ground-based sensors because ground-based sensors cannot measure elevated plumes and ISCST3 and AERMOD would realize significant benefit if lidar-derived information could be incorporated into their calculations. The present results are consistent with that claim as during this campaign we were able to generate a more consistent picture of the emission rates using both technologies.

6. LESSONS LEARNED

The sampling difficulties encountered during this field study, specifically concerning filter-based measurements, prompt us to provide a list of practices and procedures that can mitigate these problems in future field measurements. There are several lessons to be learned from the experiences of this study.

1) Each kind of instrument has a specific operational range in terms of concentration, mass, temperature, etc. Therefore, adequate accommodations must be made during the planning stages of the field exercise such that each instrument can operate within its specified range. In this study, $PM_{2.5}$ and PM_{10} MiniVol samplers were very likely overwhelmed by concentrated plumes from the tillage operations during five sample periods. To prevent overwhelming the samplers in future field measurements, they can be moved further away from the source, thereby allowing more time and distance for dispersion of the plume and a decrease in concentration.

2) Frequent (e.g. daily or even immediately prior to each sampler period) inspection of instrument condition is important and may provide early warnings of potential problems, especially in high concentration conditions. During this experiment large crustal particles and organic matter were found in the sample head assembly, pointing to potential problems with the impactor, overloading of the sampler, and/or contamination. In addition, very heavy cumulative particle loading of the silicon vacuum grease used in the impactor assembly to prevent particle bounce and/or re-entrainment was observed after the May sample periods. Heavy loading of the grease may increase the probability of particle bounce and/or re-entrainment into the air stream. These two observations lead us to the conclusion that extreme vigilance regarding instrument condition is required at all times – the MiniVols shall not be considered "set and forget" instruments. In the present case, had we performed a more thorough daily inspection of the sampler heads we would have been able to take corrective action earlier. One example of corrective action is, in the case of $PM_{2.5}$ samplers, is to install a PM_{10} impactor upstream of the $PM_{2.5}$ impactor head to act as an additional large particle filter and decrease the overall loading on the $PM_{2.5}$ impactor. Another preventative action is to clean and regrease the MiniVol impactor assemblies after each use if exposed to high aerosol concentrations.

3) Filter handling and storage must occur in a clean environment, with potential contamination factors minimized. During this experiment, filter handling was performed onsite in a trailer. While it was maintained as clean as possible, there were high winds with blowing dust on May 20 that may have been a source of contamination on the filters being handled. If an adequately clean onsite filter processing location cannot be identified, an appropriate solution might be to transport the impactor heads to an offsite location for processing (such as a hotel room).

Careful application of these lessons learned will help prevent future problems similar to those encountered during this field campaign. However, constant evaluation of actual conditions for potential problems is strongly encouraged, with proper mitigation promptly employed.

In addition to the above lessons learned, peer review of this report also brought to our attention that measurements of additional parameters should be considered in future studies. Specifically,

it was suggested that soil surface temperature measurements be made. Differences in soil surface temperature may result in different vertical and horizontal PM dispersion (with all other conditions being equal) as surface conditions are known to affect turbulence and dispersion.

7. ACKNOWLEDGMENTS

The Space Dynamics Laboratory would like to thank the individuals and groups whose efforts made this study and subsequent analysis possible. Cooperators include the USDA-ARS National Laboratory for Agriculture and the Environment (Dr. Jerry Hatfield, Dr. John Prueger, and Dr. Richard Pfeiffer), Utah State University (Mark Erupe, Dr. Randy Martin, Derek Price, Emyrei Reese, Dr. Phil Silva), U.S. EPA (Sona Chilingaryan, Kerry Drake, Ron Myers, Dr. Robert Vanderpool, and Dr. David J. Williams), the San Joaquin Valleywide Air Pollution Study Agency, the San Joaquin Valley Ag Technical Group, the San Joaquin Valley Air Pollution Control District (Jessi Fiero, Sheraz Gill, Ramon Norman, Samir Sheikh, Patia Siong, James Sweet), California Air Resources Board (Kevin Eslinger, Shelby Livingston, Karen Magliano) and the cooperative agricultural producers and industry representatives. Individuals from SDL who participated in the field measurement campaign or contributed to the report include Dr. Gail Bingham, Bill Bradford, Jennifer Bowman, Eve Day, Carrie Farmer, Eva Gillespie, Cassi Going, Dr. Allen Howard, Everett Ito, Derek Jones, Tanner Jones, Spencer Kitchen, Richard Larsen, Christian Marchant, Kori Moore, Brad Peterson, Andrew Pound, Shane Topham, Nathan Whipple, Dr. Tom Wilkerson, Dr. Michael Wojcik, Cordell Wright and Dr. Vladimir Zavyalov.

8. PUBLICATIONS

G. E. Bingham, C. C. Marchant, V. V. Zavyalov, D. J. Ahlstrom, K. D. Moore, D. S. Jones, T. D. Wilkerson, L. E. Hipps, R. S. Martin, J. L. Hatfield, J. H. Prueger, R. L. Pfeiffer. 2009. Lidar based emissions measurement at the whole facility scale: Method and error analysis. Journal of Applied Remote Sensing 3(1):033510 [doi: 10.1117/12.829411].

C. C. Marchant, T. D. Wilkerson, G. E. Bingham, V. V. Zavyalov, J. M. Andersen, C. B. Wright, S. S. Cornelsen, R. S. Martin, P. J. Silva, J. L. Hatfield. 2009. Aglite lidar: A portable elastic lidar system for investigating aerosol and wind motions at or around agricultural production facilities. Journal of Applied Remote Sensing 3(1):033511 [doi: 10.1117/12.829412].

C. C. Marchant, K. D. Moore, M. D. Wojcik, R. S. Martin, R. L. Pfeiffer, J. H. Prueger, J. L. Hatfield. 2011. Estimation of dairy particulate matter emission rates by lidar and inverse modeling. Transactions of ASABE 54:1453-1463.

K. D. Moore, M. D. Wojcik, C. C. Marchant, R. S. Martin, R. L. Pfeiffer, J. H. Prueger, J. L. Hatfield. 2011. "Comparisons of measurements and predictions of PM concentrations and emission rates from a wind erosion event," in *Proc. International Symposium on Erosion and Landscape Evolution (ISELE) 2011*, D. C. Flanagan, J. C. Ascough II, and J. L. Nieber, eds., American Society of Agricultural and Biological Engineers, St. Joseph.

K. D. Moore, M. D. Wojcik, R. S. Martin, C. C. Marchant, G. E. Bingham, R. L. Pfeiffer, J. H. Prueger, J. L. Hatfield. 2013. Particulate emissions calculations from fall tillage operations using point and remote sensors. Journal of Environmental Quality [doi: 10.2134/jeq2013.01.0009].

M. D. Wojcik, G. E. Bingham, C. C. Marchant, V. V. Zavyalov, D. J. Ahlstrom, K. D. Moore, T. D. Wilkerson, L. E. Hipps, R. S. Martin, J. L. Hatfield, J. H. Prueger. "Lidar based particulate flux measurements of agricultural field operations," in IGARSS 2008, Boston, Massachusetts, July 2008.

M. D. Wojcik, K. D. Moore, "Laboratory for Atmospheric and Remote Sensing (LARS)", Wind Erosion Workshop organized by the Agriculture Research Service – Wind Erosion Research Unit, Manhattan, Kansas, April 2008.

M. D. Wojcik, R. S. Martin, J. L Hatfield. 2012. "Using lidar to characterize particles from point and diffuse sources in an agricultural field," in *Environmental Remote Sensing and Systems Analysis*, ed. N.-B. Chang, CRC Press, Taylor and Francis Group, Boca Raton, pp. 299-331.

V. V. Zavyalov, C. C. Marchant, G. E. Bingham, T. D. Wilkerson, J. L. Hatfield, R. S. Martin, P. J. Silva, K. D. Moore, J. Swasey, D. J. Ahlstrom, T. L. Jones. 2009. Aglite lidar: Calibration and retrievals of well characterized aerosols from agricultural operations using a three-wavelength elastic lidar. Journal of Applied Remote Sensing 3(1):033522 [doi: 10.1117/12.833365].

9. REFERENCES

[1] U.S. EPA. 1995. User's guide for the Industrial Source Complex (ISC3) Dispersion Models. Research Triangle Park, NC: U.S. Environmental Protection Agency, Office of Air Quality Planning and Standards Emissions. Monitoring, Analysis Division. January, 2008. http://www.epa.gov/scram001/userg/regmod/isc3v2.pdf.

[2] U.S. EPA. 2005. Revision to the Guideline on Air Quality Models: Adoption of a Preferred General Purpose (Flat and Complex Terrain) Dispersion Model and Other Revisions; Final Rule. 40 CFR Part 51. Washington, D.C., U.S. Environmental Protection Agency. January 2008. http://www.epa.gov/ttn/scram/guidance/guide/appw_05.pdf.

[3] Pope, C.A. 1991. Respiratory hospital admissions associated with PM10 pollution in Utah, Salt Lake, and Cache Valleys. Archives of Environmental Health 46(2):90-97.

[4] Hinds, W. C. 1999. Aerosol Technology: Properties, Behavior, and Measurement of Airborne Particles, 2nd Edition. John Wiley & Sons, New York. 233-242.

[5] 40 CFR 50.6. National primary and secondary ambient air quality standards for PM_{10}.

[6] 40 CFR 50.7. National primary and secondary ambient air quality standards for $PM_{2.5}$.

[7] Williams, D.J., Chilingaryan, S., Hatfield, J. 2012. Los Banos, CA Fall 2007 Tillage Campaign: Data Analysis. U.S. Environmental Protection Agency Report EPA/600/R-12/734, U.S. Government Printing Office, Washington, D.C. Available: http://cfpub.epa.gov/si/si_public_record_report.cfm?dirEntryId=248752. Date accessed: March 1, 2013.

[8] Holmen, B.A., Eichinger, W.E., Flocchini, R.G. 1998. Application of elastic LIDAR to PM_{10} emissions from agricultural nonpoint sources. Environmental Science and Technology 32:3068-3076.

[9] Conservation Management Practices Program Report. January 2006. San Joaquin Valley Air Pollution Control District for 2005.

[10] Holmen, B.A., James, T.A., Ashbaugh, J.L., Flocchini, R.G. 2001a. LIDAR-assisted measurement of PM_{10} emissions from agricultural tilling in California's San Joaquin Valley—Part I. LIDAR. Atmos. Env. 35:3251-2364.

[11] Holmen, B.A., James, T.A., Ashbaugh, J.L., Flocchini, R.G. 2001b. LIDAR-assisted measurement of PM10 emissions from agricultural tilling in California's San Joaquin Valley—Part II: Emission factors. Atmos. Env. 35:3265-3277.

[12] Flocchini, R.G., James, T.A., Ashbaugh, L.L., Brown, M.S., Carvacho, O.F., Holmen, B.A., Matsumura, R.T., Trezpla-Nabalgo, K., Tsubamoto, C. 2001. Interim Report: Sources and sinks of PM_{10} in the San Joaquin Valley. Crocker Nuclear Laboratory, UC-Davis, CA.

[13] California Air Resources Board (CARB). 2003a. Area Source Methods Manual, Section 7.4: Agricultural Land Preparation.

[14] CARB. 2003b. Area Source Methods Manual, Section 7.5: Agricultural Harvest Operations.

[15] U.S. Environmental Protection Agency (EPA). 2001. Procedures document for national emission inventory. Criteria Air Pollutants 1985-1999. EPA-454/R-01-006.

[16] Madden, N.M., Southard, R.J., Mitchell, J.P. 2008. Conservation tillage reduces PM10 emissions in dairy forage rotations. Atmospheric Environment 42:3795-3808.

[17] Wang, J., Miller, D.R., Sammis, T.W., Hiscox, A.L., Yang, W., Holmen, B.A. 2010. Local dust emission factors for agricultural tilling operations. Soil Science 175:194-200.

[18] Kasumba, J., Holmen, B.A., Hiscox, A., Wang, J., Miller, D. 2011. Agricultural PM_{10} emissions from cotton field disking in Las Cruces, NM. Atmospheric Environment 45:1668-1674.

[19] Clausnitzer, H., Singer, M.J. 1996. Respirable-dust production from agricultural operations in the Sacramento Valley, California. Journal of Environmental Quality 25:877-884.

[20] Clausnitzer, H., Singer, M.J. 2000. Environmental influences on respirable dust production from agricultural operations in California. Atmospheric Environment 34:1739-1745.

[21] Baker, J.B., Southard, R.J., Mitchell, J.P. 2005. Agricultural dust production in standard and conservation tillage systems in the San Joaquin Valley. Journal of Environmental Quality 34:1260-1269.

[22] Mitchell, J.P., Southard, R.J., Madden, N.M., Klonsky, K.M., Baker, J.B., De Moura, R.L., Horwath, W.R., Munk, D.S., Wroble, J.F., Hembree, K.J., Wallender, W.W. 2008. Transition to conservation tillage evaluated in San Joaquin Valley cotton and tomato rotations. Journal of California Agriculture 62(2):74-79.

[23] Veenstra, J.J., Horwath, W.R., Mitchell, J.P., Munk, D.S. Conservation tillage and cover cropping influence soil properties in San Joaquin Valley cotton-tomato crop. Journal of California Agriculture 60(3):146-153.

[24] Upadhyaya, S.K., Lancas, K.P., Santos-Filno, A.G., Raghuwanshi, N.S. 2001. One-pass tillage equipment outstrips conventional tillage method. Journal of California Agriculture 55(5):44-47.

[25] Mitchell, J.P., Munk, D.S., Prys, B., Klonsky, K.K., Wroble, J.F., De Moura, R.L. 2006. Conservation tillage production systems compared in San Joaquin Valley cotton. Journal of California Agriculture 60(3):140-145.

[26] U.S. EPA. March 17, 2008. NONROAD Model (nonroad engines, equipment, and vehicles). Accessed: August 21, 2008. Available: http://www.epa.gov/otaq/nonrdmdl.htm#techrept.

[27] U.S. EPA. 2004. Exhaust and Crankcase Emission Factors for Nonroad Engine Modeling – Compression-Ignition. EPA420-P-04-009. April 2004.

[28] U.S. EPA. 1991. Nonroad Engine and Vehicle Emission Study – Report. EPA 460/3-91-02. November 1991.

[29] CARB. 1999. Emissions inventory of off-road large compression-ignited engines (≥25hp) using the new OFFROAD Emissions Model. Mail-Out #MSC99-32. December 1999.

[30] Kean, A.J., Sawyer, R.F., Harley, R.A. 2000. A fuel-based assessment of off-road diesel engine emissions. Journal of the Air and Waste Management Association 50:1929-1939.

[31] RTI International. 2007. Emissions Factor Uncertainty Assessment, Review Draft. 29 March 2013. http://www.epa.gov/ttn/chief/efpac/uncertainty.html.

[32] USDA National Resource Conservation Service (NRCS). 2009. Web Soil Survey 2.0. 2 January 2009. http://websoilsurvey.nrcs.usda.gov/app/.

[33] Geology.com. May 2009. http://geology.com/state-map/california.shtml.

[34] Live Search Maps. December 2008. http://maps.live.com.

[35] California Irrigation Management Information System (CIMIS). 2009. Data for Station #15 (Stratford) for May and June of 2005 through 2007. July 2009. http://wwwcimis.water.ca.gov/cimis/data.jsp.

[36] Cooper, D.C., Alley, F.C. 2002. Air pollution control: A design approach. Waveland Press Inc. Prospect Heights, Illinois. 575.

[37] Doran, J.W., Jones, A. 1996. Methods for assessing soil quality. SSSA Special Publication Number 49. Soil Science Society of America. Madison, Wisconsin.

[38] Soil Sampling and Methods of Analysis, ed. by M.R. Carter, Canadian Society of Soil Science. Lewis Publishers, 1993:508-509.

[39] *Ibid.* 659-662.

[40] Chen, F.-L., Williams, R., Svendsen, E., Yeatts, K., Creason, J., Scott, J., Terrell, D., Case, M. 2007. Coarse particulate matter concentrations from residential outdoor sites associated with the North Carolina Asthma and Children's Environment Studies (NC-ACES). Atmospheric Environment 41:1200-1208.

[41] Chow, J. C., Watson, J. G., Lowenthal, D. H., Chen, L.-W A., Tropp, R. J., Park, K., Magliano, K. A. 2006. PM2.5 and PM10 Mass Measurements in California's San Joaquin Valley. Aerosol Science and Technology 40(10):796–810.

[42] Airmetrics MiniVol Portable Air Sampler Operation Manual v. 5.

[43] Hinds, W. C. 1999. Aerosol Technology: Properties, Behavior, and Measurement of Airborne Particles, 2nd Edition. John Wiley & Sons, New York. 75-82.

[44] Rupprecht & Patashnick, n.d. Series 5400 Elemental Carbon/Organic Carbon Analyzer Instrument Manual.

[45] Malm, W.C. and J.L. Hand. 2007. An examination of the physical and optical properties of aerosols collected in the IMPROVE program. *Atmospheric Environment*, 41, 3407-3427.

[46] Marchant, C. 2008. Algorithm Development of the AGLITE-LIDAR Instrument, MS Thesis, Utah State University.

[47] Zavyalov, V. V., Marchant, C. C., Bingham, G. E., Wilkerson, T. D., Hatfield, J. L., Martin, R. S., Silva, P. J., Moore, K. D., Swasey, J., Ahlstrom, D. J., Jones, T. L. 2009. Aglite lidar: Calibration and retrievals of well characterized aerosols from agricultural operations using a three-wavelength elastic lidar. Journal of Applied Remote Sensing 3(1):033522 [doi: 10.1117/12.833365].

[48] Klett, J.D. 1985. LIDAR inversion with variable backscatter/extinction ratio. Appl. Opt. 24: 1638-83.

[49] U.S. EPA. 2009. Guideline on Air Quality Models. Appendix W. U.S. Code of Fed. Regulations, 40 CFR Part 51. May 2009. http://www.epa.gov/scram001/guidance/guide/appw_05.pdf.

[50] Cooper, D.C., Alley, F.C. 2002. Air pollution control: A design approach. Waveland Press Inc. Prospect Heights, Illinois. 611-626.

[51] Turner, D.B. 1970. Workbook of Atmospheric Dispersion Estimates. Washington, D.C., U.S. Environmental Protection Agency.

[52] Paine, R.J., Lee, R.F., Brode, R., Wilson, R.B., Cimorelli, A.J., Perry, S.G., Weil, J.C., Venkatram, A., Peters, W.D. 1998. Model evaluation results for AERMOD. Research Triangle Park, NC:U.S. Environmental Protection Agency, Office of Air Quality Planning and Standards Emissions, Monitoring, Analysis Division. March 2008. http://www.epa.gov/scram001/7thconf/aermod/evalrep.pdf.

[53] National Research Council, National Academies of Science. 2003. Air emissions from animal feeding operations: Current knowledge, future needs. The National Academies Press. Washington, D.C. 95.

[54] Arya, S.P. 1998. Air Pollution Meteorology and Dispersion. Oxford University Press.

[55] Lakes Environmental. 2009. Terrain Data: 7.5-Min DEM Native Format – United States. July 2009. http://www.webgis.com/terr_us75m.html.

[56] U.S. Department of Agriculture, Natural Resources Conservation Service. 2007. National Soil Survey Handbook, title 430-VI. Available: http://soils.usda.gov/technical/handbook/.

[57] Bingham, G.E., Marchant, C. C., Zavyalov, V. V., Ahlstrom, D. J., Moore, K. D., Jones, D. S., Wilkerson, T. D., Hipps, L. E., Martin, R. S., Hatfield, J. L., Prueger, J. H., Pfeiffer, R. L. 2009. Lidar based emissions measurement at the whole facility scale: Method and error analysis. Journal of Applied Remote Sensing 3(1):033510 [doi: 10.1117/12.829411].

[58] Cooper, D.C., Alley, F.C. 2002. Air pollution control: A design approach. Waveland Press Inc. Prospect Heights, Illinois. 100.

[59] Hinds, W. C. 1999. Aerosol Technology: Properties, Behavior, and Measurement of Airborne Particles, 2nd Edition. John Wiley & Sons, New York. 402-408.

10. APPENDICES

10.1 APPENDIX A: DATA AND SETTINGS TABLES

Table 30. Settings for the ISCST3 and AERMOD dispersion models for the tillage study in the ISC-AERMOD View software by Lakes Environmental, Inc. All settings were held constant across the sample periods except the source area size and shape, which changed each day, and the downwind receptor locations, which were specific to each field studies. (--- = not applicable)

Setting	ISCST3	AERMOD
Control Pathway		
Dispersion Options	Regulatory Default	Regulatory Default
Output type	Concentration	Concentration
Plume Deposition	None	---
Pollutant	Other – PM	Other – PM
Averaging Time	Period	Period
Dispersion Coefficient	Rural	Rural
Terrain Height Options	Elevated	Elevated
Terrain Calculation Algorithms (ISC), Receptor Elev./Hill Hghts (AERMOD)	Simple terrain only	Run using the AERMAP Receptor Output file
Source Pathway		
Source type	Area Poly	Area Poly
Base Elevation	0.0 m	0.0 m
Release height	0.0 m AGL	0.0 m AGL
Emission rate	8.6 E-6 g/(s-m^2)	8.6 E-6 g/(s-m^2)
Initial Vertical Dim. of the plume	Blank	Blank
Building downwash	None	None
Receptor Pathway		
Uniform Cartesian Grid (# Receptors: 4200)	138x130, 10x10m spacing, flagpole height z = 2.0 m AGL	138x130, 10x10m spacing, flagpole height z = 2.0 m AGL
Discrete Cartesian Receptors (# Receptors: 10)	Placed at sample locations, z = 2, 5, and 9 m AGL	Placed at sample locations, z = 2, 5, and 9 m AGL
AERMET View Settings		
Hourly Surface Data	---	Source: on-site data, mixing height = 1000 m AGL
Adjustment to Local Time	---	8 hr (Pacific)
Application Station Elevation MSL	---	76.2 m
Upper Air Data	---	Source: calculated based on on-site data, mixing height = 1000 m AGL
Mode	---	Upper Air Estimator
Sectors Parameters	---	
Time Zone	---	8 (Pacific)
Randomize NWS Wind Directions	---	Yes
Anemometer Height	---	6.2 m AGL
Wind direction sectors	---	1: Start = 0°, End = 360°
Land Use Type	---	Cultivated Land

Setting	ISCST3	AERMOD
Surface parameters per sector	---	Annually, using spring-time default values for Midday Albedo = 0.14, Bowen Ratio = 0.3, and Surface Roughness = 0.03 m
Meteorology Pathway		
Surface Met Data	Source: on-site data, mixing height = 1000 m AGL	Source: calculated from on-site data and default values
Profile Met Data	---	Source: estimated from on-site data
Anemometer Height (agl)	6.2 m	---
Primary Met Tower Base Elevation above MSL	---	76.2 m
Read Entire Met Data File	No	No
Specify Data Periods to Process	Set to sample period times, varied by sample	Set to sample period times, varied by sample
Wind Speed Categories	Default	Default
Output Pathway		
Tabular Outputs		
All	Not available, no short term averaging times selected	Not available, no short term averaging times selected
Buildings	None	None
Terrain	Calculated values from AERMAP using 7.5 Min DEM	Calculated values from AERMAP using 7.5 Min DEM

Table 31. Calculated PM concentrations (μg/m^3) measured during May 2008 at all sample locations.

Location (height agl)	Size	Sample Period						
		May 17 R1	May 17 R2	May 18	May 19 R1	May 19 R2	May 20 R1	May 20 R2
T1 (9)	TSP	138.2	330.0	118.2	242.0	153.5	242.3	343.4
	PM_{10}	64.6	239.3	*	83.2	65.1	115.7	469.8
	$PM_{2.5}$	59.7	128.1	133.8	35.2	23.2	31.6	205.5
10.0 (2)	TSP	135.4	628.2	266.1	178.6	267.9	260.5	355.1
	PM_{10}	75.7	205.5	38.1	*	*	*	*
	$PM_{2.5}$	43.5	266.8	27.1	29.2	24.8	51.2	89.3
11.0 (2)	TSP							
	PM_{10}							
	$PM_{2.5}$							
T2 (9)	TSP		533.8	479.6	1138.2	965.0	1511.7	2276.9
	PM_{10}		199.6	100.1	231.5	195.9	253.5	258.4
	$PM_{2.5}$		92.0	46.2	71.7	41.4	77.5	324.4
T3 (9)	TSP	559.3						
	PM_{10}	154.4						
	$PM_{2.5}$	48.8						
AQT (5)	TSP	380.0	368.3	154.3	188.3	224.5	286.1	709.1
	PM_{10}	167.0	109.0	59.4	*	76.9	98.1	172.9
	$PM_{2.5}$	53.9	141.6	65.1	38.2	34.5	52.3	107.3
2.4/2.5 (2)	TSP	610.7	*	1233.4	*	1894.2	*	*
	PM_{10}	161.3	186.4	135.3	312.1	387.8	347.1	399.2
	$PM_{2.5}$	49.4	187.8	63.3	135.0	232.4	459.7	215.7
6.4/6.5 (2)	PM_{10}	157.7	1458.4	140.2	278.2	408.4	287.3	730.6
	$PM_{2.5}$	65.2	3244.9	90.1	132.7	491.0	465.9	171.1
7.4/7.5 (2)	TSP							
	PM_{10}	140.5	83.8	75.7	268.7	215.9	250.9	364.8
	$PM_{2.5}$	62.3	153.8	60.9	153.5	202.6	398.0	136.5
8.4/8.5 (2)	PM_{10}	191.4	300.9	141.2	562.5	402.4	*	437.0
	$PM_{2.5}$	57.4	179.8	36.9	171.0	102.8	284.9	139.3
9.4/9.5 (2)	PM_{10}	140.6	203.6	149.1	570.6	335.3	347.3	348.9
	$PM_{2.5}$	65.9	144.4	*	265.5	344.8	392.7	186.7
12.0 (2)	TSP							
	PM_{10}							
	$PM_{2.5}$							

* Filter sample had a noted problem during or after sampling
(blank) = no sample collected

Table 32. Calculated PM concentrations (μg/m^3) measured during June 2008 at all sample locations.

Location (height agl)	Size	Sample Period					
		June 5 R1	June 5 R2	June 7	June 11	June 18	June 24
T1 (9)	TSP	102.9	158.5	110.7	73.6	195.4	180.1
	PM_{10}	47.4	*	57.2	188.8	56.5	101.8
	$PM_{2.5}$	26.7	68.0	27.5	117.9	30.1	71.2
10.0 (2)	TSP	227.9	231.4	*	183.1		
	PM_{10}	86.2	272.6	80.7	137.6		
	$PM_{2.5}$	101.5	165.2	38.8	106.3		
11.0 (2)	TSP					233.6	195.6
	PM_{10}					68.6	89.6
	$PM_{2.5}$					28.2	64.4
T2 (9)	TSP	*	353.8				
	PM_{10}	58.0	109.6				
	$PM_{2.5}$	32.2	138.8				
T3 (9)	TSP			204.6	262.9		
	PM_{10}			61.5	96.7		
	$PM_{2.5}$			29.5	76.1		
AQT (5)	TSP	104.3	243.8	158.7	250.0		
	PM_{10}	58.6	221.3	78.0	75.1		
	$PM_{2.5}$	38.2	252.5	30.8	122.7		
2.4/2.5 (2)	TSP	*	*	335.7	246.9	1896.9	554.2
	PM_{10}	80.4	137.5	80.3	80.2	333.6	142.2
	$PM_{2.5}$	57.6	174.3	47.8	213.6	42.9	74.0
6.4/6.5 (2)	PM_{10}	102.5	229.4	78.0	172.9	489.4	116.7
	$PM_{2.5}$	62.6	123.1	36.9	102.6	38.9	70.7
7.4/7.5 (2)	TSP					1495.1	717.0
	PM_{10}	53.5	246.2	59.0	176.3	195.3	142.4
	$PM_{2.5}$	42.8	140.4	33.2	149.8	60.2	64.3
8.4/8.5 (2)	PM_{10}	80.8	163.4	88.3	182.6	207.1	126.9
	$PM_{2.5}$	86.9	110.0	56.1	73.2	35.1	76.4
9.4/9.5 (2)	PM_{10}	77.9	131.6	98.4	111.9	61.6	196.9
	$PM_{2.5}$	43.9	114.6	33.1	101.4	30.0	65.0
12.0 (2)	TSP						700.7
	PM_{10}						203.4
	$PM_{2.5}$						74.9

* Filter sample had a noted problem during or after sampling
(blank) = no sample collected

Table 33. PM concentrations (µg/m^3) used in emission rate calculations from sample periods in May 2008.

Location (height agl)	Size	Sample Period						
		May 17 R1	May 17 R2	May 18	May 19 R1	May 19 R2	May 20 R1	May 20 R2
T1 (9)	TSP	138.2	330.0	§	§	§	§	§
	PM_{10}	64.6	---	*	§	§	§	§
	$PM_{2.5}$	59.7	---	§	§	§	§	§
10.0 (2)	TSP	135.4	+	§	§	§	§	§
	PM_{10}	75.7	+	§	*	*	*	*
	$PM_{2.5}$	43.5	+	§	§	§	§	§
11.0 (2)	TSP							
	PM_{10}							
	$PM_{2.5}$							
T2 (9)	TSP		533.8	§	§	§	§	§
	PM_{10}		§	§	§	§	§	§
	$PM_{2.5}$		§	§	§	§	§	§
T3 (9)	TSP	559.3						
	PM_{10}	154.4						
	$PM_{2.5}$	48.8						
AQT (5)	TSP	380.0	368.3	§	§	§	§	§
	PM_{10}	167.0	§	§	*	§	§	§
	$PM_{2.5}$	53.9	§	§	§	§	§	§
2.4/2.5 (2)	TSP	610.7	*	§	*	§	*	*
	PM_{10}	161.3	§	§	§	§	§	§
	$PM_{2.5}$	49.4	§	§	---	§	§	§
6.4/6.5 (2)	PM_{10}	157.7	§	§	§	§	§	§
	$PM_{2.5}$	65.2	§	§	§	§	§	§
7.4/7.5 (2)	TSP							
	PM_{10}	140.5	§	§	§	§	§	§
	$PM_{2.5}$	62.3	§	§	§	§	§	§
8.4/8.5 (2)	PM_{10}	191.4	§	§	§	§	*	§
	$PM_{2.5}$	57.4	§	§	§	§	§	§
9.4/9.5 (2)	PM_{10}	140.6	§	§	§	§	§	§
	$PM_{2.5}$	65.9	§	*	§	§	§	§
12.0 (2)	TSP							
	PM_{10}							
	$PM_{2.5}$							

* = Filter sample had a noted problem during or after sampling
--- = Removed due to ring particle density classification of medium or higher
+ = Removed due to exceptionally high or low value and not supported by OPC time series
◊ = $PM_{2.5}$ and PM_{10} levels indicated filters switched during sampling, concentrations switched
§ = Removed due to contaminated background or overloaded downwind filters
(blank) = no sample collected

Table 34. PM concentrations (µg/m^3) used in emission rate calculations from sample periods in June 2008.

Location (height agl)	Size	Sample Period					
		June 5 R1	June 5 R2	June 7	June 11	June 18	June 24
T1 (9)	TSP	102.9	158.5	110.7	+	195.4	180.1
	PM_{10}	47.4	*	57.2	188.8	56.5	101.8
	$PM_{2.5}$	26.7	68.0	27.5	117.9	30.1	71.2
10.0 (2)	TSP	§	§	*	183.1		
	PM_{10}	---	---	80.7	137.6		
	$PM_{2.5}$	---		38.8	106.3		
11.0 (2)	TSP					233.6	195.6
	PM_{10}					68.6	89.6
	$PM_{2.5}$					28.2	64.4
T2 (9)	TSP	*	353.8				
	PM_{10}	58.0	§				
	$PM_{2.5}$	32.2	---				
T3 (9)	TSP			204.6	262.9		
	PM_{10}			61.5	96.7		
	$PM_{2.5}$			29.5	76.1		
AQT (5)	TSP	104.3	243.8	158.7	250.0		
	PM_{10}	58.6	---	---	122.7 ◊		
	$PM_{2.5}$	38.2	+	30.8	75.1 ◊		
2.4/2.5 (2)	TSP	*	*	335.7	246.9	1896.9	554.2
	PM_{10}	80.4	§	80.3	213.6 ◊	333.6	142.2
	$PM_{2.5}$	---	---	---	80.2 ◊	42.9	74.0
6.4/6.5 (2)	PM_{10}	102.5	§	---	172.9	489.4	116.7
	$PM_{2.5}$	---	123.1	---	102.6	38.9	70.7
7.4/7.5 (2)	TSP					1495.1	717.0
	PM_{10}	53.5	§	59.0	176.3	195.3	142.4
	$PM_{2.5}$	42.8	140.4	33.2	149.8	60.2	64.3
8.4/8.5 (2)	PM_{10}	80.8	§	88.3	182.6	207.1	126.9
	$PM_{2.5}$	---	---	56.1	73.2	35.1	76.4
9.4/9.5 (2)	PM_{10}	77.9	§	98.4	111.9	61.6	196.9
	$PM_{2.5}$	43.9	114.6	33.1	101.4	30.0	65.0
12.0 (2)	TSP						700.7
	PM_{10}						203.4
	$PM_{2.5}$						74.9

* = Filter sample had a noted problem during or after sampling
--- = Removed due to ring particle density classification of medium or higher
+ = Removed due to exceptionally high or low and not supported by OPC time series
◊ = $PM_{2.5}$ and PM_{10} levels indicated filters switched during sampling, concentrations switched
§ = Removed due to contaminated background or overloaded downwind filters
(blank) = no sample collected

Table 35. PM concentrations (μg/m^3) as measured by OPCs from sample periods in May 2008. (OPC PM_k = V_k x MCF_k)

Location (height agl)	Size	Sample Period						
		May 17 R1	May 17 R2	May 18	May 19 R1	May 19 R2	May 20 R1	May 20 R2
T1 (9)	TSP	95.3	181.6	109.1	181.7	127.8	224.7	
	PM_{10}	50.6	68.6	48.9	70.3	58.6	74.5	
	$PM_{2.5}$	9.2	4.3	7.7	12.8	8.4	12.6	
10.0 (2)	TSP				159.0	275.9	296.3	
	PM_{10}				61.9	89.1	87.9	
	$PM_{2.5}$				12.4	9.7	12.2	
11.0 (2)	TSP							
	PM_{10}							
	$PM_{2.5}$							
T2 (9)	TSP		1777.6	490.0	1585.2	1296.9	1282.2	
	PM_{10}		197.0	110.3	283.4	241.6	252.3	
	$PM_{2.5}$		6.3	9.7	18.9	12.5	16.5	
T3 (9)	TSP	597.1						
	PM_{10}	142.3						
	$PM_{2.5}$	12.2						
AQT (5)	TSP	636.3	417.1	164.6	227.8	207.1	331.3	
	PM_{10}	174.7	75.5	54.4	74.0	71.3	102.3	
	$PM_{2.5}$	13.2	4.8	7.9	12.9	8.9	13.2	
2.4/2.5 (2)	TSP	601.4	3251.9	813.2	2263.5	3271.9	2550.4	
	PM_{10}	165.2	318.8	178.0	375.8	641.1	462.7	
	$PM_{2.5}$	12.9	7.5	11.1	19.9	20.0	20.7	
7.4/7.5 (2)	TSP	816.6	2767.5	692.0	2523.2	2553.9	1656.4	
	PM_{10}	199.0	292.0	141.5	406.8	451.5	342.1	
	$PM_{2.5}$	13.7	7.7	10.1	20.5	15.9	18.5	
8.4/8.5 (2)	TSP							
	PM_{10}							
	$PM_{2.5}$							
12.0 (2)	TSP							
	PM_{10}							
	$PM_{2.5}$							

Table 36. PM concentrations (μg/m^3) as measured by OPCs from sample periods in June 2008. (OPC PM_k = V_k x MCF_k)

Location (height agl)	Size	Sample Period					
		June 5 R1	June 5 R2	June 7	June 11	June 18	June 24
T1 (9)	TSP	95.3	170.5	104.8	222.4	179.5	127.0
	PM_{10}	41.2	47.7	43.1	122.4	47.0	85.0
	$PM_{2.5}$	11.7	5.7	16.2	11.4	4.8	56.9
10.0 (2)	TSP	172.4	571.5	194.6	198.4	153.6	
	PM_{10}	69.5	160.2	94.4	120.7	44.2	
	$PM_{2.5}$	13.6	12.1	19.3	10.7	5.4	
11.0 (2)	TSP						172.4
	PM_{10}						81.7
	$PM_{2.5}$						55.8
T2 (9)	TSP	205.9	364.4			475.1	334.9
	PM_{10}	63.8	80.9			97.0	109.4
	$PM_{2.5}$	13.3	6.9			6.4	57.8
T3 (9)	TSP			190.9	213.4		
	PM_{10}			59.2	132.6		
	$PM_{2.5}$			16.9	11.2		
AQT (5)	TSP	113.3	221.8	194.2	257.4		
	PM_{10}	47.2	67.2	62.3	141.1		
	$PM_{2.5}$	11.6	6.4	16.8	11.4		
2.4/2.5 (2)	TSP	386.1	1162.4	318.3	282.4	2816.4	720.8
	PM_{10}	93.2	213.0	83.4	155.8	467.4	165.8
	$PM_{2.5}$	14.7	12.9	18.3	11.4	22.0	60.2
7.4/7.5 (2)	TSP	180.4	769.2	245.8	357.1	2084.4	822.3
	PM_{10}	64.0	193.9	72.2	171.0	295.0	177.1
	$PM_{2.5}$	12.6	11.6	17.1	12.0	12.7	58.5
8.4/8.5 (2)	TSP					1703.5	
	PM_{10}					214.5	
	$PM_{2.5}$					9.6	
12.0 (2)	TSP						868.3
	PM_{10}						203.6
	$PM_{2.5}$						58.3

Table 37. PM concentrations (μg/m^3) as measured by OPCs used in emission rate calculations from sample periods in May 2008. (OPC $PM_k = V_k$ x MCF_k)

Location (height agl)	Size	Sample Period						
		May 17 R1	May 17 R2	May 18	May 19 R1	May 19 R2	May 20 R1	May 20 R2
T1 (9)	TSP	95.3	181.6	109.1	156.5*	127.8	224.7	
	PM_{10}	50.6	68.6	48.9	63.3*	58.6	74.5	
	$PM_{2.5}$	9.2	4.3	7.7	12.6*	8.4	12.6	
10.0 (2)	TSP				159.0	137.1*	169.0*	
	PM_{10}				61.9	56.1*	64.2*	
	$PM_{2.5}$				12.4	8.4*	11.7*	
11.0 (2)	TSP							
	PM_{10}							
	$PM_{2.5}$							
T2 (9)	TSP		1777.6	490.0	1585.2	1296.9	1282.2	
	PM_{10}		197.0	110.3	283.4	241.6	252.3	
	$PM_{2.5}$		6.3	9.7	18.9	12.5	16.5	
T3 (9)	TSP	597.1						
	PM_{10}	142.3						
	$PM_{2.5}$	12.2						
AQT (5)	TSP	636.3	417.1	164.6	227.8	207.1	331.3	
	PM_{10}	174.7	75.5	54.4	74.0	71.3	102.3	
	$PM_{2.5}$	13.2	4.8	7.9	12.9	8.9	13.2	
2.4/2.5 (2)	TSP	601.4	3251.9	813.2	2263.5	3271.9	2550.4	
	PM_{10}	165.2	318.8	178.0	375.8	641.1	462.7	
	$PM_{2.5}$	12.9	7.5	11.1	19.9	20.0	20.7	
7.4/7.5 (2)	TSP	816.6	2767.5	692.0	2523.2	2553.9	1656.4	
	PM_{10}	199.0	292.0	141.5	406.8	451.5	342.1	
	$PM_{2.5}$	13.7	7.7	10.1	20.5	15.9	18.5	
8.4/8.5 (2)	TSP							
	PM_{10}							
	$PM_{2.5}$							
12.0 (2)	TSP							
	PM_{10}							
	$PM_{2.5}$							

* Significant plumes at upwind location removed

Table 38. PM concentrations (μg/m^3) as measured by OPCs used in emission rate calculations from sample periods in June 2008. (OPC $PM_k = V_k$ x MCF_k)

Location (height agl)	Size	Sample Period					
		June 5 R1	June 5 R2	June 7	June 11	June 18	June 24
T1 (9)	TSP	95.3	170.5	104.8	222.4	179.5	127.0
	PM_{10}	41.2	47.7	43.1	122.4	47.0	85.0
	$PM_{2.5}$	11.7	5.7	16.2	11.4	4.8	56.9
10.0 (2)	TSP	93.9*	127.9*	98.6*	198.4	153.6	
	PM_{10}	41.0*	42.6*	41.9*	120.7	44.2	
	$PM_{2.5}$	11.8*	6.2*	16.3*	10.7	5.4	
11.0 (2)	TSP						172.4
	PM_{10}						81.7
	$PM_{2.5}$						55.8
T2 (9)	TSP	205.9	364.4			475.1	334.9
	PM_{10}	63.8	80.9			97.0	109.4
	$PM_{2.5}$	13.3	6.9			6.4	57.8
T3 (9)	TSP			190.9	213.4		
	PM_{10}			59.2	132.6		
	$PM_{2.5}$			16.9	11.2		
AQT (5)	TSP	113.3	221.8	194.2	257.4		
	PM_{10}	47.2	67.2	62.3	141.1		
	$PM_{2.5}$	11.6	6.4	16.8	11.4		
2.4/2.5 (2)	TSP	386.1	1162.4	318.3	282.4	2816.4	720.8
	PM_{10}	93.2	213.0	83.4	155.8	467.4	165.8
	$PM_{2.5}$	14.7	12.9	18.3	11.4	22.0	60.2
7.4/7.5 (2)	TSP	180.4	769.2	245.8	357.1	2084.4	822.3
	PM_{10}	64.0	193.9	72.2	171.0	295.0	177.1
	$PM_{2.5}$	12.6	11.6	17.1	12.0	12.7	58.5
8.4/8.5 (2)	TSP					1703.5	
	PM_{10}					214.5	
	$PM_{2.5}$					9.6	
12.0 (2)	TSP						868.3
	PM_{10}						203.6
	$PM_{2.5}$						58.3

* Significant plumes at upwind location removed

10.2 APPENDIX B: INVESTIGATIONS INTO AND CONCLUSIONS FROM FILTER-BASED DATA

During the post-weighing process it was noticed that filters used for $PM_{2.5}$, PM_{10}, and TSP had particles large enough to be visible to the naked eye, not all of which were embedded in the filter medium and thus could move around and off the filter. Particles small enough to pass through the impactor assembly in the sample head are typically too small to be seen with the naked eye, almost always being less than 10 μm and 2.5 μm in diameter for PM_{10} and $PM_{2.5}$, respectively. Particles collected during sampling that were not stuck into or onto the filter medium may move off of the filter, yielding a variable low bias in reported PM concentrations. In addition, several of the calculated $PM_{2.5}$ concentrations significantly exceeded the collocated PM_{10} concentrations, which is theoretically impossible under the ideal sampling scenario since $PM_{2.5}$ is a subset of PM_{10} and should always be less than or equal to the PM_{10} concentration. These inverted $PM_{2.5}$ and PM_{10} concentrations, as we will call them, were very prevalent in the data for several sample periods, with up to 75% of the downwind $PM_{2.5}$ and PM_{10} concentrations inverted for the lister

pass on May 20, 2008. These size-inverted concentrations and the presence of visible particles on the filters prompted an investigation to determine their causes as well as potential solutions for the current data set and prevention methods for future measurements. This section describes these investigations, as well as the conclusions drawn about the suitability of the dataset for use in emission rate calculations, and options for preventing such problems in the future.

All aspects of the pre-, intra-, and post-sampling filter handling were examined in detail for potential problems. Filter identification numbers were recorded throughout the preparation, sample, and analysis phases, which allowed each filter to be tracked throughout the entire process. It was thought that the cause could be improper and/or inaccurate weighing methods and instruments. This possibility, however, was ruled out as all filters were preconditioned according to U.S. EPA standards in dessicators before both pre- and post-weights were determined. Measurements of weight to the 1 μg ($1x10^{-6}$ g) level were performed by experienced personnel using a vibration-isolated micro-balance at the UWRL that had been calibrated on-site by manufacturer personnel earlier in 2008; a certified 1.000 mg calibration mass was used to monitor balance accuracy and drift every ten readings. The correct calculation and use of average pre- and post-weights for all filters were verified, and the filter numbers recorded on sample run sheets were checked for potential errors. A few errors were found during this verification process in the calculation and use of average pre- and post-weights, but they did not explain the majority of the suspect filters with the problems stated above. The errors found have been corrected in the concentrations reported in Section 4.2.1 and found in Table 31 and Table 32.

Another potential cause of inverted collocated $PM_{2.5}$-PM_{10} concentrations was that the filters were switched during sampling due to human error, causing the filter designated for $PM_{2.5}$ to actually sample PM_{10} and vice versa. Data were examined on a location-by-location basis by switching the suspected $PM_{2.5}$ and PM_{10} concentrations and comparing them with other downwind PM concentrations of the same size fraction measured during the same sample period. The results suggested that this likely occurred on a total of four occasions at two sample locations and across two sample periods. Switching these $PM_{2.5}$ and PM_{10} concentrations yielded a more consistent set of concentrations in all cases. In addition, examination of the OPC time series yielded no irregularities that would suggest problems with either one or both samples. The collocated $PM_{2.5}$ and PM_{10} concentrations were therefore switched for subsequent analysis. Similar to the verification of correct filter tracking and the average weights used, this investigation found some inverted collocated $PM_{2.5}$-PM_{10} concentrations could be explained by the filters being switched during sampling but that a significant number of instances of the phenomena were unexplained. It was determined that this was likely not the cause in most cases due to the pervasiveness of this phenomenon during only a few sample periods and because the personnel that were operating the filter-based measurements were experienced and capable.

Further investigations were made through visual inspection of the filters through microscopy. Several representative filters were examined through a microscope to size and count collected particles. Examined filters included some from each of the following categories: collocated $PM_{2.5}$ and PM_{10} samples where the $PM_{2.5}$-PM_{10} concentrations were inverted; samples collected in upwind/background locations on days with multiple suspect filters; and blank filters that were taken to the field but not used. The microscope used was a BX51 from Olympus (Center Valley, PA) with a stage that could be controlled either manually or through computer software. An Olympus Model DP71 camera was mounted on the microscope to capture digital images of the microscope field of view. The MicroSuite Five Imaging software, also by Olympus, controlled

the camera and stage automatically to photograph a user-specified area of the filter, combine adjacent images, and identify and size particles in the images. The 5x, 10x, 50x, and 100x lenses were all tested, but the software analysis on images taken using 50x and 100x lenses under the given light, microscope, and software settings were not used due to inaccurate sizing and counting. The 5x lens was mainly used to scan over the filter area for large particles (> ~25 μm in diameter), while most images used for counting and sizing particles were taken with the 10x lens because smaller particles could be detected. The minimum particle diameters detected by the 5x and 10x, lenses under the light, microscope, and software settings were 5.22 μm and 2.61 μm, respectively. Projected area particle diameter (d_{PA}) is the diameter of a circle having the same area as the 2D projected area of the 3D particle and is a common representation of particle size based on microscopic sizing [59]; the d_{PA} were calculated based on individual particle area values provided by the MicroSuite Five Imaging software. Smaller particles could be visually identified in the images, but the software could not sufficiently resolve them from the background light intensity variation inherent in the Teflon filter medium. The entire microscope and computer imaging system were housed in a room maintained at Class 100 clean room standards to prevent particle deposition on the filters during analysis. All of the microscope work was performed by just one person in order to maintain consistent procedures and settings.

The 47 mm diameter Teflon filters used in PM mass sampling have a collection area composed of an exposed mesh of Teflon fibers about 41 mm-diameter and a 3 mm-wide plastic ring which holds the Teflon fibers in place; this plastic ring is used for filter handling and also for securing the filter into the MiniVol sampling fixture. The Teflon area is fragile. The sample collection area is about 1320 mm^2. The sampling fixture is a two-part, push-on assembly which sandwiches the Teflon filter between two plastic fittings. Figure 43 shows an example of an image of a PM_{10} filter sample collection area taken using the microscope and the 10x lens. This image is composed of four adjacent pictures that were automatically combined by the software. Note the varying shades of the grey background from the Teflon fibers. Particles are shown as both dark and bright white spots, depending on chemical composition, size, and orientation with respect to the light source and microscope lens. The average $d_{PA} \pm 1\sigma$ of detected particles in this image was 4.47 ± 2.56 μm (n 2977) and the median mean diameter was 3.50 μm with 25 and 75 percentile values of 2.86 and 5.08 μm; 95.9 % of the detected particles had a d_{PA} less than 10.0 μm. The largest particle, marked by the blue ring, was measured at a d_{PA} of 31.94 μm.

Due to the magnification and time limits of this analysis at each position, a total of about 1% of the collection area on most filters was sampled after integration over three to four sample locations. Sample locations were chosen randomly within quadrants, with each sample from a quadrant that was previously not sampled. While a total sample area of at least 10% is preferred, the variability of the cumulative distribution between sample locations on the same filter was less than 10%. Therefore, multiple sample areas per filter with a total area of about 1% of the potential collection area were deemed adequate for the purposes of this analysis.

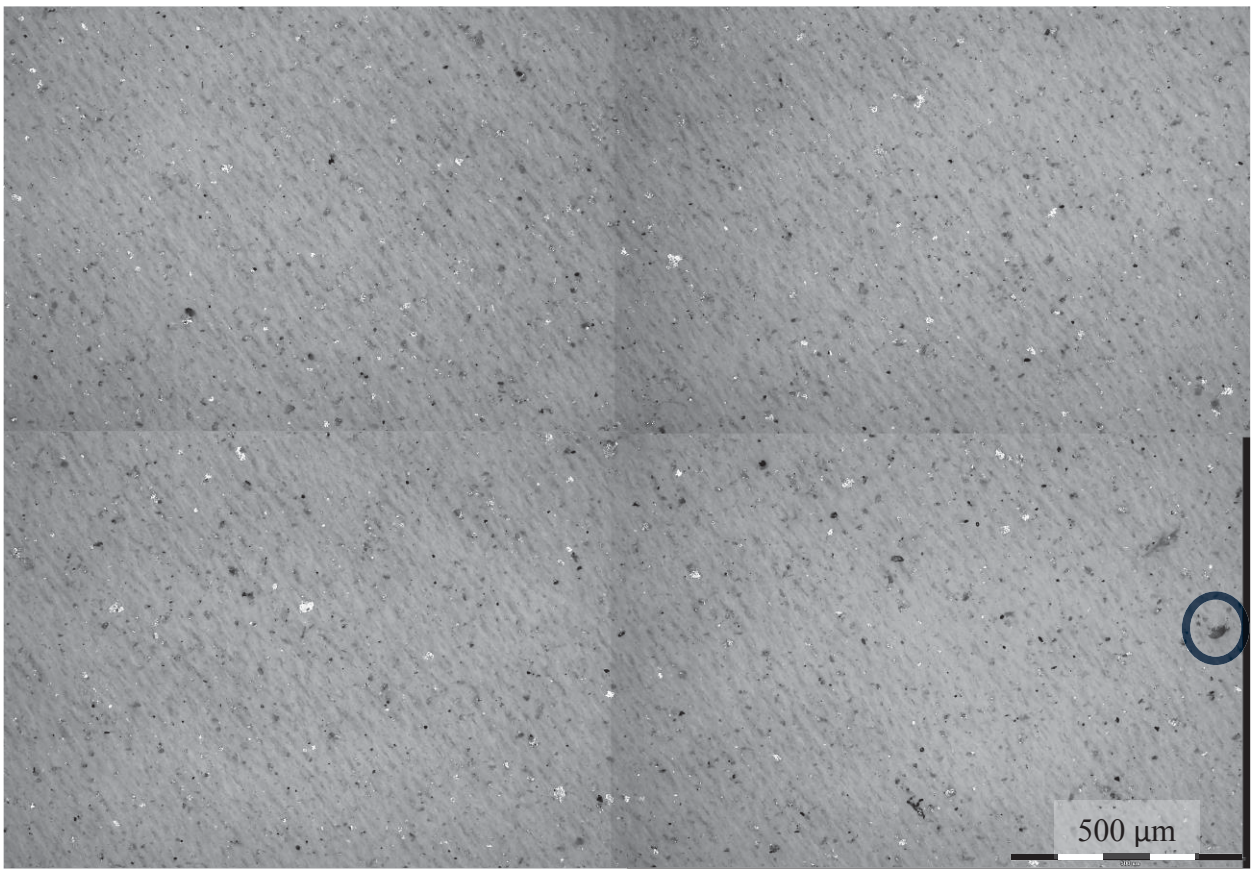

Figure 43. Four adjacent microscopic images taken with the 10x lens that have been combined for determining the particle size distribution and count at this location on a PM_{10} sample filter. The largest particle with d_{PA} = 31.94 µm is shown by the blue circle.

Results of the microscope particle sizing and counting on two sets of $PM_{2.5}$ and PM_{10} samples where the concentrations were inverted showed that the d_{PA} size distributions on the sample collection areas were similar in shape, with the PM_{10} filters having a much higher particle density than the $PM_{2.5}$ filter, as seen in Figure 44. Note that the size distribution is given in number of particles per square mm of filter surface per µm of bin width; incorporating the bin width into the denominator removes the bin number concentration dependence on bin width. Also, it must be remembered that the MDL was 2.61 µm and that d_{PA} is related to but different from aerodynamic diameter (d_{aero}). For a given particle, d_{PA} and d_{aero} values should be similar but will vary according to shape, density, and orientation at the time of detection. These data, coupled with visual scans of the entire collection area to find and size large particles, suggest that the inverted $PM_{2.5}$-PM_{10} concentrations for these filters cannot likely be explained by large particle contamination on the $PM_{2.5}$ collection area. Additionally, the data show that there was neither a complete failure of the size fractionating impactors nor were many of the filters switched during sampling. Very similar particle count densities in each size fraction between the two downwind sites, 7.4 and 2.4, suggest that in-plume number size distribution was roughly spatially homogenous during the May 20 Run 1 sample period, assuming spatially homogeneous deposition on the filter area. The differences between the upwind $PM_{2.5}$ size distribution and the downwind $PM_{2.5}$ size distributions are due to the plumes that impacted the downwind samplers.

A potentially significant number of larger-than-expected particles (d_{PA} > ~2.5 µm for $PM_{2.5}$ and d_{PA} > ~10 µm for PM_{10}) were found on the downwind PM_{10} and $PM_{2.5}$ filters; there were even particles greater than 100 µm in diameter. Particles with d_{PA} greater than 25 µm were found on the downwind $PM_{2.5}$ and PM_{10} filters whose size distributions are presented in Figure 44. Such large particles are not unexpected on TSP samples collected downwind of agricultural tillage operations, but they should not be present on samples with a PM_{10} or $PM_{2.5}$ size-separating device upstream of the filter in the sample head assembly. In addition, large particles were found on the annular plastic ring of many of the examined filters by both the microscope and inspection with the naked eye. This was troubling since this annular area is completely covered by the sampling fixture itself and therefore cannot collect particles during active sampling. Most observed particles on the annular filter ring area were sitting on the surface, suggesting either migration from the collection area or deposition after removal from the sampling device. Several particles were even pressed into the plastic, suggesting that they were either present on the filter prior to being loaded for sampling or were on the bottom of the filter holder piece when pressed down onto the plastic ring medium and remained there upon removal from the sampling fixture.

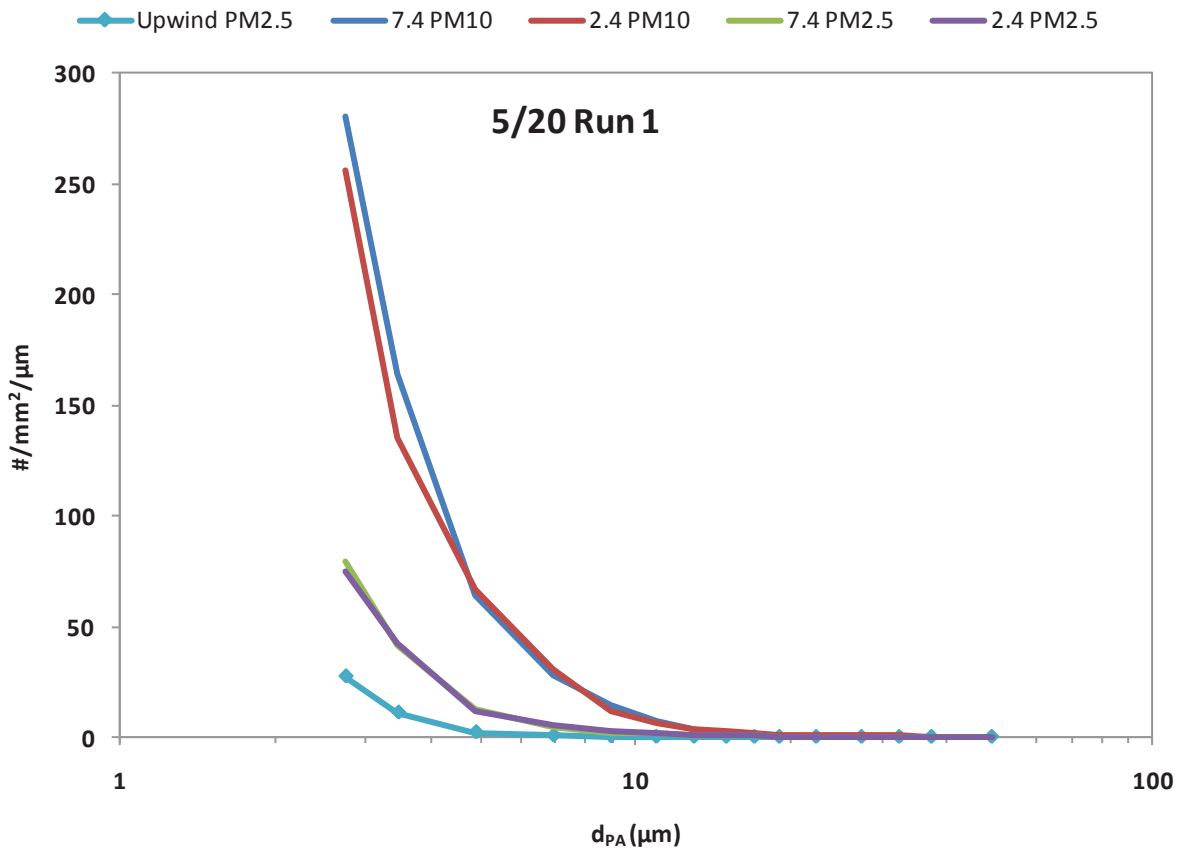

Figure 44. Number distributions based on projected area diameter as measured via microscopy for two downwind and one upwind $PM_{2.5}$ filters and two downwind PM_{10} filters used during the Lister pass on May 20, 2008.

The presence of such large particles on both the collection area and the annular area of multiple filters may be explained by several potential factors, including but not limited to:

1) The collection efficiency curve of the PM_{10} and $PM_{2.5}$ size fractionation devices employed by both FRMs and MiniVols are S-curves with respect to particle aerodynamic diameter, designed to mimic the particle removal efficiency of the human respiratory system. The removal efficiency curves have a 50% collection efficiency at the designed cut-off size, with some smaller particles being removed and some larger particles passing through the system. The potential exists for high numbers of large particles to be present in plumes emitted from sources such as agricultural tillage activities and, if the plume is being sampled by an instrument a short distance away as was the case in this study, some particles larger than the cut size would be expected to pass through the size-separating devices. This potential factor would best apply to particles close to the cut size as the collection efficiency curve theoretically approaches 100% soon after passing the design cut-off diameter, with the MiniVol S-curve being less steep than the FRM and approaching 100% at a larger size.

2) Improper assembly of the size-fractionating impactor is another potential explanation for passing larger-than-expected particles through the impactor. While possible on an individual basis, such an improper assembly problem across up to 75% of the downwind samplers is not likely (75% of downwind PM_{10} and $PM_{2.5}$ samples had significant numbers of visible particles). In addition, two full sets of sample heads were used throughout the study period to minimize the time required for preparation between sample periods, and the problematic PM concentrations were present in filters which were placed in both sets of sample heads.

3) A phenomenon commonly referred to as "particle bounce" may have occurred. Particle bounce refers to when a particle collides with the impactor assembly but then returns to the airstream and is collected downstream at the filter. To aid in removal of particles colliding with the impactor plate, grease may be applied on the impaction surface. If too many particles accumulate in the grease, however, the impaction surface loses its "stickiness" and larger particles may bounce off, leading to higher reported $PM_{2.5}/PM_{10}$ concentrations than actually existed. Impactor plate stickiness is influenced by a combination of total exposure time and PM concentrations during exposure. The smaller effective impact area and increased particle velocity in the MiniVol $PM_{2.5}$ impactor assembly makes it more susceptible to particle bounce than the PM_{10} assembly under the same conditions, which could result in higher reported levels of $PM_{2.5}$ than PM_{10}. Airmetrics, Inc. suggests cleaning and regreasing of the impactor plates every five to seven samples to maintain the design removal efficiency, but states that the need to renew the plate may change based on exposure levels. In the case of this study, silicone-based, high-vacuum grease was applied to all impaction surfaces on-site prior to sampling in May. Personnel noted that impactor assemblies in downwind samplers had collected significant amounts of particles near the end of the seven sample periods in that month (May 17-20), which suggests that particle bounce likely occurred during some sample periods. The sample heads and impactor assemblies were cleaned and greased during the break in measurements, with evaluation and re-greasing if necessary after each measurement in June. In addition, the enhanced susceptibility of the $PM_{2.5}$ assembly to particle bounce could explain the inverted $PM_{2.5}$ and PM_{10} concentrations observed at downwind locations during the May 19 and May 20 sample periods.

4) Exposure to dust plumes while the sampler was deployed but not actively pulling air through its system is another potential cause. In such a case, settling of particles may allow some to reach the filter. Dirt access roads surround each field at this location and the standoff distance for the samplers usually put them on the downwind side of these access roads. While travel was limited to farm activity, it is possible that a vehicle driving on these roads may have passed shortly before a programmed start time and resulted in large particles being deposited on the filter.

5) Contamination prior to or after sampling is a potential cause that cannot be ruled out, especially in a dry, dusty environment. Filters were held in individual Petri dishes at all times except during sample collection. The filters and Petri dishes were stored on-site in dessicators. All required filter handling for sampling was performed on-site in a trailer over white laboratory paper which was changed as needed. Personnel handling the filters wore latex gloves and used tweezers to move filters; the tweezers were rinsed with DDI water as needed. Any filters dropped prior to sampling were not used, and those that were dropped after sampling were noted and not used in further calculations. While the trailer was kept as clean as possible, the environment outside of the trailer was dusty. In fact, blowing dust was a problem during a couple sample periods, especially May 20 R1 and R2.

While any one of these potential causes can significantly impact the mass collected on a filter, there is evidence from examination of the filters under the microscope that a combination of several of these phenomena potentially occurred. It was suspected that contamination prior to or after sampling accounted for the largest portion of the problems in the MiniVol mass concentration data, with additional contributions at locations heavily impacted by agricultural activity, or traffic on nearby dirt roads from particle bounce, and the passage of large particles due to the S-shaped collection efficiency curve of the impactor assembly.

While the microscopic analysis of the filters provided insight into the number/size of particles on the filters and causes of possible contamination, it did not provide a feasible solution to correct this problem in the current data set. Microscopically examining and analyzing both the collection area and the ring of each of the 296 filters used was prohibitively time intensive. A surrogate method for determining the compromised/contamination level of each filter was devised in order to feasibly remove those samples that were compromised. The ring on each filter was visually inspected by just one person with a Doublet 10x single lens magnifier by Selsi Company, Inc. (Midland Park, NJ) against a white background and the relative amount of particles found on the ring was classified into one of the following ring particle density categories: 1) None, 2) Very light, 3) Light, 4) Medium, 5) Heavy, 6) Very heavy, and 7) Extremely heavy. The following two categories were also used for the specified reasons: 8) Not available – filters were not available for visual inspections because the IC ion analysis had already been performed; and 9) Filters with notes – filters that had noted problems either during or after sampling that could affect the mass collected, such as being dropped after sampling or a malfunction of the flow system. While this method is subjective it has the virtue of minimizing the impact of grossly contaminated filters on the final PM emission values.

A significant number of particles were found on the rings of upwind/background and downwind samples for all three PM mass fractions measured. In fact, none of the inspected filters had a completely clean ring that would correspond to the “None” category. Table 39 presents the

results of the visual categorization according to the measured PM fraction. Filters with noted problems (i.e., stable post-weights could not be obtained, filter was dropped during post-sample handling, large particles/organic matter were present on the filter immediately after sampling) numbered 17, 5.7% of the 296 samples collected during the study. Most samples (66.9%) were classified as very light or light, having just a few small detectable particles. As TSP sampling does not use an impactor assembly, a TSP filter would be expected to have larger and much more numerous particles that may more easily move to the ring of the filter. Therefore, more TSP filters would be expected to have a significant number of particles on the ring than the collocated PM_{10} and $PM_{2.5}$ filters collected at locations exposed to heavy PM plumes. This expected result was supported in the ring particle density categorization of the filters: the only filter classified as extremely heavy was a TSP filter. TSP filters dominated the very heavy category, most of which had visible particles in the Petri dish in addition to the filter ring.

Table 39. Size fractionated results of the visual inspection of annular filter rings.

Size	Ring Particle Density Category									Sum
	None	Very Light	Light	Medium	Heavy	Very Heavy	Extremely Heavy	Not available	Filter w/ notes	
TSP	0	2	22	19	8	4	1	0	8	64
PM_{10}	0	45	51	9	2	0	0	1	8	116
$PM_{2.5}$	0	35	43	19	8	1	0	9	1	116
Total	0	82	116	47	18	5	1	10	17	296
% of Total	0	27.7	39.2	15.9	6.1	1.7	0.3	3.4	5.7	

A troubling finding was that a significant percentage (24%) of $PM_{2.5}$ filters was categorized as medium or greater. Most of these occurred on downwind samples collected May 18-20, while the collocated PM_{10} samples are generally in the very light and light categories. This finding suggests that contamination during non-sample times is likely not a significant cause of the problems in the data for these days because all the filters used on a given day were treated the same during filter handling and storage and it would be expected that filters of all size fractions would be impacted equally. This disparity in the number of $PM_{2.5}$ and PM_{10} filters in the medium or greater ring particle density categories suggests that the dominant cause of larger-than-expected particles and $PM_{2.5}$ concentrations higher than PM_{10} occurs at the impactor assembly in the sample head, which was the only difference between the $PM_{2.5}$ and PM_{10} MiniVol samplers used. As the $PM_{2.5}$ impactor assembly removes more particles from the airstream than a collocated PM_{10} impactor, it is likely that particle bounce would occur sooner and at a higher rate in the $PM_{2.5}$ impactor than in the PM_{10} impactor under the same plume conditions.

Table 40 presents the ring particle density category results by sample period, with a graphical presentation in Figure 45. In general, the light category has the greatest number of filters, followed by the very light category. The greatest frequency of filters classified as medium and greater occurs in samples collected May 18-20, which corresponds to the greatest occurrence of $PM_{2.5}$ samples classified as medium or greater. One conclusion drawn from this is that the downwind filter-based PM samplers were likely overloaded during those sample periods, suggesting that the reported downwind concentrations should not be used for emission rate calculations. This removes 104 samples, leaving 175 samples for emission rate calculations and six others with noted problems. Table 41 shows the operation(s) examined in each sample

period, whether or not the filter-based PM dataset for each period was suitable for calculating emission rates, and, if it was not used, the reasons for excluding the entire dataset.

Table 40. Results of the visual inspection of filter rings by sample date.

Sample Period	Ring Particle Density Category								Sum
	Very Light	Light	Medium	Heavy	Very Heavy	Extremely Heavy	Not available	Filter w/ notes	
May 17 R1	6	13	3	0	0	0	1	0	23
May 17 R2	3	13	4	1	0	0	1	1	23
May 18	3	7	8	1	1	0	1	2	23
May 19 R1	6	5	6	1	1	0	1	3	23
May 19 R2	7	8	3	1	1	1	1	1	23
May 20 R1	7	3	2	5	2	0	1	3	23
May 20 R2	5	11	3	1	0	0	1	2	23
June 5 R1	0	12	3	5	0	0	1	2	23
June 5 R2	0	12	7	1	0	0	1	2	23
June 7	4	12	5	0	0	0	1	1	23
June 11	10	13	0	0	0	0	0	0	23
June 18	12	6	1	1	0	0	0	0	20
June 25	19	1	2	1	0	0	0	0	23
Sum	82	116	47	18	5	1	10	17	296
% of Total	27.7	39.2	15.9	6.1	1.7	0.3	3.4	5.7	100.0

For the remaining samples, the ring particle density classifications were used to separate out problematic PM concentrations. In the $PM_{2.5}$ and PM_{10} size fractions, all filters that were classified as medium or greater and those with noted problems were removed, totaling 12 (6.9%) and 8 (4.6%) $PM_{2.5}$ and PM_{10} samples, respectively, for remaining sample periods. In addition, two $PM_{2.5}$, one PM_{10}, and two TSP samples were removed from consideration due to exceptionally high or low concentrations, often with significantly greater $PM_{2.5}$ or PM_{10} concentrations than PM_{10} or TSP, respectively. Two of the five were collocated with an OPC and the OPC time series (based on 20-second sample times) in each case was examined and provided no evidence of contamination/concentrations significantly above background during sampling. Four of the five removed for this reason were collected at background locations, and the fifth was at the AQT location while the tillage operation was occurring in Field 4, several hundred meters to the north. The other three samples removed were background TSP, PM_{10}, and $PM_{2.5}$ samples for May 17 Run 2, which were not collocated with an OPC at the time. Unfortunately, this did not leave a background PM_{10} or $PM_{2.5}$ concentration to use in calculating the operation's contribution to downwind concentrations for this run as the PM_{10} and $PM_{2.5}$ filters at the other background location had ring particle density categorizations of medium and were also removed. Therefore, a TSP emission rate will be calculated using inverse modeling for May 17 Run 2, but not PM_{10} and $PM_{2.5}$ emission rates.

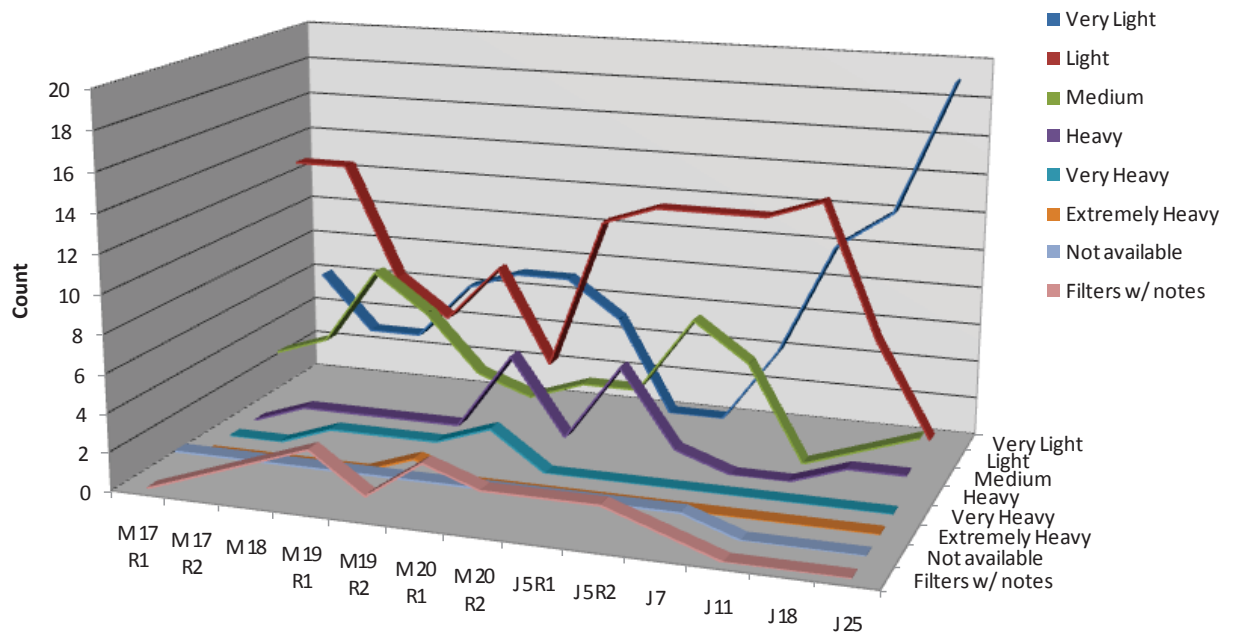

Figure 45. Line graphs showing the number of filters in each ring particle density category for each sample period.

Traffic on access roads adjacent to upwind/background locations was recorded by field personnel during most sample periods. Therefore, possible contamination due to sources nearby the upwind sample locations was closely investigated during each sample period. This was accomplished by examination of the available OPC time series for significant spikes in particle counts that indicate such an event. The OPC time series for upwind location 10.0 on June 5 Run 1 (R1) and June 5 Run 2 (R2) showed that nearby road traffic significantly impacted the PM samplers: between 50% and 80% of the TSP volume concentrations were attributed to such events. In addition, the ring particle density categories of the six filters collected at this location on June 5 were: $PM_{2.5}$ heavy and medium; PM_{10} heavy and medium; and TSP = medium and light. Based on these categorizations, the $PM_{2.5}$ and PM_{10} values had previously been removed for being medium or greater. In light of this, the two TSP concentrations at location 10.0 were also removed from emission rate calculations. Samples collected at the other background location, T1, were not compromised by road traffic.

Table 41. Sample period filter datasets used in calculating emissions, with reasons for why some datasets were not used in further calculations.

Sample Period	Operation(s)	Used	If not, reason excluded
Conservation Tillage			
May 17 R1	Strip-Till	Yes	---
June 7	Plant and Fertilize	Yes	---
June 11	Herbicide application	Yes	---
Conventional Tillage			
May 17 R2	Break down in-field borders	TSP – Yes PM_{10}, $PM_{2.5}$ - No	Problems with most background samples
May 18	Chisel	No	Downwind samplers overloaded by plumes
May 19 R1	Disc 1	No	Downwind samplers overloaded by plumes
May 19 R2	Disc 2	No	Downwind samplers overloaded by plumes
May 20 R1	Lister	No	Downwind samplers overloaded by plumes
May 20 R2	Build ditch and field-edge borders	No	Windblown dust contamination
June 5 R1	Break down ditch and field edge borders, Cultivator passes 1 and 2, and Roller	Yes	---
June 5 R2	Plant	TSP, $PM_{2.5}$ – Yes PM_{10} – No	Problems with both PM_{10} background samples
June 18	Fertilize	Yes	---
June 25	Cultivator pass 3	Yes	---

Results of these investigations into the inverted $PM_{2.5}$-PM_{10} concentrations and visible particles led to the removal of many collected filter samples from emission rate calculations using inverse modeling, including all downwind samples collected during five consecutive sampling periods. A graphical representation of the filters used and reasons for not using others is presented in Figure 46. Note that the four samples for which it was determined that the $PM_{2.5}$ and PM_{10} filters had been switched were corrected (i.e., the concentration values were reassigned) and used in emission rate calculations. The final PM concentrations used in emission rate calculations are tabulated in Table 33 and Table 34. Most of the samples removed during this investigation were not used in MCF calculations, as explained in Section 4.3.2.

There are several practices and procedures which may prevent such problems in future filter-based sampler deployments in such conditions. Filter handling steps include, but are not limited to, the following: use EPA-recommended filter storage, handling, and mass determination

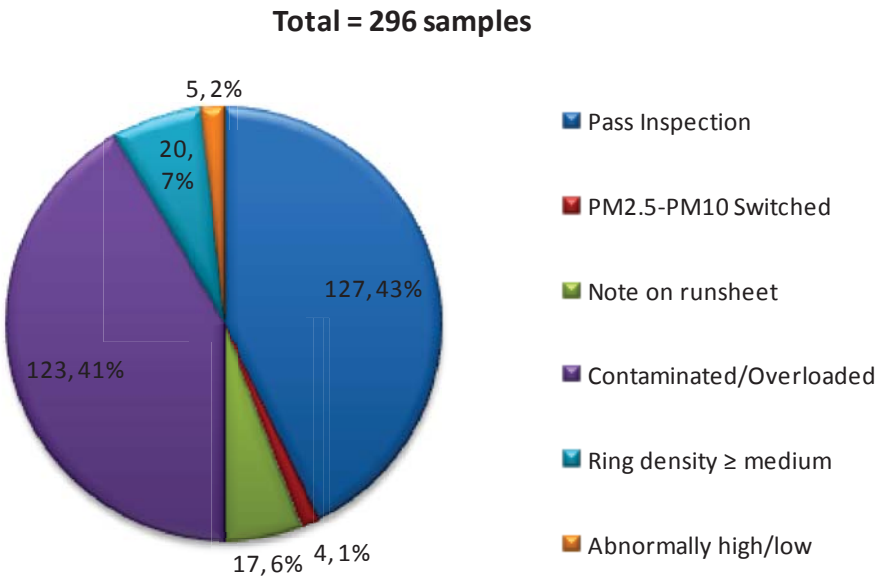

Figure 46. Categorization of filter samples to determine suitability for use in emission rate calculations in inverse modeling.

methodologies; use a calibrated mass balance, with continuing calibration verification; carefully track each filter throughout the pre-weighing, sampling, and post-weighing steps; and ensure that the filter storage and handling areas, both in the lab and the field, are clean and will minimally contribute to the particles present on the filter. During the sample preparation and sampling periods, the following practices will help to prevent problems with filter samples: inspect each sample assembly before and after use for potential problems, specifically checking the condition of the layer of high-vacuum grease on the impactor plate; place sample locations at a sufficient distance downwind from the source(s) such that heavy plumes will not overload the sampler; if possible, restrict access to upwind areas to prevent contamination of upwind samplers, but if it is not possible place upwind samplers in positions that will not be impacted by nearby activities. Additionally, record in detail all activities under study (e.g., tractor operation time, tractor position via GPS) and any activities in upwind areas that may potentially affect upwind and/or downwind samplers. Proper training of personnel is also critical, both in prevention and identification of potential problems. Placing a more time-resolved PM sampler, such as the OPCs employed herein, with filter-based samplers provides the opportunity to examine changes in aerosol loadings to identify impacts from source activities, as well as potential contamination during sampling. It should be noted that most of these procedures were already in use when the problems in this campaign occurred; future mitigation of such problems requires more careful evaluation and application.

As discussed in the conclusions, the fact that we had to dedicate so many resources to extracting any useable data from our MiniVol samplers tells us that some field situations are in fact "too dusty" for the sampling techniques as we applied them. Furthermore, even when we tried to counter some of these effects (by using a PM_{10} impactor as a pre-filter for the $PM_{2.5}$ impactor) we continued to run into difficulty. By employing as many of the best-practices listed above we expect to avoid many of these difficulties in the future.

10.3 APPENDIX C: RESPONSES TO COMMENTS RECEIVED RE: CALIFORNIA SPRING 2008 TILLAGE CAMPAIGN: DATA ANALYSIS REPORT

Responses to comments are in *italics* with all changes to the report text indented. Note that all page numbers mentioned refer to the page number in the final version.

10.3.1 Draft Date: 16 March 2011 (Organization: U.S. EPA)

10.3.1.1 General Comments

1) Since the goal of this project was to calculate emissions for the purposes of assessing control efficiencies and any emission calculations were ultimately used to compare emissions from a conventional practice with one that reduces emissions, we believe that it is appropriate to use a combination of point samplers and inverse modeling as a part of the methodology used to calculate emissions. EPA would want to further scrutinize this methodology if the main goal of the study was to inform baseline emission factors.

   No response required

2) The dependence on the use of historical emissions factors and the comparison to emissions factors estimated in this study is understandable. In addition, the discussions describing the variations of measured emissions and the uncertainties associated with historical emissions factors is refreshing. However, some of the cited uncertainties appear quite low compared to some recent assessments of emissions factors uncertainties of several sources which would be thought to be less variable than tilling emissions (see http://www.epa.gov/ttn/chief/efpac/uncertainty.html). It is suggested that the uncertainties associated with the historical emissions factors and the estimated emissions factors associated with this study be re-evaluated based upon the conclusions in the draft emissions factor uncertainty report (i.e. the number of independent test runs and the underlying variability of the measured emissions). Then some of the processes which are described as not being in close agreement may be more in line with the overall uncertainties associated with the emissions factors and variabilities.

   The authors agree that a better analysis of tillage emissions factors uncertainty is warranted and have done so to the extent data are available, following the emissions factor dataset analysis procedure used in the emissions factor variability assessment referenced above. Results of two additional studies that have been released since submittal of this document to EPA have been included in the literature review. The following paragraph describing the uncertainty analysis methodology and results has been added to the end of the literature review section (page 10). Refer to page 11 in the document to view the tables and figures.

   > *"An uncertainty analysis was conducted to determine the statistics of the preceding PM10 emissions factors reported from measurements. This analysis was performed following the emissions factor dataset analysis technique used by RTI International in 'Emission Factor Uncertainty Assessment, Review Draft' [29]. Data points were categorized according to the following tillage operations, with the number of values given in parenthesis: chisel (2), disc (67), land planing (1), listing (8), ripping (5), root cutting (3), standard tillage planting (11), strip-*

till planting (9), strip-tilling (6), and weeding (15). In cases where a report/paper only provided an average emissions factor, the average value was used only once. RTI International found that two parametric models, the lognormal and Weibull distributions, best fit the analyzed datasets. These same two parametric models were fitted to the tillage operation datasets with eight or more data points. The estimated parameters for these models and the corresponding goodness-of-fit to the available data points, expressed as the root mean square error (RMSE), are given in Table 5 with the better fit model values in bold. Note that a smaller RMSE represents a better fit to the data. The Weibull distribution proved to be a better fit for four out of the five examined datasets. The fits to the disc and weeding datasets were better than that for the remaining three, both visually and based on the RMSE values. Figure 1 presents the histogram for the disc operation dataset and cumulative density functions developed from the data and the Weibull distribution fit to the data. The mean and median values of the fitted Weibull distribution are shown on the cumulative density function line, along with the emissions factor value given by ARB for a disc operation. The ARB emissions factor of 134.5 mg/m2 is very close to the Weibull distribution median of 136.3 mg/m2. The emissions factor values corresponding to the 5%, 25%, median, 75%, and 95% levels along the cumulative distribution curve, as well as the average emissions factor, were calculated for the five operations and are presented in Table 6. The 95% level emissions factors for the three operations with poorer fits (i.e., higher RMSE) seem very high; this is likely an artifact of fitting the distributions to a limited number of datapoints. In this analysis, the better fits were obtained for datasets with n ≥ 15."

The discussion of the results on page 86 of the document has been updated to reflect the findings of the uncertainty analysis, which did indeed include a portion of the higher values as suspected by the reviewer. The paragraph now reads:

"Some of the values herein reported are in agreement with those reported by Flocchini et al. (2001) and Madden et al. (2008), as well as the PM10 emission factors used by CARB, such as the strip till and plant passes in the conservation tillage method and the cultivate and roll passes in conventional tillage [12][16][13]. Other emission rates are significantly different and larger than previous values reported in the literature, especially the discing 1 and 2, chisel, and lister passes of the conventional tillage, though those derived through inverse modeling are below the estimated 95% level for their respective distributions as presented in the uncertainty calculations in this report. The lidar-derived emission rates for the disc 1, disc 2, chisel, and lister passes are high when compared to values found by inverse modeling coupled with OPC PM data, values in the literature for the same operations, and values reported in the 2007 fall CMP tillage study which used the same lidar methodology. These relatively high emission rates provide indirect support for the conclusion that downwind PM samplers were likely overloaded during those sample periods by high aerosol concentrations. While the values from listed published studies are generally not in close agreement, they are relatively well fit by lognormal or Weibull distributions, which have previously been shown to represent emissions factors datasets well [31]. In addition, they are within the range of the variability expected from

measurements made under different meteorological and soil conditions, as demonstrated by the wide range of values from Flocchini et al. (2001) [12] summarized in Table 2. The results from this campaign are not in as good agreement as previous results have been [7]. In general our results are larger than their corresponding literature values."

A sentence has also been added to the executive summary on page 2 about the comparative results with the uncertainty analysis:

"Emissions factor values estimated through inverse modeling for these operations are below the 95% level predicted by statistical distributions fitted to published data; emissions estimates from lidar for the same operations are above the 95% level"

3) The use of reverse modeling for particulate matter is of concern since the deposition and removal mechanisms are limited in EPA models. The EPA models only have a percentage of the particulate reflect off a smooth surface when in reality, the ground surface is not smooth and if there is vegetation more removal may occur. In addition, electrostatic and other forces may cause small particulate to aggregate to form larger particulate. These effects are not included in EPA models and as a result a reverse model would tend to underestimate the actual source strength. The amount of underestimation may depend upon not only these items but also the distance at which the measurement is removed from the emissions source.

The authors agree with the limitations of the ISC and AERMOD models stated by the reviewer concerning deposition and removal mechanisms, resulting in an underestimation of the actual source strength. The effect of the distance at which the measurement is removed from the source was minimized in this study by locating the sampling sites immediately adjacent to the field under study; additionally, the constant motion of the tractor and implement lead to varying distances between the measurement and source. It should also be noted that any emission estimation methodology for a tillage source that does not include a correction for the deposition and removal of PM due to surface roughness, vegetation, etc. as a function of distance from the source will underestimate actual emissions. The following text has been added to the inverse modeling methodology section on page 38:

" In addition, the deposition and particle removal mechanisms are limited in the ISCST3 and AERMOD models herein employed. Insufficient correction within a given model for these and other processes that decrease downwind pollutant concentrations will lead to an underestimation of emission rates based on measured downwind impacts."

10.3.1.2 Comments about Appendix B

1) While the selection and use of low-cost, battery-powered samplers is understandable in a study of this type (particularly requiring a large number of concurrently operated samplers), it should first be recognized that the MiniVol samplers are not EPA-approved reference method or equivalent method samplers for making either PM2.5 or PM10 compliance measurements. Although the MiniVol samplers have sometimes been shown to provide similar PM concentrations to collocated FRM

samplers under some sampling conditions, their ability to extract representative samples of large particles under high wind speeds has not been demonstrated. In fact, a limited wind tunnel evaluation of the MiniVol samplers (conducted by Research Triangle Institute in 1991) indicated that the sampler's ability to obtain representative aerosol samples degrades rather dramatically as a function of wind speed. In agricultural environments where elevated wind speeds are the not at all uncommon, representative sampling of large aerosols characteristic of tilling operations cannot be assumed. This is particularly the case when interpreting data from MiniVol samplers operated as "TSP" samplers. For this reason, data obtained with the MiniVol samplers in this type of study should only be considered as approximate measures of PM2.5, PM10, and "TSP" concentrations.

We thank the reviewer for bringing to our attention the collection efficiency versus wind speed issued found in the 1991 MiniVol study. This is an issue of concern, especially when dealing with aerosols with relatively large size distributions as found downwind of most agricultural sources. It should be noted that the sampler model of those tested in 1991 were ≤ 3.x, while the model number of the units employed during this study were 4.2. Attempts to contact Airmetrics to inquire about potential changes to the sampling inlet/size separator that might affect sampling efficiency between the models have not yet been successful.

Text was added to the Section 3.1.4.1, page 27, which describes the MiniVols, to clarify that the MiniVol is neither a FRM nor a FEM.

> *"The MiniVol is a battery operated, ambient air sampler that gives results that closely approximate air quality data collected by a Federal Reference Method (FRM) PM sampler. The MiniVol is neither designated as an FRM nor a Federal Equivalency Method (FEM) by the EPA, and results should be considered as approximate measures of PM."*

A short discussion of general meteorological conditions observed during the sampling periods and a table listing period-average values has been included in section 4.1.2.2, page 43. The period-average wind speeds observed during this study varied between 2 and 6 m/s, within the range of 0.5 m/s and 6.7 m/s at which the 1991 study was conducted.

Section 4.1.2.2, page 43, reads:

> *"Meteorological characteristics were monitored on-site throughout the field study. Sample period average conditions were calculated and are presented in Table 14 based on measurements taken at the WM and EM locations. As can be seen from these data, all measurements were made during warm and dry conditions. Winds were consistently out of the northwest with average speeds between 2 and 6 m/s."*

2) Appendix B provides an account of discrepancies noted during visual observations of collected field filters and offers several possible explanations for these observations. While the discussion on page 108 correctly points out that there may be differences in the position and shape of the MiniVol and FRM's fractionation curves, it is <u>not</u> correct to state "Ideally, the collection efficiency of the size fractionation

device would be a step function that goes from 0% to 100% at the desired cut-off size." In fact, the slope of the FRM's PM10 fractionation curve was intentionally designed to match the performance of the human respiratory system - which does not provide step-function performance. The fractionation curve of the PM2.5 FRM was also not designed to provide step-function performance.

This error has been corrected in the text with the first and second sentences of this paragraph, page 113, now stating

> *"The collection efficiency curve of the PM10 and PM2.5 size fractionation devices employed by both FRMs and MiniVols are S-curves with respect to particle aerodynamic diameter, designed to mimic the particle removal efficiency of the human respiratory system. The removal efficiency curves have a 50% collection efficiency at the designed cut-off size, with some smaller particles being removed and some larger particles passing through the system."*

3) As hypothesized on page 109 of the report, observations of very large particles on collected field filters and of uncharacteristic deposition patterns are almost certainly due to "particle bounce" occurring in the MiniVol samplers. Unlike EPA's PM2.5 FRM which uses either the WINS well or the very sharp cut cyclone (VSCC) to minimize substrate overloading and particle bounce, the MiniVol samplers were not designed to handle high concentrations of ambient aerosols. The design of the impaction substrate for both the PM2.5 and PM10 MiniVols is such that particle bounce may occur from the impaction stage once a few monolayers of particle deposits occurs during sampling. Once particle bounce begins, the cutpoint of the stage can shift dramatically upwards and result in inaccurate PM concentration measurements. In the case of the MiniVol design, the reduction in a cutpoint from 10 micrometers to 2.5 micrometers requires a reduction in impaction jet diameter from approximately 0.69 cm to approximately 0.29 cm. As a result, the jet velocity through the PM2.5 MiniVol is approximately 5.5 times that of the PM10 MiniVol. This increase in jet velocity results in an increase in particle kinetic energy and makes the PM2.5 MiniVol more susceptible to particle bounce than the PM10 MiniVol. And because the PM2.5 MiniVol has a much smaller stage deposition area than that of the PM10 MiniVol, it is possible for the mass gain of PM2.5 MiniVol's filter to exceed that of the PM10 MiniVol filter. As a result, measured PM2.5 concentrations may often exceed those of collocated PM10 concentration measurements. Although occasional inadvertent switching of PM2.5 and PM10 filters was noted in the report, substrate overloading was almost certainly the cause of the majority of the "inverted" PM2.5 and PM10 measurements.

The authors thank the reviewer for providing a very good analytical description of the particle bounce phenomenon as it may occur in the MiniVol impactor assembly. The discussion under point 3 on page 113 in the report has been changed to include portions of this description. It now reads:

> *"A phenomenon commonly referred to as "particle bounce" may have occurred. Particle bounce refers to when a particle collides with the impactor assembly but then returns to the airstream and is collected downstream at the filter. To aid in removal of particles colliding with the impactor plate, grease may be applied on*

the impaction surface. If too many particles accumulate in the grease, however, the impaction surface loses its "stickiness" and larger particles may bound off, leading to higher reported $PM_{2.5}/PM_{10}$ concentrations than actually existed. Impactor plate stickiness is influenced by a combination of total exposure time and PM concentrations during exposure. The smaller effective impact area and increased particle velocity in the MiniVol $PM_{2.5}$ impactor assembly makes it more susceptible to particle bounce than the PM_{10} assembly under the same conditions, which could result in higher reported levels of $PM_{2.5}$ than PM_{10}. Airmetrics, Inc. suggests cleaning and regreasing of the impactor plates every five to seven samples to maintain the design removal efficiency, but states that the need to renew the plate may change based on exposure levels. In the case of this study, silicone-based, high-vacuum grease was applied to all impaction surfaces on-site prior to sampling in May. Personnel noted that impactor assemblies in downwind samplers had collected significant amounts of particles near the end of the seven sample periods in that month (May 17-20), which suggests that particle bounce likely occurred during some sample periods. The sample heads and impactor assemblies were cleaned and greased during the break in measurements, with evaluation and re-greasing if necessary after each measurement in June. In addition, the enhanced susceptibility of the $PM_{2.5}$ assembly to particle bounce could explain the inverted $PM_{2.5}$ and PM_{10} concentrations observed at downwind locations during the May 19 and May 20 sample periods."

4) If funding were not a limitation, a much better alternative to the use of the MiniVols would be BGI PQ100 samplers. These 16.7 Lpm, filter-based samplers are EPA-designated for both PM2.5 and PM10 compliance testing, and operate with 120 VAC line power or internal 12 VDC battery (with solar panel option). The PM2.5 version of the BGI PM2.5 PQ100 can be equipped with a 2.5 micrometer cutpoint VSCC which has been shown to maintain its fractionation performance under high loading conditions. Use of PQ100 samplers should totally prevent the occurrence of PM2.5 and PM10 data inversion that was reported in the study. Even if a suite of these BGI samplers could not be procured, it would be useful to collocate a pair of them with the currently operating MiniVol samplers in order to help isolate and resolve the performance issues currently noted with the MiniVol samplers. Funding required to purchase a pair of the PQ100 samplers would more than be compensated for the resources currently being expended attempting to extract and interpret useful information from field data of uncertain quality.

   The BGI PQ100 units have recently been investigated as potential future purchases. The reviewer's description and suggestion for comparison with the MiniVols currently deployed are compelling and a future purchase of some PQ100s is planned. This comment highlights our ongoing effort to utilize instruments of higher fidelity, such as the BGI PQ100.

5) If continued use of the MiniVol samplers is envisioned, <u>it is absolutely critical that the MiniVol's impaction surface be renewed after every sampling event</u>. In the MiniVol design, this is not a difficult or time consuming process. While this procedure will not totally prevent substrate overloading during sampling of high concentration aerosols, it will at least minimize the effect and should substantially

reduce the frequency of the PM2.5 and PM10 concentration "inversion" that s currently being observed.

It is anticipated that the MiniVols will continue to be used to measure ambient and near-source PM. The reviewer's suggestion to renew the impaction surface between each use will be implemented in future uses. This has also been included as a potential preventative action in the Lessons Learned section, page 90, under the second point:

> *"Another preventative action is to clean and regrease the MiniVol impactor assemblies after each use if exposed to high aerosol concentrations."*

10.4 DRAFT DATE: 15 APRIL 2013 (ORGANIZATION: SAN JOAQUIN VALLEY AIR POLLUTION CONTROL DISTRICT)

1) Page 45 Section 4.2.1 discussion of 165 of 296 samples rejected by QA requires some immediate discussion as well as reference to Appendix B. This amount of QA rejection is very high and will raise an immediate red flag. The importance of this issue merits added text in the paragraph.

A summary of likely causes of the high failure rate has been included. The section on page 47 now reads as follows:

> *"Of the 296 filter samples collected, 165 did not pass quality analysis/quality control (QA/QC) steps applied to the dataset, leaving 131 for use in calculating emission rates using inverse modeling. An investigation into this high rate of failure was conducted and a detailed description is provided in Appendix B. In summary, filters that did not pass QA/QC were suspected to have been contaminated either during sampling or during storage and handling. Evidence of "particle bounce" was found on many $PM_{2.5}$ and PM_{10} samples collected during May sample periods. Particle bounce occurs when particles that collide with the impactor plate, the mechanism used by the MiniVols to exclude particles larger than the design size, are re-entrained in the airstream and collected on the filter downstream and result in higher measured levels than actually existed. This issue is most likely due to exposing the MiniVol samplers to dust plumes exceeding the maximum recommended exposure level and improper instrument maintenance and cleaning through the May sample periods. Corrective action was taken during the June sample periods and no issues associated with particle bounce were observed in the second portion of the study.*
>
> *"Additionally, some particles were observed on top of and imbedded into the plastic annular ring around the Teflon filter material – the plastic ring is covered by the filter holder assembly during deployment. This was likely due to contamination during on-site filter storage or handling. Efforts were made to minimize this issue throughout, especially during the June sample periods. However, windblown dust did impact the handling and storage area during the last sample periods in May. In addition, contamination of upwind samplers prevented emission rate calculations for some size fractions for two other operations. The size fraction distribution of approved filters was nearly identical to the total sample set: 51 (39%) were $PM_{2.5}$, 50 (38%) were PM_{10}, and 30 (23%)*

were TSP. These finalized concentrations are given in Table 33 and Table 34 in Appendix A. *See Appendix B for a detailed discussion of the QA/QC steps, filter inspection failure, possible causes of the failures, and preventative solutions for future sampling."*

2) In sharp contrast to section 4.2.1, sections 4.2.3 through 4.3.3 (starting at page 49) never mention QA. Some discussion of data completeness and redactions should be included for these sections.

Sentences and paragraphs addressing QA have been included in each of the sections referred to above. Some of the material were previously in the methodology portion of the report and have been pulled into the results section. While the lidar concentration measurements section had some discussion of QA screening, it has been augmented, clarified, and moved to the first paragraph of the section.

Page 48, 4.2.2.1 Organic Carbon/Elemental Carbon Analyzer

"As mentioned previously, the organic carbon/elemental carbon analyzer passed the manufacturer's suggested in-field audits and after completion of the field project the data were manually screened for completeness and potential outliers. During the two distinct periods of sampling, May 13-20 and June 3-21, 2008, the EC/OC instrument operated continually except for brief periods for QA/QC checks, servicing of the system generator, or significant breaks in the producer operations. An unanticipated consequence of the one hour sample times, coupled with the dual channel operation of the R P 5400 EC/OC Analyzer, was that the sampling/analysis/cleaning cycles extended beyond the planned two hours. The net result was a sampling profile wherein every third hour of data was missing (66% sample collection efficiency over the entire deployment). However, because the actual farm practice periods varied from one to eight hours, the actual, observed data periods ranged from one to eight hours, the data coverage was from 50-100%, averaging 78.2% ± 10.3%."

Page 50, 4.2.2.2 Ion Chromatographic (IC) Analysis

"As such, a total of nine filters were analyzed for soluble ions. However, two of these filters, from 5/20/08 and 6/5/08, were subsequently suspected as potentially having contamination issues (see Section 4.2.1) and were discarded from further analysis."

Page 54, 4.2.3 Aerosol Mass Spectrometer

"During the tillage experiment, the AMS acquired chemical composition data from May 14-May 19 with some significant gaps in the data due to mass spectrometer malfunctioning. This required manual screening of the AMS data. Approximately 35% of data over the time period was found to be valid. Large gaps occurred throughout the sampling period with, for example, no data acquired on May 17."

Page 56, 4.3.1 Met One Optical Particle Counter

"The collected OPC data were analyzed for particle size distribution, particle volume concentrations, and converted to particle mass concentration through

multiplication with the MCF, as described in Section 3.1.4.2. Table 35 and Table 36 present the $PM_{2.5}$, PM_{10}, and TSP concentrations as reported by the OPCs. Three to four OPCs were in positions immediately downwind of the field under study in each sample period, with between one and four OPCs in upwind locations. Unlike the downwind MiniVol samplers, the downwind OPCs were not overwhelmed by the dust plumes from the tillage activities – the manufacturer specified range of the OPC of 0 to 318,000,000 particles/m^3 was never exceeded – and thus provided usable data throughout all sample periods. Upwind OPC time series data were examined for contamination from activities upwind of the site, such as unpaved road traffic. Contamination was found in six of the 12 sample periods, with five of those occurring at the 10.0 sample site that was immediately downwind of an unpaved road (see Figure 7). Large spikes indicative of contamination were removed from the upwind OPC time series data in these instances to estimate the background aerosol concentration; the estimated background levels were in very good agreement with those measured by an OPC at a different, uncontaminated upwind location (see Table 37 and Table 38).

Data completeness for the OPC datasets was calculated as a ratio of the number of valid samples per sample period over the possible number of valid samples and expressed as a percentage. Data completeness was less than 100% due to communication errors between the OPCs and the computer logging the data, resulting in lost packets of 20 second sample data. Communication error frequency was variable between OPCs and across time. Data completeness per sample period ranged from 81.8% to 100.0%, and averaged (± 1σ) 97.4 ± 3.7%."

Page 61, 4.3.2 Optical to PM mass concentration conversion

"As OPC data collected at each site and during each sample period passed QA/QC, the calculation of MCF values was dependent solely on the presence of a valid filter-based PM measurement."

Page 66, 4.3.3 Lidar Aerosol Concentration Measurements

"Lidar data was collected throughout all sample periods, except for the Cultivator 3 pass monitored on June 25 due to an equipment failure after the previous measurement. All lidar scans collected during times when no tillage activity was occurring, based on detailed field notes, were removed from further calculations. The remaining scans were visually checked to remove scans with data acquisition errors and to prevent the use of data that was contaminated by other sources; sources of observed contamination were vehicular traffic on unpaved roads, agricultural activities immediately upwind, activities associated with the adjacent dairy, and windblown dust. Contaminated upwind scans, as well as the corresponding downwind scans, were removed from further emission rate calculations. In most cases two or more downwind scans use the same upwind scan as a reference because multiple downwind scans were made for each upwind scan. Downwind scans were not used in further calculations if the corresponding wind direction was outside of ± 70° from perpendicular to the downwind lidar beam path; if the lidar scan contained apparent plumes from an outside source (such as from unpaved road traffic or the dairy); if no plumes were detected; or if

the tillage plume had a potentially significant portion crossing the lidar beam closer than 500 meters down beam. In addition, upwind scans were invalidated if none of the associated downwind scans were usable. Light wind speeds (< 1 m/s) were recorded during portions of some measurement periods. Light winds challenge the measurement system and resulted in additional invalidation of some lidar scans. The total number of lidar scans made along both upwind and downwind planes is presented in Table 19*, along with the number of valid scans, i.e. those that passed all quality checks, and the percent of valid scans compared to the total number of scans.*

In several cases, the percent of valid scans was very low. Although wind and background conditions were good during the herbicide application on 6/11, none of the scans taken were deemed valid because the mass difference between the upwind and downwind scans was below the minimum detection level (MDL). This means that the operation didn't produce plumes significant enough to be detected by the lidar; this operation was performed by a very small tractor pulling a small spraying apparatus – the only disturbance of the ground was due to moving tires. Plumes of insufficient concentration differences from background levels led to downwind scan invalidation in many other instances also. The dairy pen areas adjacent to Field 4 proved to be sufficient PM sources such that lidar scans showing dust plumes passing over the pens prior to crossing the scanning plane were nearly always invalidated. Additionally, windblown dust was entrained off of both Field 4 and upwind field surfaces during both the May 20 sample periods. All of these factors combined to significantly decrease the number of valid lidar scans available for emissions estimation from most operations."

3) Strip till is mentioned beginning at page 1, but never clearly defined. Page 13 comes close but there is no adjacent description for comparison to conventional tilling. The two terms, as observed for the study, should be clearly defined.

A sentence has been added to Section 2.2, Operation Description, to describe a conservation tillage CMP and some text has also been added further down in that paragraph to contrast the level of soil disturbance between the strip-till and discing and plowing passes of the conventional method. It now reads as follows:

"As described in the Conservation Management Practices Program Report (2006), the conservation tillage CMP "involves using a system in which the soil is being tilled or cultivated to a lesser extent compared to a conventional system" and it is"intended to reduce primary soil disturbance operation such as plowing, discing, ripping, and chiseling". The Conservation Tillage CMP under study is a strip-till method which combines multiple operations to reduce the number of passes required and disturbs the soil only in 8"-wide strips centered every 30" instead of disturbing the entire surface like the plowing, discing, and listing operations of a conventional method."

4) One question is why the total $\mu g/(m^2 \times s)$ PM emission rates were used to derive the percent emission reductions when comparing the conventional tillage and conservation tillage methods rather than comparing the total mg/m^2 emission rates.

Please provide some clarification on why this metric was selected to compare PM emissions from the practices.

PM emission factors for tillage are generally given in mass per area for each operation (e.g. lb-PM10/acre-pass, mg-PM10/m^2-pass, etc.) and this was also the basis for comparing PM emission rates from this study with emission rates found in literature and used by ARB (see Page 4, Table 1; Page 6, Tables 2 and 3; Page 7, Table 4 and following paragraph; and Page 87, Table 28). It would seem that comparing the total mg/m^2 PM emission rates for conventional tillage and conservation tillage would provide a more useful and accurate representation of the change in PM emissions. At a minimum, the percent reductions based on the total mass of PM emitted per area tilled should also be shown and included in the conclusions. This would not really change the conclusions of the report but would probably be a more accurate representation of the total PM emission reductions.

The authors agree that this comparison should be made using an emission factor rather than an emission rate. The values and corresponding control efficiency calculations in Table 29 have been changed to emissions in mg/m^2 format. Text in the conclusion, page 86, has been changed to the following and numbers in the executive summary have been updated:

> *"Emission rates for $PM_{2.5}$, PM_{10}, and TSP from both lidar data and inverse modeling coupled with OPC data by operation are presented in Table 29 in units of mass emitted per unit area tilled per operation pass…. The conservation tillage method produced 9.5% as much $PM_{2.5}$, 6.3% as much PM_{10}, and 9.1% as much TSP as the conventional method according to the lidar data and 14.7% as much $PM_{2.5}$, 12.8% as much PM_{10}, and 9.7% as much TSP as the conventional method according to the AERMOD-OPC combination. Therefore, the control efficiency of the CMP for particulate emissions from these three data sets was as follows: lidar – 0.91, 0.94, and 0.91 for $PM_{2.5}$, PM_{10}, and TSP, respectively; and AERMOD-OPC – 0.85, 0.87, and 0.90 for $PM_{2.5}$, PM_{10}, and TSP, respectively."*

10.4.1.1 Comment for Further Discussion

1) Interagency discussion should review the difference between entrained and emitted. Measuring too close to a source will observe entrained material that will not remain in the air; it is entrained but will not be observed as an atmospheric contaminant downwind. We need to be sure that we have reasonable definitions for quantification of emissions. This impacts review of the best modeling approach to determine emissions – do we mean everything entrained or only that portion of material that will mix in the atmosphere sufficiently to be observable downwind and impact public health.

   EPA and SJVAPCD agree that additional discussions need to occur about definitions and methodologies.

10.4.2 Presentation of Results and Discussion with the San Joaquin Valley Air Pollution Control District's Ag Technical Group: 22 April 2013

10.4.2.1 Notes

USDA and the Space Dynamics Lab (SDL) did a presentation on the study results, emphasizing that the conservation tillage practice that was assessed reduced emissions by over 85% . USDA also noted that while different conservation management practices (CMPs) have differed reductions, the method with the greatest reduction in passes and soil disturbance of those studied had the greatest reduction in emissions. EPA stated that it would use the study results to help create incentives to implement conservation tillage, and that the Agency understands that variable conditions on farms restrict the applicability of this measure. Stakeholders and USDA also noted that producers needed flexibility to address different crops and on-farm conditions, and that the measure that was assessed in this research is not appropriate for every farm. Stakeholders also pointed out that in addition to reducing emissions through reductions in passes, California agriculture has reduced emissions by switching to equipment with cleaner burning diesel engines. The discussion included the questions below from stakeholders, which were answered by USDA and SDL.

> *The following sentence was included in Section 2.1 Site Description, page 12, to state the point brought out by stakeholders and USDA that tillage operations are not used in all agricultural crop production systems: "Tillage management practices are often crop specific and are not appropriate for use in all crop production activities. The effectiveness of CMPs used in other crop systems at reducing PM emissions should be investigated."*

10.4.2.2 Questions and Answers

Additional comments and portions of the report related to questions are provided after the answer in the indented sentences

Q: Do the results effectively capture the emission reductions associated with less fuel usage?

A: *We were able to calculate this on the previous study because the producer quantified the amount of fuel going into his tractor. We anticipate that it's tied to the amount of time using fuel, and would guess that there's probably a close to 85% reduction in fuel emissions also.*

> *The previous study referenced in this answer is Williams et al. (2012; available: http://cfpub.epa.gov/si/si_public_record_report.cfm?dirEntryId=248752) in which the control effectiveness of a Combined Operations CMP was investigated by USDA and SDL in Fall 2007.*
>
> *The following sentences have been added to the conclusion section of the report on page 89 to address the additional reductions through reduced tractor operation time:" It should be noted that other reductions in emissions between the two tillage management practices are likely to have occurred, mainly due to decreased fuel usage in tractor engines. Unlike the previously conducted companion study, fuel usage was not quantified in this study and prevented accounting for the associated reductions in emissions. However, these reductions are expected to be similar to the reduction in tractor operation time (~85%)."*

Q: Is it possible that there are some extra reductions to be claimed?

A: *Yes, if we looked at carbon emissions as well as potential PM coming from fuel usage we could get additional reductions— we didn't capture all of that with the samplers we had in the field for this study.*

See the response to the above question.

Q: Did you analyze yield differences?

A: *We were primarily interested in emission aspects and didn't do any yield comparisons in this study.*

The following sentence has been added on page 12 to clearly state this in the report: "The focus of this study was comparing emissions resulting from the tillage operations in each field. Therefore, no data were collected to make comparisons of other potentially varying characteristics, such as crop yield, soil organic matter, etc., between the two management practices."

Q: Were either of the fields already in conservation tillage?

A: *The field that was under conservation tillage had been under conservation tillage for several years; the other one was still being operated with conventional tillage with all the passes.*

This is addressed on page 13 of the report

Q: Did you look at the difference between soil temperature or ambient air temperature?

A: *We did not make soil surface temperature measurements. We agree that this factor may have a significant effect on emissions transport. We plan to make such measurements in future studies.*

An additional paragraph has been added to the Lessons Learned section, pages 90-91, to address this comment in the report: "In addition to the above lessons learned, peer review of this report also brought to our attention that measurements of additional parameters should be considered in future studies. Specifically, it was suggested that soil surface temperature measurements be made. Differences in soil surface temperature may result in different vertical and horizontal PM dispersion (with all other conditions being equal) as surface conditions are known to affect turbulence and dispersion."

Q: Were different tractors used for conventional vs. conservation tillage?

A: *It was usually the same tractor but for some of the passes a different tractor may have been used.*

The equipment, including the tractor, used for each tillage operation are provided in Table 8, page 17

Q: Did you do anything with N20?

A: *No. We didn't have the equipment at the time of the study.*

All equipment deployed for this study is provided in Section 3, pages 20-40.

United States
Environmental Protection
Agency

Office of Research
and Development (8101R)
Washington, DC 20460

Please make all necessary changes on the below label, detach or copy and return to the address in the upper left hand corner.

If you do not wish to receive these reports CHECK HERE ☐; detach, or copy this cover, and return to the address in the upper left hand corner.

PRESORTED STANDARD
POSTAGE & FEES PAID
EPA PERMIT No. G-35

Official Business
Penalty for Private Use
$300

EPA/600/R-14/191
August 2014
www.epa.gov